STUDIES ON SOIL-FOUNDATION INTERACTION IN THE SABKHA ENVIRONMENT OF EASTERN SAUDI ARABIA

BY

WALID MOHAMMED EL-MAHDI SIDDIG ALI

A Thesis Presented to the

DEANSHIP OF GRADUATE STUDIES

KING FAHD UNIVERSITY OF PETROLEUM & MINERALS

DHAHRAN, SAUDI ARABIA

In Partial Fulfillment of the

Requirements for the Degree of

MASTER OF SCIENCE

In

CIVIL ENGINEERING

January 2004

KING FAHD UNIVERSITY OF PETROLEUM AND MINERALS

DHAHRAN 31261, SAUDI ARABIA

DEANSHIP OF GRADUATE STUDIES

This thesis written by

WALID MOHAMMED EL-MAHDI SIDDIG

Under the direction of his thesis advisor and approved by his thesis committee, has been presented to and accepted by the Dean of Graduate Studies, in partial fulfillment of the requirements for the degree of

MASTER OF SCIENCE IN CIVIL ENGINEERING

Thesis Committee

Prof. Omer S. B. Al-Amoudi (Thesis Advisor)

Prof. Sahel N. Abduljauwad (Member)

Dr. Mohammed Maslehuddin (Member)

Dr. Talat A. Bader (Member)

Dr. Osman M. Abdullatif (Member)

Prof. H. I. Al-Abdul Wahhab
(Department Chairman)

Dr. Mohammad A. Al-Ohali
(Dean of Graduate Studies)

٩/١٢/١٤٢٠ هـ ١٢/٩/١٩٩٩ م

Date

Dedication

To the memory of

……my grandfather

To my uncle ……Mahdi

To ……my family

To my teacher

……..Hassan Zakariya

ACKNOWLEDGEMENT

All praise be due to ALLAH the most beneficent, the most compassionate, and prayers and peace be upon his Prophet Mohammed.

I wish firstly to express my sincere gratitude and thanks to KFUPM for providing me the financial support during the entire research period. My deep thanks go to my main advisor, Prof. Omer S. Baghabra Al-Amoudi, and Dr. Mohammed Muslehuddin, a committee member, for their continuous guidance, encouragement and advice that made this work possible. Special thanks are due to Prof. Sahel N. Abduljawad, a committee member, who introduced the sabkha-clay liner study and guided me through the experimental and analytical processes. I would like also to thank Dr. Talat A. Badr and Dr. Osman M. Abdullatif for serving as committee members.

My special appreciation is to Mr. Hassan Zakaria Saleh and Eng. Mohammed Mukaram Khan for their unlimited technical and expertise guidance as well as their fatherhood. A word of thanks also go to Prof. Hamad I. Al-Abdul Wahhab, Chairman, Department of Civil Engineering for his support and guidance through my MS program. Special thanks are for all the technicians and the scientists who made this work a reality.

Special recognition is given to my family at home for their patience and sacrifices during the course of my study.

ABSTRACT

Name of Student: **Walid Mohammed El-Mahdi Siddig Ali**
Title of the Thesis: **Studies on Soil-Foundation Interaction in the Sabkha Environment of Eastern Saudi Arabia**
Date of Degree: **January 2004**

This study was conducted to assess the possibility of utilizing clay as a stabilizer and liner in sabkha. The durability of plain and blended cement concretes in sabkha environment was also evaluated. The sabkha soil was characterized and investigated for the soil compressibility and infiltration of hazardous ions. Plain and blended cement specimens were exposed to a typical sabkha solution and their performance was evaluated by measuring compressive strength, sulfate resistance, chloride diffusion, and reinforcement corrosion. The effect of wet-dry and heat-cool cycles on the performance of blended cements was also evaluated.

The results of this study indicated that the addition of clay to sabkha increases its compressibility and inhibits the permeation of hazardous ions through the soil liner and significantly mitigates the percolation of the trace metals. However, an increase in the chloride diffusion was noted when clay was added to the sabkha soil.

Blended cements performed better than plain cements. However, the presences of magnesium sulfate in the solution exacerbated the deterioration of blended cements, especially silica fume cement. This cement was also affected by heat-cool cycles leading to higher water absorption. On the other hand, blended cements were found to have higher resistance to reinforcement corrosion than plain cements. The chloride permeability and chloride diffusion of blended cements were also less than that of plain cements.

King Fahd University for Petroleum and Minerals
January 2004

ملخص البحث

اسم مقدم البحث: وليد محمد المهدي صديق علي نميري

عنوان الرسالة: دراسات على تداخل التربة-الاساسات في البيئة السبخية للمنطقة الشرقية بالمملكة العربية السعودية

تاريخ منح الدرجة: ذو القعدة 1423هـ (يناير 2004م)

أجريت هذه الدراسة لتقييم احتمالية استخدام الطين كبطانة وكمثبت للتربة السبخية. تم تقييم ديمومة خرسانات الإسمنت العادي والإسمنت المضاف في البيئة السبخية. تم توصيف التربة السبخية وتحقق من إنضغاطية التربة وترشيحها للأيونات الخطرة. عرضت عينات من الإسمنت العادي والإسمنت المضاف لمحاول سبخة مثالي وتم تقييم أدائهم بقياس مقاومة الضغط، مقاومة الكبريت، تغلغل الكلورايد وصدأ حديد التسليح. تم أيضا تقييم تأثير دورات الرطوبة-الجفاف والتسخين-البرودة على أداء الاسمنت المضاف

أوضحت نتائج هذه الدراسة أن إضافة الطين للسبخة يزيد من خصائص إنضغاطيتها ويمنع مرور الأيونات الخطرة عبر البطانة ويحد بكفاءة من ترشيح العناصر المعدنية. بالرغم من ذلك، لوحظ زيادة في تغلغل الكلورايد عند اضافة الطين للتربة السبخية.

ان أداء الإسمنت المضاف أفضل من الإسمنت العادي. بالرغم من ذلك، فان وجود كبريت المغنيسيوم في المحاول يسرع تدهور الإسمنت المضاف، خاصة إسمنت غبار السيليكا. يتأثر هذا الاسمنت أيضا بدورات التسخين-البرودة مؤديا لإمتصاص ماء أعلى. من ناحية ثانية، وجد أن الإسمنت المضاف لديه مقاومة لصدأ حديد التسليح أعلى من الإسمنت العادي. ان نفاذية وتغلغل الكلورايد في الاسمنت المضاف أقل من تلك التي في الاسمنت العادي.

جامعة الملك فهد للبترول والمعادن

يناير 2004

TABLE OF CONTENTS

LIST OF TABLES

LIST OF FIGURES

CHAPTER ONE

INTRODUCTION

1.1 BACKGROUND

The Arabian Gulf countries have gone through a spectacular era of unparalleled industrialization and establishment of the infrastructure in the last three decades. These activities have led to the use of all types of concrete to construct all kinds of structures. However, the Arabian Gulf region is characterized by aggressive geomorphic and environmental conditions. These conditions have contributed to an alarming degree of concrete deterioration that takes place within ten to fifteen years after construction. Partly, the deterioration, particularly of columns and footings, is ascribable to the presence of sabkha soil in the region. Sabkha is a salt-encrusted soil that possesses little bearing capacity with large settlements when in a wetted condition. Its extreme salinity, which is about four to six times as much as seawater, and shallow groundwater make the sabkha medium an aggressive environment for foundations and sub-structures of all types, leading to rapid deterioration of concrete due to sulfate attack and reinforcement corrosion. The climate of the Arabian Gulf region is hot and humid and there is a large variation in the daily and seasonal temperature and humidity. The environmental and

geomorphic factors accelerate the deterioration of reinforced concrete structures in the region.

Research has to be directed towards the improvement of both the sabkha soil and the durability characteristics of reinforced concrete materials to enhance the performance of reinforced concrete structures in sabkha media. The improvement of sabkha soil may be achieved by the methodology of soil stabilization and adding fine-grained soil to the sabkha to form a low-permeability insulating material surrounding the structural utilities. Review of literature indicates that the first aspect, i.e., soil stabilization, has not been thoroughly investigated; particularly regarding its performance as a soil liner. Regarding improving the durability of reinforced concrete structures in sabkha, several investigations have recently been conducted at KFUPM. However, the use of different blending materials, particularly the use of densified and undensified silica fumes, has not been very well reported. Moreover, the chloride diffusion in concrete exposed to sabkha has not been studied.

The aim of this research was to investigate the possibility of modifying the sabkha soil to act as a liner, i.e., an impermeable layer, to decrease the diffusion of sulfate and chloride ions into reinforced concrete structural materials. Blended cements were used in order to inhance the durability of concrete in sabkha environment. The beneficial effect of using blended cements in sabkha exposure was evaluated by comparing their performance with that of concrete made with ordinary Portland cements (Type I and Type V).

1.2 PROBLEM DEFINITION

As stated earlier, the interaction of sabkha soil with foundation materials is of special concern to the construction industry in the Arabian Gulf area where sabkha prevails in most of the coastal areas along the Arabian Gulf and the Red Sea. Though many constructional problems have been reported, the durability of foundation materials is of special concern as the sabkha brine contains harmful salts that can attack reinforced concrete structures through:

a- Sulfate attack on concrete;

b- Chloride-induced reinforcement corrosion; and

c- Salt weathering due to salt crystallization in the pores of concrete above the groundwater table.

Several studies (Al-Amoudi, 1995; Algahtani et. al., 1994; Alsaadoun et. al., 1993 and Haque and Kawamura, 1990) have recently been conducted at KFUPM and elsewhere on the durability of plain and blended cements in sulfate-chloride environments. However, there is an exigent need to continue and build-up the studies on durability of plain and reinforced concrete in sabkha in order to understand the behavior of construction materials in sabkha and develop a databank on the performance of these materials in such an extremely aggressive environment. In particular, there is a need to conduct studies regarding the use of densified and undensified silica fume in producing durable structural concrete units, and determining the coefficient of chloride diffusion in plain and blended cement concretes when exposed to sabkha. Moreover, it may be necessary to provide insulation to all the structural members to be buried in the sabkha medium in order to

protect them from chloride and sulfate exposures. Accordingly, there is a need to investigate the possibility of mixing the sabkha soil with clayey materials (in different proportions) in order to make such a mixture perform as an insulating material.

1.3 RESEARCH OBJECTIVES

The overall objective of this research is to study the interaction of sabkha soil with the foundation materials. The specific objectives are as follows:

i. Characterize the geotechnical properties of sabkha-clay mixtures and determine the optimum dosage of clay to be added to sabkha, to improve its insulating behavior;
ii. Assess the compressibility of the sabkha-clay mixture by the use of modified oedometer;
iii. Assess the leachability of harmful dissolved ions and salts in the sabkha brine in order to evaluate the insulating properties of the mixtures;
iv. Assess the properties of plain and blended cement concretes exposed to chloride and sulfate-chloride (sabkha) media and determine their corrosion resistance;
v. Determine the extent of chloride diffusion in plain and bleneded cements when exposed to sabkha; and
vi. Study the performance of densified and undensified silica fume in sabkha.

1.4 THESIS ORGANIZATION

In order to accomplish the above-stated objectives, a thorough survey of the published literature was conducted to provide basis to this research. Literature review was presented in Chapter Two. This chapter mainly focuses on various aspects of sabkha soils, such as their characteristics, formation and their stabilization processes. Also in this chapter, a presentation of the literature on durability of concrete structures in sabkha soils was presented. In Chapter Three, details of the experimental program, including experiments and procedures, were presented. Chapter Four was devoted to data analysis and results obtained from the experimental program. In Chapter Five, conclusions from the results and recommendations emanating from this research were presented. Finally, a list of references was supplemented to document the literature on this thesis program.

CHAPTER TWO

LITERATURE REVIEW

2.1 SABKHA SOIL

The expression “sabkha” is originally an Arabic name for saline flats that are underlain by sand, silt and clay, and often encrusted with salt (Abu-Taleb and Egeli, 1981). These soils are products of the evaporative environment. There are essentially two types of sabkhas, coastal and continental, which are both equilibrium geomorphic surfaces. The coastal sabkhas are the result of depositional off-lap of marine sediments of subtidal, intertidal and supratidal facies, while continental sabkhas are landward and comprise earlier cycle marine sediments (Kinsman, 1969). It differs from a salt pan (or an evaporite basin) in that its depositional interface is subaeral, whereas that of a saltpan is subaqueous (Al-Amoudi, 1992). Sabkha soils have loose, permeable, sandy to gritty textures. The encrusted surface is composed usually of hygroscopic salts (Abduljawad et, al., 1994). Sabkha’s surface is usually hard enough to support a medium-weight vehicle, and become so impassible when wetted that a person would sink in nearly to knee depth (Al-Amoudi, 1995).

The variability of sabkha soil in the horizontal direction is related to its proximity to the shoreline, while the vertical variations represent stages of development of the sabkha cycle (Akili, 1981).

2.1.1 Coastal Sabkhas

Coastal sabkhas are the normal end product of nearshore marine sedimentation whereby the sediments are laid down just above the high-water mark, and the shoreline gradually moves seaward (Kinsman, 1969). A coastal sabkha is typically bordered on the seaward side by a semi-restricted lagoon, and on the landward side by a desert or rock outcrops. This sabkha is usually stark, salt-encrusted, and virtually flat, except for possible scattered storm tide channels and small isolated sand dunes. Its surface dips very gently seaward at imperceptible rates, and does not normally exceed a few centimeters to one or two meters elevation above the mean high-water level, as depicted in Figure 2.1. Since virtually the whole spectrum of sedimentation in the Arabian Gulf is carbonates, the major constituents of these types of sabkhas are aragonite and calcite, and by virtue of their proximity to the coasts, the carbonate content decreases as the sabkha grades landward (Al-Amoudi, 1995).

The formation of coastal sabkha is believed to be related to the regressive sedimentation which occurred during the past 4,000 to 5,000 years (Kinsman, 1969). The sabkha is a wedge of marine sediments of facies similar to those accumulating in the present marine and intertidal areas, capped by a thin supratidal facies which is overlain by a thin eolian facies (Kinsman, 1969). In addition to their primary marine sedimentological characteristics, the coastal sabkhas have many other features, particularly the early

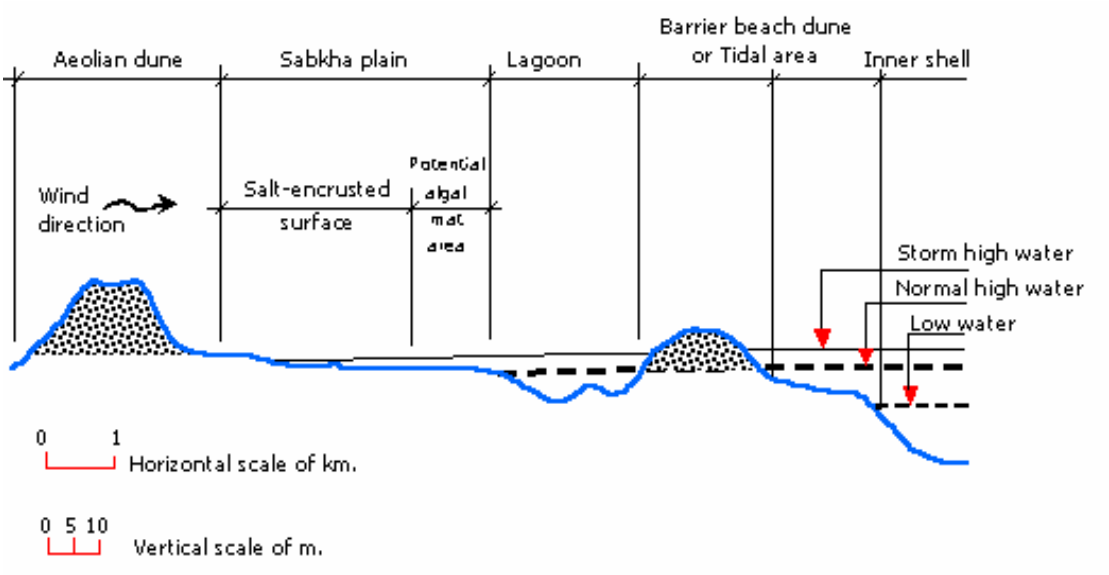

Figure 2.1: Coastal sabkha (Akili and Torrance, 1981)

diagenetic minerals. The new minerals are formed in response to the chemical and physical conditions of the sabkha environment. The minerals of the marine carbonate sediments represent a relatively stable marine assemblage, even though aragonite, the dominant mineral, is metastable at earth-surface temperatures and pressures (Kinsman, 1969). Coastal sabkhas may also evolve into continental sabkhas as the coastal plain progrades and marine-derived brines are replaced by continental waters (Kendall and Harwood, 1996), whereas the change can be occurred without noticeable change in surface morphology.

2.1.2 Continental Sabkhas

These types of sabkha are originally much older than coastal sabkhas, and their formation was linked to the transgression of sea water 300,000 years ago, when its level was well above its present one, and about that time started to regress leaving behind salt flats which formed these deposits (Kinsman, 1969). They are often interpreted as deflation surfaces, from which the wind removes the dry small particles, parallel to the water table at a level controlled by the dampness of the sediments (Kinsman, 1969). The ground-water table has to be higher than the bedrock surface, and the base level of deflation has to lie just above the capillary fringe in the sediments. The rate of evaporation in these sabkhas is supposedly higher than that in the coastal ones due to the more arid conditions. Consequently, the ground-water table plays a substantial role in the development of continental sabkhas, which are usually less developed than coastal sabkha flats and are predominantly tectonically and/or topographically controlled (El-Naggar, 1988). The

sediments of these sabkhas consist predominantly of gypsum (desert roses), quartz and calcite, with halite always existing at the crust (Kinsman, 1969).

2.1.3 Distribution of Sabkha

Sabkha distribution in Saudi Arabia is shown to be quite extensive, especially in the well-populated cities along both the Red Sea and the Arabian Gulf coasts. The distribution of sabkha along the Southern and Southwestern shores of Arabian Gulf is well documented in Figure 2.2, and found to be extending intermittently for more than 1,700 km with varying inland extensions of about 20 km on the average. Along the Western coasts of Saudi Arabia, sabkha exists at Abhor, Al-Lith, Rabigh and Yanbu, while in the Southwestern region, sabkha exists near the town of Jizan. In the North, continental sabkhas are distributed in WadiAs-Sirhan, as documented in Figure 2.3 (Al-Amoudi, 1995).

Globally, it has been reported that sabkha soils are present in Mexico, Utah, California and Texas in the United States of America and Ethiopia. Active coastal sabkha soils are also reported to exist in Australia, Sudan, North Africa and Libya. In summary, sabkha soils typically exist in semi-arid, arid or extremely arid climatic regions, excluding the polar areas, and cover about 30% of the total land area of the earth, principally within 10º 50’ N and 20° 30’ S, as documented in Figure 2.4 (Al-Amoudi, 1995).

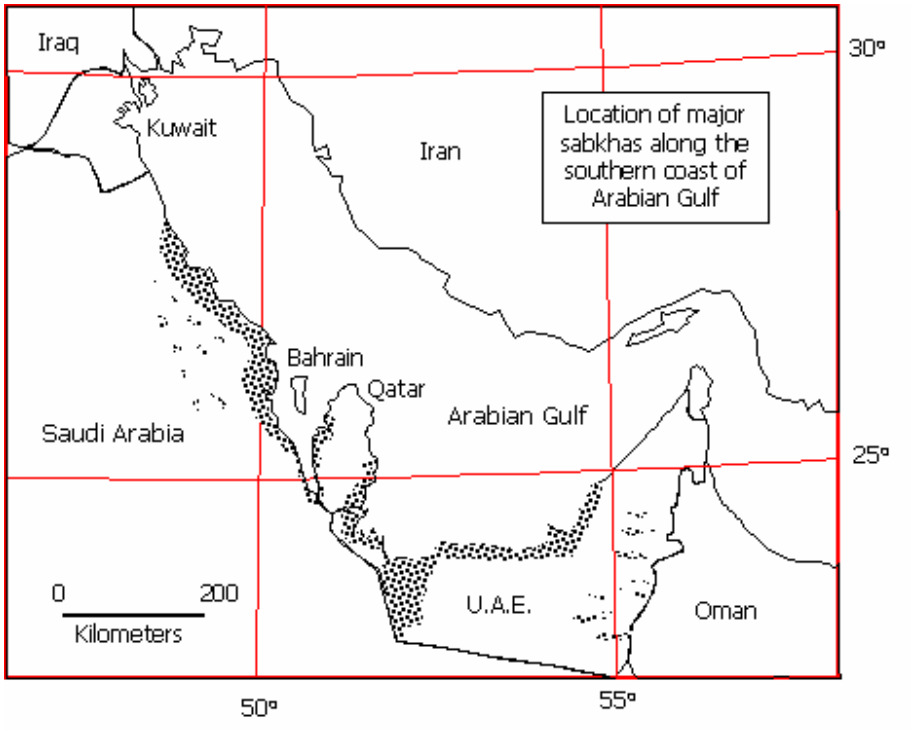

Figure 2.2: Distribution of sabkha along the Arabian Gulf coasts (Akili and Torrance, 1981)

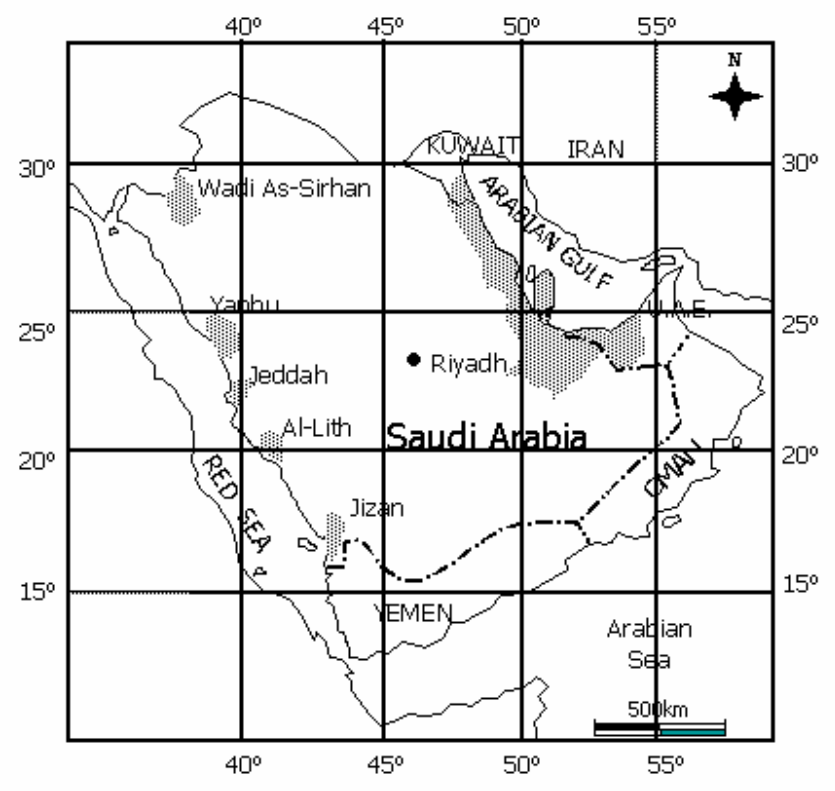

Figure 2.3: Sabkha distribution in Saudi Arabia (Al-Amoudi, 1995)

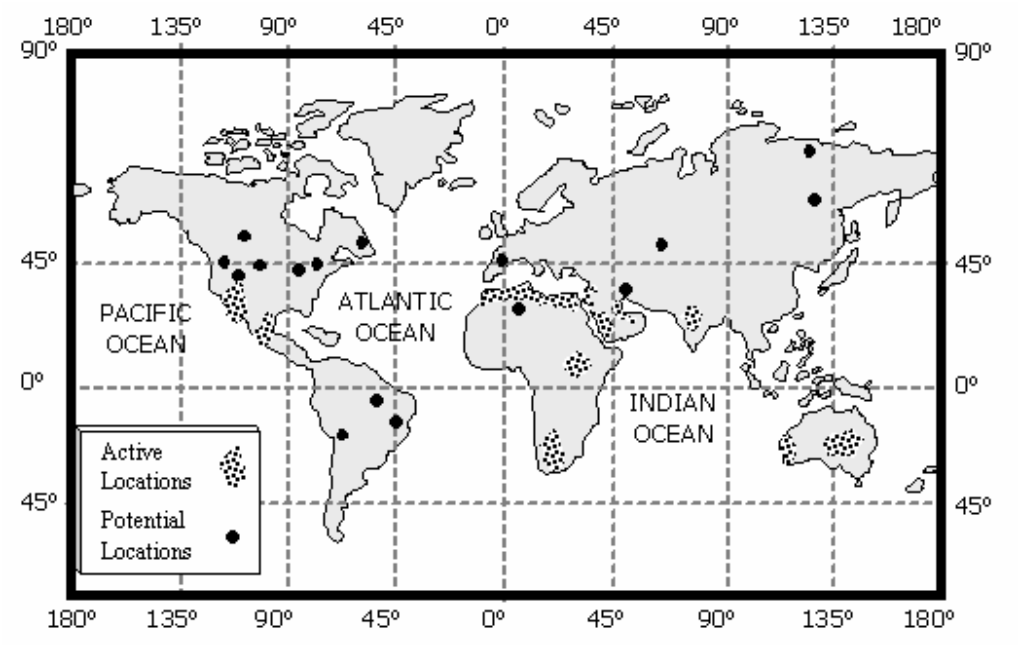

Figure 2.4: World map showing active and potential sabkha locations (Fookes et. al., 1985)

2.1.4 Geology of Sabkha

In order to study the geology of the sabkha soils in the region, the sequence of major palaeogeographic events in the Arabian Gulf is presented first with reference to Figure 2.5:

- At the end of the Pliocene periods (about 400,000 Y.B.P.), the Arabian Gulf water was about 150 m higher than its present-day mean and submerged most of the present coastal areas. Sabkhas terrains were formed along the ancient coasts of the Gulf (now inland sabkhas) in the same manner of formation of the present sabkhas (Kassler, 1973).

- During the Pleistocene glaciations (shortly before 100,000 Y.B.P), the Gulf water were lowered to a level of about 120 m below its present level. The Gulf basin dried out completely, except for a small arm at the Hormuz Strait. During maximum regression, the basin was a very large river valley carrying Tigris-Euphrates waters directly into the Gulf of Oman. This stage was reached at about 70,000 to 17,000 Y.B.P. (Kassler, 1973).

- The drying out of the Gulf basin was followed by a gradual rising of the sea level, and the re-filling of the basin with waters from the Indian Ocean during the post-glacial transgression (latest Pleistocene – earliest Holocene), between 20,000 and about 17,000 Y.B.P. (Kassler, 1973).

- In the early and middle Holocene (7,000 – 4,000 Y.B.P.), oscillations in the eustatic sea level brought in local marine transgressions, during which the water level was slightly higher than the present level (El-Naggar, 1988).

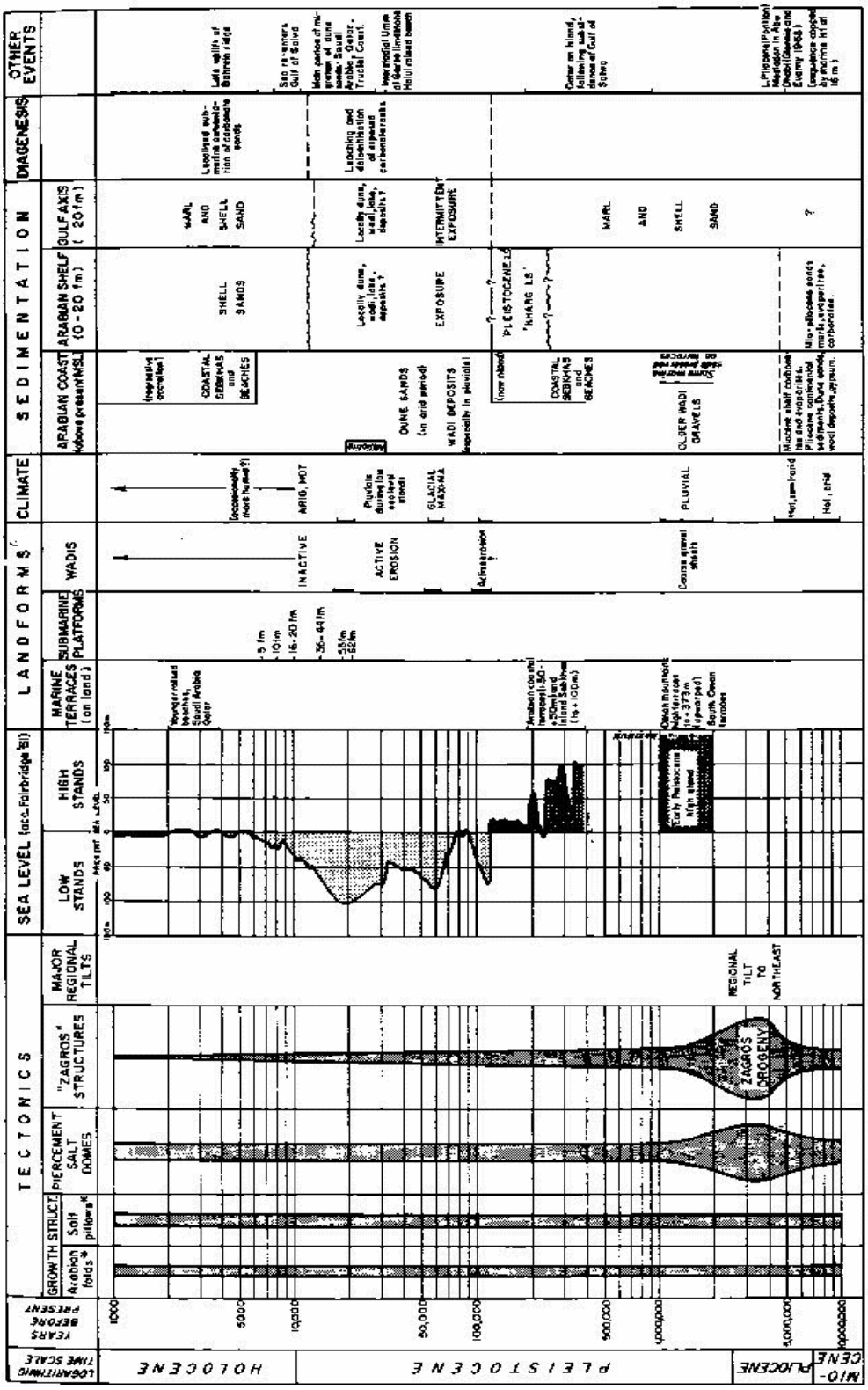

Figure 2.5: Generalized history of the Arabian Gulf coastal areas (Kassler, 1973)

- The sea level was still oscillating in minor transgressions and regressions that left their marks in the form of abraded, raised terraces in many coastal areas that took place from about 4,000 till 1,000 Y.B.P. These oscillations were accompanied by a relatively quick fall in the sea level of about 1 m at about 3,750 Y.B.P. and another drop of about 0.6 m to the present-day level during the period from 3,750 to 1,000 Y.B.P. (El-Naggar, 1988).

According to these sequences, El-Naggar (1988) suggested that during that period, the present-day sabkha area in the Arabian Gulf would have been laid under a free-water surface. This area extended for more than 1 km west to the present shoreline, with strand coastal banks and barriers that represent series of transgressions, vertical build-ups or regressions (Al-Amoudi, 1992)

The sequences of events which led to the formation of sabkhas was summarized as follows (Bush, 1973):

Approximately 7,000 Y.B.P., the Gulf waters transgressed over the site of the present sabkha plain, which at that time were covered by sub-aerial dunes, composed of quartzose carbonate sand. The extent of this transgression varied from place to place. In the area of the southwestern of Abu Dhabi, the maximum transgression reached a point between a 5 and 6 km landward of the present low water mark by approximately 4,000 Y.B.P., and a beach ridge developed at the margin of the lagoon so formed. Landward of the ridge, the dunes were deflated to the level of the water table, as their source of sediment had been submerged beneath the waters of the lagoon.

Seaward of the beach ridge, the original, aeolian, quartzose carbonate sand was reworked during transgression, and then gradually buried under newly formed skeletal carbonate sand which contained considerable amounts of re-worked aeolian sand in its

lower parts. It was finally covered with gray, muddy carbonate sand as the lagoon environment became established. Deposition continued until the lagoon became very shallow and further accumulation of sediment was prevented by the action of waves and currents (Bush, 1973).

A lithified crust, cemented with high magnesium calcite, formed on the surface of the sediments in the area of non-deposition (a similar crust is found on the lagoon floor at the present time). The sediments were transported by waves and currents to be deposited at the margins of the lagoons to form intertidal flats. This resulted in the lateral filling of the lagoon and the progradation of the coastline (Bush, 1973).

An apparent fall of sea level by approximately 1 m occurred between 4,000 Y.B.P. and 3,750 Y.B.P. This resulted in some of the sediments of the inner lagoon becoming intertidal instead of subtidal. An algal mat colonized the new intertidal area. At first, the algal mat grew out over the lithified crust, but later it continued to grow over the sediments pushed to the margins of the lagoons by the waves and the currents. As this algal mat grew seaward, the sediments carried onto its surface by winds and the occasional storms slowly covered it. About 1,000 Y.B.P., this algal mat ceased to grow and was buried by intertidal sediments, but the plain continued to prograde seaward and finally a new algal mat developed and has continued to grow until the present day (Bush, 1973).

2.1.5 Factors Influencing the Sabkha Formation

According to Al-Amoudi (1992), the factors that play a role in the formation of sabkha are the following:

1. Climatic factors;
2. Geochemical factors;
3. Geomorphological factors;
4. Hydrological factors; and
5. Biological factors.

2.1.5.1 Climatic Factors

The Arabian Gulf sabkhas lie within the northern sub-tropical zone, and are surrounded, mostly, by vast deserts with generally arid climate. The major climatic factors that control the formation of the sabkha are:

1. Rainfall: It is one of the three main water sources that feed the sabkha system. Purser and Seibold (1973) quotes an average annual rainfall for the Arabian Gulf sabkhas of less than 5 cm; however, it is probably mainly between 3 to 4 cm; compared to an average annual evaporation rate of approximately 124 cm/year (Bush, 1973).

Rain waters tend to dissolve the precipitated salts within the sabkha strata, particularly in torrential downpours, when the temperature is relatively low and evaporation loss would be minimum. Rainfall might also temporarily dilute the sabkha brine and might raise the water table level (Al-Amoudi, 1992).

2. Temperature: It is the principal driving factor for the evaporative mechanism. The climate of the Arabian littoral area is hot and humid, with a daily average temperature range of 16˚C to 44˚C (Butler, 1969: Bush, 1973), and a summer range of 40˚C to 50˚C (Purser and Seibold, 1973).

The inland margins of the sabkha have a wider range of temperature reaching up to 50˚C during summer days and droping down to almost 0˚C during winter nights (Purser and Seibold, 1973). The average temperature of the sabkha watertable surface is 34˚C (Kinsman, 1969), while just below the sediment surface of the sabkha, the daily temperature ranges from 18˚ C to 53˚ C (Butler, 1969).

3. **Relative humidity**: It is proposed as constraint on the final salinity of the sabkha brine and, hence, the ultimate evaporative mineral facies. For arid coastal evaporative areas, the relative mean humidity ranging from 70 to 80%, which is mainly suitable for sulfate minerals precipitation (Al-Amoudi, 1992).

4. The persistence of the prevailing winds: Their seasonability and direction play an important role in the genesis of sabkha in the Arabian Gulf. The Shamal winds, being north to northwest winds accompanied by hazy conditions, as a result of suspended dust, can transport huge quantities of aeolian sands onto and across the sabkha flats (Purser and Seibold, 1973). The sand adheres to both the damp surfaces and the algal mats. Often, entire sand dune fields can migrate across the sabkha in an offshore conditions, and this is the main reason for producing arenaceous (siliciclastic) sabkhas (called deflation basins) (Al-Amoudi, 1992).

The Shamal, seasonal, strong offshore winds in the southeast direction, can cause flooding of sabkha surfaces, providing critical replenishment of its water (Purser and Seibold, 1973). Such wave-driven sabkhas are mostly calcareous in composition with minor amounts of quartzose sand if any (Al-Amoudi, 1992).

2.1.5.2 Geochemical Factors

The high salinity of the Arabian Gulf waters and its sabkhas as compared with other open seas, is dictated by the excessive rate of evaporation and the restrictive nature of the Gulf basin. The geochemical factors influencing the formation of the sabkha can be categorized as follows:

1. **Lagoon and Sabkha Brine Chemistry**:

a) Lagoon Chemistry: Due to the low precipitation and high evaporation rates coupled with the restricted nature of the Gulf, the salinity ranges from 37 to 40‰ in the outer shelf areas, and from 40 to 50‰ in the inner shelf areas, to a range of 60 to 70‰ in very restricted lagoons (Purser and Seibold, 1973).

Lagoon waters are recorded as having pH values of about 8.3, interstitial algal flat waters of 7.5, while in mid and inner sabkhas, the pH values fall to 6.0 to 6.4 (Butler, 1969). The overall acidity of the brines in the sabkha sediments, as reflected by the pH measurements, has probably been caused by the decomposition of organic matters releasing carbon dioxide and hydrogen sulfide. The variation of the pH values is also in the vertical direction (Sonnenfeld, 1984).

b) Brine Chemistry:

i. Chlorinity: From the lagoon across the sabkha, brine chlorinity rises to a maximum and decreases again towards the inland margin (Butler, 1969). Chlorinities across the sabkha, excluding the high supratidal zone, are consistent with the process of flood recharge. During and immediately following flooding, the sea water concentrates by dissolution of soluble salts from the surface and within the sediments (Butler, 1969). Between flooding, brines concentrate by evaporation. Chlorinity

increases with depth across the 2 to 3-mile wide belt of sabkha just inland from the lagoon margin. On the other hand, it decreases with depth across the outer flood recharge zone. The brines in the outer flood recharge zone are saturated with respect to sodium chloride (Butler, 1969).

ii. **Sulfate**: The lateral and vertical distribution of the sulfate in the brines across the sabkha is similar to that of the chlorinity. Sulfate increases from 3.2 to 3.9 gm/kg in the lagoon to a maximum of about 16 gm/kg at the landward margin of the inner flood recharge zone, and then decreases rapidly to less than 1 gm/kg in the outer flood recharge zone (Butler, 1969). Across a large portion of this zone, sulfate remains constant within values of about 0.5 gm/kg. Sulfate concentration increases to more than 2 gm/kg across the high supratidal zone and probably reaches values in excess of 4.4 gm/kg (Butler, 1969).

iii. **Magnesium to Calcium Ratio**: This ratio increases from about 5.3 in the lagoon to a mximum of approximately 35 at the landward margin of the inner flood recharge zone and decreases rapidly to about 10 across the intermediate flood recharge zone. Across the outer flood recharge zone, the ratio remains constant between 3 and 4. The brines from the high supratidal zone have ratios that vary between 1.4 and 4, with an average of 3.5. Vertically within the sediment, seaward of the high supratidal zone, the ratio decreases in value downward from the surface. The ratio balance of evaporite brines is controlled partially by evaporation leading to precipitation of calcium carbonate and gypsum, and partially by the concomitant dolomitization causing precipitation of gypsum (Butler, 1969).

2. **Diagenetic Minerals**:

The sediments of the coastal sabkha consist mainly of either carbonate muds or calcareous sands carried up by the high tides and onshore winds in the first place, or by offshore winds in the second case. However, the characteristic feature of the sabkha sediments is the continuous development of diagenetic minerals. Sabkha diagenesis involves interstitial emplacement of the evaporite minerals within the host sediments and the continuous interaction between these interstitial minerals and the host sediments (Kinsman, 1969).

Bush (1973) divided the diagenetic minerals of sabkha deposits into the following two groups:

a) **Diagenetic Minerals Produced by Evaporation**:

i. **Aragonite**: It is precipitated in the lagoon, particularly during the early stages of concentration of the brine both within the sabkha sediments and also in its surface (Bush, 1973). It is the primary cement of the quartzose sabkha, especially in its uppermost parts. Its frequency decreases inland until, in places, it disappears completely, probably as a result of dolomitization. It is thermodynamically unstable at surface temperatures and pressures and reaches its maximum precipitation at a molar Mg/Ca ratio of 5.0. Aragonite is formed under rapid rate of precipitation under aquarium conditions. Mg ions act as a catalyst for aragonite precipitation and it becomes a stable phase above 85 mole %, it predominates at lower temperatures. The fresh water supply removes the magnesium ions from the solution allowing precipitated aragonite to convert to calcite (Sonnenfeld, 1984)

ii. **Gypsum**: It is the most common evaporite mineral in sabkhas, constituting, in some places, more than 50% of the top meter of the sabkha sediments. It occurs as

well-developed crystals of varying sizes and shapes, and locally as poikilitic cement. The crystals are rarely free from fine-grained carbonate inclusions. This mineral always develops in the interstitial spaces, but never as precipitate upon the upper sediment surface (Kinsman, 1969). Gypsum is the principal primary marine sulfate which precipitates by the aim of the removal of carbon dioxide from the brine. The ground water enriched in calcium chloride plays a role in forming gypsum crusts in intertidal and supratidal environments. Gypsum crystallization changes both the ionic and isotropic composition of the residual brine enriching it with heavy oxygen. The shape of the crystals is a function of pH and foreign cations. Calcium sulfates precipitate above the interface between oxygenated surface water and brine (in the rainy season). They are stable in waters saturated with oxygen. Moreover, another cause of precipitation of the gypsum is the oxidation of H_2S and H_2SO_4. The high gypsum content makes the soil have a high moisture holding capacity and requires high hydrostatic potential and more time to flush waters through (Sonnenfeld, 1984).

iii. **Anhydrite**: It is abundant in the sediments of the sabkha, occurring as nodules in the sabkha facies above the old algal mats. The nodular anhydrite forms in the sediments of the capillary zone. Its first appearance is shortly inland of normal high spring-tide mark and tends to increase in abundance inland (Shearman, 1966). Most of the anhydrite in the sabkha is of secondary origin. There is no conclusive evidence to suggest that any anhydrite has formed by direct precipitation (in coastal sabkha) (Butler, 1969). In continental sabkha, anhydrite precipitates from the continental ground water-derived brines. Also it is found that gypsum at the surface is dehydrated to anhydrite (Kinsman, 1969).

iv. **Halite**: It is precipitated as the dominant salt on the top surface layer. Brines, if present on sabkha surfaces, evaporate readily leaving halite crusts. It is also precipitated at lower levels, which are governed by the upper limits of the capillary movement, above the permenant water table. The halite is ephemeral, as it is promptly dissolved by water, unless in cases when the halite crust is buried (Kinsman, 1969; Bush, 1970). Halite will be probably preserved in ultra-dry and restricted sabkhas further inland, provided the terrestrial groundwater table is too low to dissolve it (Al-Amoudi, 1992). Halite precipitates in dry seasons, when evaporation's concentration is a maximum, and at night, at the peak of evaporative water loss (Sonnenfeld, 1984).

v. **Celestite**: It is a minor accessory mineral of coastal sabkha (Kinsman, 1969). The celestite ($SrSO_4$) could form as a primary mineral with the sea water as the source of strontium, or as an early diagenetic mineral with the strontium acquired during the dolomitization of aragonite (Kinsman, 1969; Bush, 1970). Along the Arabian Gulf coasts, celestite is found in small quantities as individual crystals or aggregates in the uppermost gypsum layers. It occurs more abundantly inland where strontium-rich aragonite converted to strontium-poor dolomite (Sonnenfeld, 1984).

vi. **Other Accessory Minerals**: The other minerals discovered in sabkha environments include: polyhalite (Bush, 1970) and huntite (Kinsman, 1969).

b) Diagenetic Minerals Produced by the Reaction Between Brines and Sediments:

i. **Dolomite**: It occurs in the sediments together with gypsum (Sonnenfeld, 1984). The precipitation of diagenetic aragonite, gypsum and anhydrite raises the

magnesium to calcium ratio of the pore fluid brines, and values of over 12 have been recorded (Kinsman, 1969). When this ratio reaches 10, dolomitization of fine-grained aragonite occurs to produce fine-grained dolomite. The calcium released is combined with sulfate from the brines to precipitate as gypsum (Kinsman, 1969). It is thermodynamically a stable phase in seawater with a normal salinity and Mg/Ca ratio (Sonnenfeld, 1984).

ii. **Magnesite**: It occurs in areas of high magnesium concentration in the brines. Although it is considered volumetrically as an unimportant member of the diagenetic mineral suite, it may constitute up to 50% of the material finer than 0.0625 mm. Magnesite [$Mg(CO_3)_2$] is formed by further dolomitizing the dolomite, according to the following reaction (Bush, 1970):

$$Mg^{++} + CaMg(CO_3)_2 \rightarrow 2Mg(CO_3)_2 + Ca^{++}$$

In a study conducted by Al-Guwaizani (1994) on Al-Qurayyah sabkha, eastern Saudi Arabia, quartz was found within the sabkha sediments mixed with the aragonitic grains and within the lithified aragonitic layer. It was suggested that the sources of quartz are old beach deposits and from Zabnat Zulum eolian dune.

2.1.5.3 Geomorphological Factors

These factors are composed of the following:

i. **Surface Gradient**: It is a primary condition in the development of sabkhas. Gradients usually controls the shape, the recharge ability and the general morphology of a

sabkha. A most unusual feature of the Arabian Gulf sabkhas is their almost planar surfaces, which rise inland from the lagoon with slopes of about 1:1000 (Butler, 1969).

ii. **Seaward Exposure of Sabkhas**: Movement of water onto the sabkha surface plays a vital role in the development of the chemistry of the interstitial brines. A direct correlation exists between the frequency of flooding, the composition of the interstitial brines and the nature of the diagenetic minerals developed (Butler, 1969).

2.1.5.4 Hydrological Factors

Both porosity and permeability play an extremely important role in the diagenesis of the sabkha; as the whole processes of brine seepage and evaporative rise depend on good permeability (El-Naggar, 1988). The hydrological phenomenon in the sabkha is influenced by the following seven factors:

i. **Lagoon and Terrestrial Waters**: Based on the concept that the hydrology of coastal sabkhas is the resultant of interaction between lagoon and terrestrial waters, and on the nature of the diagenetic minerals developed as well as the nature of the host sediments, Butler (1969) has divided the coastal sabkha into the following five zones:

1. **Intertidal Zone**: It is largely flooded by the tide waters. The upper intertidal zone is covered by living mats of blue-green algae. The algal mats are interlayered with lime muds and landwards contain pots of small euhedral gypsum crystals. Below the algal mats are lagoonal and intertidal carbonate muds.
2. **Inner Flood Recharge Zone**: It is subjected to monthly or more frequent flooding. The limits of this zone coincide with a surface layer of randomly oriented gypsum crystals. Most of the flood waters sink into the underlying

sediments while the rest flows back into the lagoon along shallow surface channels. The underlying carbonate muds contain small amounts of dolomite and small aggregates of gypsum crystals.

3. **Intermediate Flood Recharge Zone**: It is flooded at intervals longer than one month. The gypsum mush is overlain by a skin of reworked detrital quartzose sand. The surface gypsum crystals are replaced by anhydrite nodules. The underlying carbonate muds contain much dispersed fine-grained dolomite and large lenticular gypsum crystals.

4. **Outer Flood Recharge Zone**: It is flooded at about four to five years' interval. The anhydrite progressively replaces the gypsum mush until, at the landward margin of this zone, the anhydrite forms a layer composed of small nodules of anhydrite separated by thin films of dolomitic carbonate sediment and quartzose sand.

5. **High Supratidal Zone**: This zone is bordered by Pleistocene and Miocene sedimentary rocks. This zone is not flooded by sea water and the groundwaters are in part terrestrial. The underlying sediments are eolian Pleistocene sands, largely uncemented, which contain both gypsum and anhydrite, halite, and some polyhalite and sylvite

ii. **Watertable**: It is found to be always above the high-tide level and slopes gently, but consistently, seaward, indicating that the direction of groundwater flow is towards the sea. Even in the seaward region that is periodically flooded, the water table is never found to slope inland. The depth to water table increases gradually with the distance from the present-tide strandline, but never deeper than 1.5 m (Al-Amoudi, 1992).

iii. Net Evaporation Rate: The rate of net evaporation of the Arabian Gulf waters is 124 cm/year (Purser, 1973). The rate of evaporation is reduced by the effect of some factors, such as the sediment section above the water table, high ionic strength, high relative humidity, and vertical stratification of the air mass above the sabkha. With an average porosity of about 40% for the marine sediments, the net average upward groundwater table flow velocity across most of the coastal sabkhas is in the order of 15 cm/year (Patterson and Kinsman, 1981).

iv. Permeability of Sabkhas: Since the topography of the sabkha is flat, the true velocity of groundwater flow is unlikely to exceed 10^{-6} m/sec (Fookes et al., 1985).

v. Means of Replenishment: The following three modes of replenishment have been reported in the coastal sabkhas (Bush, 1973; Akili et al., 1981):

- **a.** The horizontal movement of water from the lagoon in the sabkha environment, mainly when the tidal level sufficiently exceeds the level of groundwater.
- **b.** The horizontal movement from the sabkha to the lagoon.
- **c.** The vertical downward movement of water which inundates the sabkha surface during the exceptionally high tides, flash floods or infrequent rains. These waters cause dissolution of precipitated salts on the crustal layer and transport them down. These waters tend to dilute sabkha brine.

vi. Upward Flow: It is the result of the aridity of the sabkha region which stimulates the upward movement of moisture, which is known as evaporative pumping. This upward flow, which is necessary for dolomitization, is not due to the capillary action in the vadose zone but to reduction in the pore pressure due to the evaporation of interstitial vapour (Hsu and Schneider, 1973).

vii. Artesian pressures: As documented by James and Little (1994), it is reported to exist in the sabkha areas at Juabil and Al-Qurayyah (Al-Guwaizani, 1994).

2.1.5.5 Biological Factors

The most important biologic factors within the sabkha environment can be classified in the following:

- Algae and Algal Mats: these represent an integral part in the sabkha system and affect it in two ways:
  - By incorporating adhered sediment particles in their growth cycles; thus directly contributing to both the upward and outward growth of the sabkha by forming an impervious base for the sediments (El-Naggar, 1988).
  - By releasing gas vents of H_2S and CH_4 from their decaying dead bodies, that escape upwardly through the sediments and serve to increase both their porosity and permeability (El-Naggar, 1988).
- Sulfate-reducing Bacteria: These bacteria produce both sulfur and hydrogen sulfide, and the reducing environment can help precipitate trace metals (El-Naggar, 1988).
- Burrowers: These are not common, due to the intense heat and salinities, but they are not totally lacking and their borrowing activities enhance the sediments porosities (El-Naggar, 1988).

2.1.6 Characteristics of Sabkha Soils

Sabkha soils are characterized by the presence of diagenetic salts of different composition and texture at different depths. The precipitation of salts below the groundwater table is ascribed to the increase in the salt concentration above its saturation limit (Al-amoudi, 1992; 1995). Gypsum, for example, is known to precipitate when the volume of sea reduces to 19% of its volume (Sonnenfeld, 1984). The deposition of salt in the surfacial layers (i.e. above the groundwater level) is attributed to the evaporation of the moisture that was drawn to the top layers by the capillary action. Sabkhas always exist in the form of alternating cemented and uncemented layers, as well as lumps of quartz and/or carbonate sand. In the cemented layers, the main cementing materials are aragonite and calcite ($CaCO_3$), gypsum ($CaSO_4.2H_2O$), anhydrite ($CaSO_4$), and halite (NaCl). The top layers of sabkha may exhibit firm and stiff characteristics in its dry state. However, when dampened with water, the strength is highly reduced, as the cementing salts are susceptible to leaching and dissolution or softening thereby leading to strength loss in wet conditions. Moreover, sabkhas are characterized by volumetric change due to alternate hydration and dehydration of unstable gypsum under hot and humid conditions (Al-Amoudi, 1992; 1995). Sabkha possesses retaining characteristics. The sabkha water retention is influenced by the salinity of the groundwater, whereas the higher salinity of the water, the greater amount of water will be retained by sabkha (Sabtan et al., 1995).

2.1.7 Problems Associated with Sabkha Soil

Due to the concentrated nature of sabkha brine and its proximity from the ground surface, several geotechnical and constructional problems may emerge. These problems are further exacerbated by the fact that sabkha terrains do prevail in several major cities in Saudi Arabia like Jeddah, Jubail, Yanbu, Rabigh, Jizan, etc. These problems can be divided into the following two parts (Al-Amoudi, 1992):

2.1.7.1 Problems Associated with Sabkha as a Construction Material

1. A potential variation in compressibility of sabkha sediments will lead to excessive differential settlements. This is ascribed to the fact that sabkha deposits, in general, are known to vary from very loose or loose to dense conditions with a relatively short distance of five to ten meters. As a sequence, sabkha possesses a high collapse potential mainly as a result of dissolution of sodium chloride, leaching of calcium ions and soil grain adjustment (Al-Amoudi and Abduljawad, 1995).

2. The surfacial sabkha layers have low strength in their natural state, leading to as low as an average unconfined compressive strength of about 20 kPa (Abduljawad et, al., 1994). Strength will significantly further reduce in the surficial sabkha layers due to rainfall, flash floods, storm tides, or merely as a result of absorption of water from the humid environments.

3. Alternate volumetric change due to alternate hydration and dehydration of unstable gypsum will damage the construction above the sabkha soil (Akili, 1981).

4. The highly concentrated chloride and sulfate salts present in sabkha sediments and its brines, lead to corrosion of the steel reinforcement and deterioration of the concrete itself (Akili, 1981; Al-Amoudi, 1995).

5. Frequent rise of subsurface water due to the evaporative pumping mechanism moves soluble salts from the water table towards the surface wherein they precipitate. The salt crystals thus formed may form salt blisters and initiate surface cracking below structures (i.e. pavements) (Akili, 1981).

6. Densification of the upper layers of sabkha by conventional means, to improve its bearing capacity and reduce its settlement characteristics, may break up the cementation bonds in the underlying layers and lower their bearing capacity (Akili and Torrance, 1981).

7. Interaction of sabkha with fresh water could dissolve some of the cementing materials and decrease the strength (Sonnenfeld, 1984; Al-Amoudi, 1992).

8. Difficulties associated with the accessibility to sabkha sites due to saturation and loss of strength may delay the construction operations and increase the cost (Akili and Fletcher, 1978).

9. The use of distilled water to determine the geotechnical properties of sabkha, as recommended by ASTM, BS, DIN, etc., seems to be inappropriate (Al-Amoudi and Abduljawad, 1994 (a)). This is because distilled water tends to dissolve the salts, which are considered as part of the soil.

2.1.7.2 Foundation Problems in Sabkha Soil

1. Problems due to the periodic changes in moisture content, will lead to large changes in density, consistency, strength and volumetric changes. These excessive volumetric changes may cause serious damage to foundations as well as to the constructions above the sabkha soil (Al-Amoudi, 1992).

2. Problems due to excessive differential settlements may take place due to the inhomogeneity of sabkha soil profile, the looseness of certain layers within the soil profile and the highly variable compressibility of the various components of the soil. This may lead to severe differential settlements and to serious cracks and tilting in the structures on the sabkha soil (Al-Amoudi, 1992; Al-Shamrani and Dhowian, 1997).

3. Problems due to the presence of highly corrosive salts and brines due to excavation and refilling will induce capillary rise which brings with it additional soluble salts to the new foundations. The sulfate and chloride ions present with high concentrations are highly corrosive to both concrete and reinforcement, respectively. Moreover, salt crystallization usually occurs in the concrete pores above the water table leading to slow disintegration of concrete due to the high crystallization pressure that is enhanced by evaporation (Al-Amoudi, 1995).

4. Problems due to the proximity of the ground water table due to the fluctuations in the ground water level can cause serious problems of settlements for structures built on such a soil. These settlements occur due to the wetting of dry, loose sands or due to the compressibility of dewatered, loose, sandy soils. In addition, the susceptibility of the sabkha soil to flooding due to the low elevation of sabkha surface may cause several problems (Al-Amoudi, 1992; Aiban, 1994).

2.1.8 Sabkha in Eastern Saudi Arabia

The sabkha sediments are predominantly sandy in nature with occasional layers of clay, clayey silts or silty clay. The fines content in the sands is significant. The sands, in terms of mineral constituents, are mostly quartz, however, the carbonate and sulfate contents are also significant. The sands are often layered and cemented, and the degree of cementation varies from lightly cemented to strongly cemented. Crystalline salts, often visible in the upper layers, are comprised of gypsum, anhydrite, calcite and halite (Akili and Ahmed, 1983).

Calcarious sands and silts are also prevalent in some eastern Saudi sabkha sediments containing 12 to 50% carbonate. Most of the sabkha materials encountred contain less than 25% carbonate (Akili and Ahmed, 1983). Due to the high carbonate content in the sabkha sediments, some construction problems may emerge resulting in undermining the foundations, due to carbonate leaching (Akili and Ahmed, 1983). The sabkha sediments reported by Akili and Ahmed (1983) consist of the following three zones:

- Upper Zone: It extends from the surface down past the water table and varies in depth to approximately two meters. This zone includes the cemented crust, the water table, and other thin stratified layers of cemented sands and silts.
- Intermediate Zone: It may contain some or all of the following: loose quartz sands, calcarious sands, cemented sand-silt layers, clay layers, muds, carbonate sands and other marine derived sediments. This zone varies in depth from approximately two to ten meters.

- Lower Zone: In this zone, the sediments generally exhibit high resistance to penetration. The likely materials encountered are: dense to very dense sands, strongly cemented sands, stiff clays or rock.

2.1.9 Sabkha Stabilization

Many studies have recently been conducted on sabkha stabilization (Al-Amoudi, 1992; Ali, 1999; Ahmed, 1997; Al-Ayedi, 1996). The output of these studies can be summarized as follows:

1. Cement is considered to be one of the best materials used in sabkha stabilization, especially when the soil is sandy. The percentage of cement to be added is determined based on a few number of tests to assess the strength and durability when subjected to inundation by water (Al-Ayedi, 1996).

At high moisture content similar to that existing in the field, cement increases the strength significantly. Cement-soil mixture requires an amount of water to achieve proper compaction and to help in the hydration process of cement in order to act as a cementing agent (Al-Amoudi et. al., 1995).

2. Lime is used to stabilize plastic sabkhas that contain a large amount of clay. Preliminary tests should be conducted to confirm the suitability of lime to strengthen sabkha, especially in the presence of moderate concentration of sulfates (i.e., gypsum and anhydrite) and chlorides. Alternatively, combination of lime and cement may be used to achieve appropriate strength and durability (Ahmed, 1997).

Lime may develop high strength when stabilizing sabkha specially for lime addition of more than 5%. However, care should be taken due to the fact that stabilized sabkhas display significant reduction in strength when prepared at higher moisture contents than the optimum (Al-Amoudi et. al., 1995).

3. Geotextiles can be used in the case of sabkha having high quantities of salts (Abduljauwad et al., 1994). It may be secondarily used as a drainage control technique in order to intercept the capillary fringe (Ali, 1999; Siddiqi, 2000).

Some trials on the usage of geotextiles to increase the bearing capacity of sabkhas and to arrest saline-water rise have been reported (Abduljawad et. al., 1994). Geotextiles can also reduce the permeanant deformations of the sabkha soils.

4. In the case of thick layers of sabkha, vibroreplacement techniques (i.e. stone columns) may be the best alternative when the loading conditions are not highly concentrated. In such a case, a number of columns are recommended to be used in order place the mat foundation on them (Akili and Ahmed, 1983).

5. If the site has a base rock at deep levels, concrete piles may be the ultimate solution. Precautionary measures to improve the durability performance of these piles, however, have to be taken into consideration (Akili and Ahmed, 1983).

6. Preloading techniques can also be applied for sabkha stabilization. This technique can be viable for compressible sabkha complex having clayey soil or having recognized organic contents (Al-Shamrani and Dhowian, 1997).

2.2 DURABILITY OF CONCRETE

2.2.1 Introduction

The exposure conditions for concrete structures in the coastal areas of the Arabian Gulf constitute one of the most aggressive environments in the world. The coastal areas of the Arabian Gulf have large fluctuations in daily and seasonal temperature and humidity conditions. The temperature can vary by as much as 30°C during a typical summer day, and the relative humidity ranges from 40% to 100% over a period of 24 hours (Al-Amoudi, 1992). Furthermore, the groundwater is relatively high and close to the ground surface and evaporation is intense. The capillary rise of moisture and frequent flooding followed by high evaporation rates leaves a heavy crust of salt in the upper layers of the soil. This leaves the ground, groundwater, atmosphere and the aggregates heavily contaminated with chloride and sulfate salts (Maslehuddin et al., 1990). The primary causes for concrete deterioration in this region are: Firstly the reinforcement corrosion, and secondly the sulfate attack.

Since reinforcement corrosion and sulfate attack are the main forms of concrete deterioration in a sulfate-chloride environment, the mechanisms of these phenomena are discussed in the following sections.

2.2.2 Reinforcement Corrosion

A good quality concrete provides protection to the reinforcing steel due to the alkaline nature of the pore solution (ACI 201-2R, 1992). Under such high pH conditions,

steel reinforcement is normally protected from corrosion by the formation of a thin surface layer of ferrous hydroxide or hydrated oxide (Kumar, 1998). The formation of this surface layer is a time dependent process and its electrochemical properties change with age. Typically, for mature Portland cement paste, the pH is 12.5 which results from the presence of calcium hydroxide, liberated when the Portland cement hydrates (ACI 201-2R, 1992). The presence of sodium and potassium hydroxides in the cement increases the pH to more than 13.5.

Whenever the passive layer protecting the reinforced concrete breaks, rust will start appearing on the steel surface. When the steel corrodes, it dissolves in the pore water and gives up electrons (Broomfield, 1997; Eglinton, 1987), as explained in the following equation:

$$Fe \longrightarrow Fe^{2+} + 2e^{-}$$

This is called the anodic reaction and the location at which it takes place is known as the anode. The electrons liberated in the anode are driven to the cathode where they react with water and oxygen forming hydroxyl ions, as explained in the following equation:

$$2e^{-} + H_2O + \tfrac{1}{2} O_2 \longrightarrow 2OH^{-}$$

Although the hydroxyl ions generated in the cathodic reaction will increase the local alkalinity leading to strengthening of the passive film, these hydroxyl ions will react with the free ferrous ions leading to a first stage of rusting followed by several more

stages. When the iron was just dissolved in the pore solution, the following chemical reactions take place (Broomfield, 1997):

$$Fe^{2+} + 2OH^- \longrightarrow Fe(OH)_2$$

$$4Fe(OH)_2 + O_2 + 2H_2O \longrightarrow 4Fe(OH)_3$$

$$2Fe(OH)_3 \longrightarrow Fe_2O_3.H_2O + 2H_2O$$

Unhydrated ferric oxide has a volume of about twice that of the steel it replaces when fully dense. When it becomes hydrated, it swells even more and becomes porous (Broomfiled, 1997). This leads to the cracking and spalling usually observed as usual consequence of corrosion (Broomfiled, 1997).

The two main causes of reinforcement corrosion are the following:

(a) Carbonation of the cover concrete; and

(b) The presence of chloride ions around the steel.

2.2.2.1 Corrosion Due to Carbonation

Carbonation is the result of the interaction of atmospheric carbon dioxide with the alkaline hydroxides in the concrete. The carbon dioxide dissolves in water to form carbonic acid which neutralizes the alkalis in the pore water forming calcium carbonate, as follows (Broomfield, 1997):

$$CO_2 + H_2O \longrightarrow H_2CO_3 \downarrow$$

$$H_2CO_3 + Ca(OH)_2 \longrightarrow CaCO_3 \downarrow + 2H_2O$$

The calcium hydroxide dissolved in the pore water maintains the pH at its usual level of around 13. When the carbonic acid reacts with this hydroxide forming calcium carbonate, the calcium carbonate produced reduces the pH of the pore water to levels of 8 to 9 due to the consumption of the high alkalinity calcium hydroxide (ACI 201-2R, 1992). With time, this will destroy the alkalinity of the surficial zone, and if this carbonated front reaches the level of the reinforcement, it will render the steel vulnerable to corrosion in the presence of moisture and oxygen (Mosley et al., 1996). The rate of carbonation depends on the quality of the concrete, the humidity and the concentration of CO_2 in the environment. However, the deterioration of concrete structures in the Arabian Gulf region due to carbonation-induced reinforcement is much less prevalent than that due to the chloride-induced corrosion of reinforcing steel.

2.2.2.2 Chloride-induced Reinforcement Corrosion

The major cause for reinforcement corrosion is chloride attack, where the chloride ions attack the passive layer. Chlorides act as catalyst to corrosion of reinforcing steel when there is sufficient concentration at the steel surface to break down the passive layer. They are not consumed in the corrosion process but help break down the passive layer of oxide on the steel and allow the corrosion process to proceed quickly, which can be described by the following equations (Broomfield, 1997; Elington, 1987; Montemor et. al., 2003):

$$Fe^{+++} + 3Cl^- + 3H_2O \longrightarrow Fe(OH)_3 + 3HCl$$

$$HCl \longrightarrow H^+ + Cl^-$$

Free chloride ions within the capillary pore water are known to increase both the electrical conductivity and solubility of the passive film that normally forms on the surface of steel in concrete. At the end of the initiation stage of the corrosion process, the passive film is destroyed or damaged and a corrosion cell is established. This signifies the onset of the corrosion growth stage (ACI 201-2R, 1992).

Chloride ions can originate from the water added to mix the concrete, chloride-contaminated aggregates, sea water spray and splash, salt-bearing soil and groundwater, marine salts carried by the wind, and possibly brackish curing water (Novokshchenov, 1995). Chlorides can also originate in the constituents of a concrete mix, e.g. the cement, aggregate, admixtures (Kumar, 1998). Once the chloride ions penetrate the concrete matrix, they will exist in one or more of the following three conditions:

(a) Part of the chloride ions will react with the tricalcium aluminate (C_3A) phase of cement, forming an insoluble compound of calcium chloro-aluminate hydrate ($C_3A.CaCl_2.10H_2O$), also known as Friedel's salt. The beneficial effect of higher C_3A contents in the increase of corrosion protection by retarding chloride-induced reinforcement corrosion has been known for some time (Roberts, 1962; Algahtani et al., 1994).

(b) Another part is adsorbed by the calcium silicate hydrate and other hydrated phases, such as ettringite, forming adsorbed chlorides (Kropp, 1995).

(c) The third part will be the free chloride ions in the pore fluid of the concrete that will attack the passive film on the reinforcing steel, causing its depassivation (Kropp, 1995).

Chloride ions can move into and through the layer of cover concrete by one of the following three main mechanisms:

i) Diffusion: Chloride diffusion occurs where the capillary pores of the concrete are effectively saturated with water. As a consequence, chloride ions outside the concrete must diffuse into the saturated cover concrete. The driving force for this movement is the concentration gradient between the outside surface and the center of the concrete (Kropp, 1995).

ii) Capillary absorption: Under alternate wetting and drying conditions, significant capillary uptake of water can occur in the outer concrete surface. Where the water absorbed into the drying capillary pores contains chloride ions, they will be left deep in the cover concrete after only one wet/dry cycle. Subsequent wet/dry cycling can give rise to the rapid build-up of high chloride ion levels deep in the concrete. It has been estimated that chloride ingress by capillary absorption is more rapid than that occuring by permeability (Kropp, 1995).

iii) Flow under pressure: Concrete is a permeable material and, if in contact with water under pressure, will allow the passage of water. If the water, which flows, is contaminated with chloride ions then chloride concentrations can build-up to high levels (Hobbs and Matthews, 1998).

A major cause of chloride intrusion into concrete is cracks, which allow infiltration at a much faster rate than by the slower diffusion process, and establish chloride concentration cells that can initiate corrosion. Crack formation can be reduced by

the use of good quality concrete having low water permeability and absorption and reduced risk of corrosion (ACI 201-2R, 1992). Of course, in real structures, chloride ingress occurs by a combination of these processes.

It is an important observation that even in the presence of free chloride ions when concrete is kept moderately dry; corrosion of the steel can be minimized (ACI 201-2R, 1992).

The free chloride ions in concrete depend on the cement type. It can be seen that sulfate resisting Portland (Type V) cement is much less able to bind the initial chloride ions than ordinary Portland (Type I) cement and, as a consequence, the limit on allowable total chloride ion content is reduced (Novokshchenov, 1995; Rasheeduzzafar, 1992). As reported by Azad (1998), reinforcement corrosion may occur with chloride content exceeding 0.355% by weight of cement. Further, Kay et al. (cited by Bungey, 1982) suggested that a value of 0.4% chloride ions by weight of cement might be sufficient to promote reinforcement corrosion, and 0.2% by weight of cement for external diffusion (Broomfield, 1997). Broomfiled (1997) attributed the variation in the threshold chloride value to the following:

- Concrete pH varies with the type of cement and the concrete mix. A tiny pH change represents a massive change in the hydroxyl ion concentration and therefore the chloride threshold value varies radically with pH.
- Chlorides can be bound chemically by the aluminate phases in the concrete or physically by adsorption on the pore walls, which removes them permanently or

temporarily from the corrosion process. Sulfate resisting cements have low aluminate content thereby leading to more rapid diffusion and lower chloride thresholds.

- In very dry concrete, corrosion may not occur even at very high chloride ion concentration as the water is missing from the corrosion reaction.
- In sealed or polymer-impregnated concrete, corrosion may not occur even at a very high chloride ion concentration if no oxygen or moisture is present to fuel the corrosion reaction.
- Corrosion can be suppressed when there is total water saturation due to oxygen starvation, but if some oxygen is present, then the pitting corrosion can occur.

Chloride-induced corrosion is prone to macro-cell formation at presence of high amount of water to carry the chloride ions into the concrete. The presence of water in the pores increases the electrical conductivity of the concrete, which allows the separation of anode and cathode of the corrosion cell as the ions can move through the water-filled pores (Broomfield, 1997).

2.2.3 Sulfate Attack

The role of sulfate ions towards concrete deterioration can be visualized as follows (Al-Amoudi, 1998):

- They react with C_3A in cement to form ettringite, which is expansive in nature and produces cracks.
- They react with $Ca(OH)_2$ producing a cohesionless mass, which progressively peels off the concrete surface.

- The concomitant presence of chlorides and sulfates may decrease the electrical resistivity of concrete (Maslehuddin et al., 1995).

Sulfate salts only attack concrete when they are in solution. There are two types of sulfate attack, according to the type of cation associated with the sulfate ions, which are magnesium sulfate attack and sodium sulfate attack (Al-Amoudi, 1998).

2.2.3.1 Magnesium Sulfate Attack

Magnesium sulfate reacts with the portlandite [$Ca(OH)_2$] present as a result of cement hydration, forming gypsum and insoluble magnesium hydroxide (brucite) (Eglinton, 1987). This insoluble hydroxide has a pH of 10.5. At this low pH, calcium silicate hydrate and ettringite become chemically unstable. As a result, secondary ettringite will not form and the magnesium sulfate will react with the calcium silicate hydrate forming gypsum, brucite, and silica gel ($SiO_2.H_2O$) (Santhanam et al., 2003). As the pH is lowered by the evolution of magnesium hydroxide, the calcium silicate hydrate will liberate lime to raise the pH to establish its equilibrium. The liberated lime reacts with the magnesium sulfate producing more magnesium hydroxide, resulting in more concentration of gypsum and brucite. Consequently, the calcium silicate hydrate loses its lime and becomes less cementitious. The excess magnesium hydroxide reacts with the silica gel produced formerly, and the product is magnesium silicate hydrate, which is non-cementitious and fibrous. This attack is characterized by softening and the deterioration of the surficial layers of the concrete, and is associated with loss in weight and reduction of strength and the aggregate will be exposed (Amoudi, 1998, Eglinton, 1987; Santhanam et al., 2003).

2.2.3.2 Sodium Sulfate Attack

Sodium sulfate reacts with portlandite present in the hydrated cement paste, forming gypsum and sodium hydroxide (Eglinton, 1987). Contrary to the action of magnesium hydroxide, sodium hydroxide tends to raise the pH of the cement paste to about 13.5. This rise in the pH has a stabilizing effect on the ettringite and the calcium silicate hydrate compound. The gypsum formed at the first phase of the sodium sulfate attack reacts with some of the hydrated and unhydrated aluminate-bearing paheses, namely calcium aluminate hydrate, monosulfate and unhydrated tricalcium aluminates, to produce secondary ettringite. This secondary ettringite has expansive characteristics on the hardened concrete thereby leading to its expansion and cracking (Al-Amoudi, 1998; Santhanam et al., 2003).

2.2.4 Concrete Durability in Chloride–Sulfate Environment

In the case of the concomitant presence of chlorides and sulfates in solution, the deterioration of concrete depends on several factors. The role of each of these ions on the durability of concrete and its reinforcing steel can be summarized in the following two sections (Amoudi, 1998):

2.2.4.1 Role of Sulfates on Chloride-induced Corrosion

When chloride and sulfate ions penetrate the concrete cover from external sources, chloride ions penetrate concrete at a faster rate than the sulfate ions, thereby inducing corrosion of the reinforcing steel. The delayed intrusion of sulfates will

exacerbate the corrosion rate due to the damaging effects of both chlorides and sulfates on the reinforcing steel (Al-Amoudi et al., 1994).

Additionally, it has been reported that the corrosion risk is likely to be significantly increased in circumstances where concrete is exposed to both chloride and sulfate salts (Al-Amoudi and Maslehuddin, 1993). Treadaway et al. (1987) indicated that reinforcement corrosion in the specimens admixed with sodium chloride plus sodium sulfate was higher compared to those specimens admixed with only sodium chloride (Dehwah et al., 2002; Al-Amoudi and Maslehuddin 1993; Al-Amoudi et al., 1994, 1992), because when both chloride and sulfate ions are present, C_3A reacts preferentially with sulfate ions. As a result, the proportion of chloride ions bound is less than that when only chlorides salts are present (Dehwah et al., 2002). Morever, the ratio of (Cl^-/OH^-) is found to increase resulting in lower chloride binding capacity of cement (Al-Amoudi, 1992). This is believed to be the major cause of the accelerated corrosion observed in the Arabian Gulf countries (Al-Amoudi et al., 1994).

2.2.4.2 Role of Chlorides on Sulfate Attack

It is found by Kind (cited in Al-Amoudi, 1992) that the sulfate resistance of cements increases in the presence of high concentrations of chlorides.

A different view was expressed by van Aardt (cited in Al-Amoudi, 1992), who showed that no improvement in the sulfate resistance could be obtained due to the presence of chlorides in the sulfate solution. Contrary to Kind's and van Aardt's opinions, Locher (cited in Al-Amoudi, 1992) concluded that sulfate attack is exacerbated by the

addition of chlorides to the solution. This view was based on strength and expansion measurement on small prisms.

The above statements can be applied mostly for sodium sulfate attack, where the sulfate ions react with C_3A to form ettringite. This reaction needs diffusion of sulfate ions that can be affected by the diffusibility of the chloride ions. On the other hand, the magnesium sulfate attack is surficial and the presence of chlorides does not mitigate the attack on the calcium silicate hydrate.

2.2.5 Durability of Concrete in the Arabian Gulf Region

The Arabian Gulf region is considered as one of the most severe exposures in the world. Table 2.1 compares the chloride content of sea waters from various regions in the world. The Arabian Gulf seawater is more concentrated than all the other seas in the world thereby indicating its aggressivity. Moreover, the dissemination of sabkha terrains in all the Arabian Gulf States is well documented (Al-Amoudi, 2002). Sabkhas are known for their high salt content in the soil itself or in its brine. Table 2.2 reveals the aggressivity of sabkha whereby the chloride ion concentration is four to five times that in the sea water from the same vicinity (Al-Amoudi et al., 1992).

Table 2.1: Chloride content of various sea waters in parts per million (Al-Amoudi, 2002)

Major Constituents	Concentration (mg/l)								
	Black Sea	Marmara Sea	Mediterranean Sea	North Sea	Atlantic Ocean	Baltic Sea	Arabian Gulf	BRE** Exposure	Red Sea
Sodium (Na^+)	4900	8100	12400	12200	11100	2190	20700	9740	11350
Potassium (K^+)	230	340	500	500	400	70	730	400	1350
Calcium (Ca^{++})	236	328	371	430	480	50	760	400	531
Magnesium (Mg^{++})	640	1035	1500	1110	1210	260	2300	1200	1867
Chloride (Cl^-)	9500	14390	21270	16550	20000	3960	36900	18200	22660
Sulfate (SO_4^{--})	1362	2034	2596	2220	2180	580	5120	2600	3050
Bicarbonate (HCO_3^-)	217	182	158	*	*	*	128	*	152
Total dissolved salts (TDS)	17085	26409	38795	33060	35370	7110	66650	32540	40960
pH	7.4	7.9	8.0	*	*	*	8.3	*	6.3
Concentration ratio***	3.90	2.52	1.72	2.02	1.88	9.37	1.00	2.05	1.63

*** Not Reported**
**** Building Research Establishment, England**
***** Concentration of total dissolved solids compared to the Arabian Gulf sea water**

Table 2.2: Chemical analysis of sabkha brine and seawater (Al-Amoudi, 1995)

Ions	Sabkha brine*	Seawater*
Na^{+}	78.8	20.7
Mg^{++}	10.32	2.30
K^{+}	3.06	0.73
Ca^{++}	1.45	0.76
Sr^{++}	0.029	0.013
Cl^{-}	157.2	36.9
Br^{-}	0.49	0.121
$(SO_4)^{--}$	5.45	5.12
$(HCO_3)^{-}$	0.087	0.128
pH	6.9	8.3
Conductivity, micro siemens	208,000	46,200

* Concentration is in parts per thousand

The arid climate of the Arabian Gulf also has influences concrete deterioration due to the large fluctuations in daily and seasonal temperature and humidity conditions. The sudden and continuous variations in temperature and humidity may cause damage due to the thermal and mechanical stresses. The micro-cracks resulting from these damages, increase the permeability of concrete thereby accelerating the penetration of aggressive species into the concrete matrix and increasing the rate of reinforcement corrosion and sulfate attack (Al-Amoudi, 1995).

Another factor playing an important role in concrete deterioration is the salt crystallization at the concrete-soil level. In this zone, capillary suction of concrete is the main mechanism of water and salt transport (Irassar et al., 1996). The maximum driving force for crystallization is related to the super-saturation for crystals growing in solution.

However, the stresses generated on the pore walls depend on other factors, including the pore size, the energy of the interface between the pore wall and the crystal, and the yield stress or buckling strength of the crystal. Even when crystallization pressure is large, the stress existing in a single pore cannot cause failure because it acts on a small volume. For fracture to occur, the crystals must propagate through a region of the network large enough for the stress field to interact with the large flaws that control the strength (Scherer, 1999)

2.2.6 Blended Cements

Blended cements involve the addition of mineralogical admixtures to the parent Portland cement to enhance the properties of concrete through chemical reaction between

them and some of the hydration products of the parent cements. They are low cost natural materials or industrial by-products (Bye, 1999). They are classified as either pozzolanic or/and cementitious materials. Granulated blast furnace slag is a hydraulic cementitious binder in its own right but requires an alkaline medium to initiate its hydration, while the pozzolanic materials break down the silica or silica-alumina networks in the particles they contain thereby forming C-S-H when interacting with alkaline medium produced by the hydrating cement (Bye, 1999).

The basic pozzolanic reaction involves the severing of Si-O-Si and Si-O-Al bonds by hyroxyl ions. In the presence of an excess of calcium ions, derived from the calcium hydroxide produced by the hydrating cement, C-S-H and, by interaction with dissolved gypsum, calcium sulfoaluminate hydrates will be precipitated. Calcium hydroxide dissolution maintains the supply of the hydroxyl ions and calcium ions necessary; the overall reaction can be followed by at a later stage in the hydration of the cement-pozzolana combination by the consumption of the crystals at this phase formed in the earlier and more rapid hydration of the Portland Cement (Bye, 1999). The pozzolanic reaction is slow, so the rate of strength development and the heat of hydration associated with reaction are low (Mehta, 1987).

2.2.6.1 Silica Fume

Silica fume (SF) is a byproduct of the production of silicon or ferro-silicon alloys by reducing quartz in an electric furnace. Some of the silicon oxide is lost as a gas and is oxidized by the air, giving very finely particulate solid. The particles are spherical, typically around 100 nm in diameter, and consist largely of glass. The material formed in

making elementary silicon typically contains 94-98% SiO_2, but for that formed in making the alloys, 86-90% SiO_2 is more usual (Taylor, 1992). Silica fume is reported to be the best mineral admixture to improve the resistance against corrosion of reinforcing steel in concrete. Therefore, the use of this "expensive" blending material may result in making silica fume concrete as the most economical alternative (as compared with other blended cements), as documented in Table 2.3. However, the usage of silica fume may be associated with the following shortcomings (Al-Amoudi et al., 2001):

a. It requires proper and extended duration of water curing to avoid plastic shrinkage cracking, especially in the hot and arid environment of the Arabian Gulf.

b. It exhibits brittle type of failure with a tendency to lower ductility.

c. It is more vulnerable to spalling by fire attack. Its thermal conductivity is higher than the normal cement concrete; therefore, the buildup of vapor pressure when exposed to fire will spall the concrete.

d. Silica fume suffers from salt scaling, due to the small sizes of the pores, which results in high pressure buildup due to salt crystallization.

e. Silica fume concrete tends to have more water demand and quick slump loss.

f. Silica fume suffers from Mg-sulfate attack due to the reaction of the magnesium sulfate with the hydrated products of the cement.

Table 2.3: Cost of adding pozzolans to concrete in Saudi Arabia (Smith, 1998)

Mix Design	Mix Cost (SR/m^3)	Time to start of Corrosion (Days)	Cost/Year of Design Life (SR/Year)
OPC + 20% MS	Not recommended as prone to cracking		
OPC + 10%MS	250	380	0.66
OPC + 5% MS	220	240	0.92
OPC + 70% G B F Slag	620 (b)	250	2.48
OPC + 30% PFA	335 (b)	250	1.34
OPC with C_3A = 8%	180	100	1.8
SRC with C_3A = 2%	185	60	3.1
All mixes have total cementitious materials content of 390 kg/m^3. Cover to reinforcement = 50 mm			

2.2.6.2 Ground Granulated Blast Furnace Slag

Blast furnace slag (GGBFS) is a by-product of the manufacture of iron in a blast furnace. It results from the fusion of a limestone flux with ash from coke and the siliceous and aluminous residue remaining after reduction and separation of the iron from the ore. The operation of the blast furnace, and hence the production of both iron and slag, is a continuous rather than a batch process, with both materials being in the molten state. When the molten slag is subjected to either fine water jets maintained at high pressure and at high water/slag ratios, or to cold air/water jets, it cools rapidly into glassy granules with a consistent particle size range and chemical composition.

The product is dried and ground to cement fineness in conventional cement clinker grinding mills with no further additions. Immediately after granulation, blast furnace slag is a light brown color, however, after milling, it becomes very pale, almost white. Freshly made GGBFS concrete has a bluish tint due to the formation of complex iron sulphides, however, this color fades rapidly as the sulphides are oxidized (Technical Report No. 40, 1991).

Particles of GGBFS are irregular in shape and have a relative density of about 2.9, compared to 3.15 for Portland cement. Therefore, exchanging GGBFS for cement on an equal mass basis will increase the total volume of the cementitious materials in the mix.

The chemical composition of blast furnace slag may vary form source to source depending on the nature of the limestone flux and the blast furnace conditions. The major oxide components of slag are lime, magnesia, silica and alumina and if slowly cooled in air these would form an assemblage of crystalline minerals. However, the rapid quenching in water to produce granulated slag results in the formation of a slag glass consisting of a

network of calcium, silicon, aluminum and magnesium ions in disordered combination with oxygen. Minor components, such as sodium, potassium and titanium, are also integral parts of this structure and further modify or disorder the glass network. Blast furnace slag also contains small quantities of sulphides, present usually as calcium sulphide. However, in the presence of air, they decompose to form hydrogen sulphide (Technical Report No. 40, 1991). In addition to this glass and depending upon the slag composition and quenching conditions, small quantities of crystalline phases may also be present.

GGBFS reacts with water, increasing the pH, generating heat and developing a particle-to-particle cementitious bond similar to Portland cement. This intrinsic hydraulicity distinguishes GGBFS from pozzolans. The intrinsic reaction of GGBFS is very slow compared to Portland cement, therefore, for practical purposes, the hydraulicity is activated by the hydroxides and sulfates present in Portland cement. These activators react with the GGBFS disturbing the structure of the glass; releasing reaction products for hydrate formation and continuation of the hydration process (Technical Report No. 40, 1991). Apart from the primary reactions between OPC and water, and GGBFS and water, secondary reactions also occur. These occur between the reaction products of the OPC with GGBFS, and the reaction products of OPC with the reaction products of GGBFS. The later reaction may be considered pozzolanic. The hydrates formed in these combinations are similar to those produced in Portland cement, i.e., calcium silicate and aluminate hydrates (Neville, 1995).

2.2.6.3 Fly Ash

Fly ashes, also known as pulverized-Fuel ashes (PFA) are materials extracted by electrostatic and mechanical means from the flue gases of power-station furnaces fired with pulverized bituminous coal (Technical Report No. 40, 1991). PFA has high glassy silica but low lime content and thus will not react on its own with water, but needs a source of calcium hydroxide before hydrates can be formed (i.e., it is pozzolanic rather than hydraulic). Ordinary Portland cement is usually used to provide the necessary calcium hydroxide.

The suitability of PFA depends on a number of factors, two important ones being the fineness to ensure reactivity and low non-reactive carbon content. A further requirement is that the water demand of a standard mortar mix Portland/PFA cement shall not exceed 95% of that for the Portland cement alone, which partly compensates for the lower cementing efficiency of PFA at early ages (Harrison and Spooner, 1996; Technical Report No. 40, 1991).

The PFA produced at power stations by the combustion of bituminous coal, consists of carbonaceous matter, and a mixture of various minerals. At power stations, the coal is pulverized in grinding mills and after this it is blown into the boiler at high speed. It burns at a temperature exceeding 1500º C, which is above the melting point of most metals present; therefore, the minerals undergo various physical changes. Most of the ash particles are carried through the furnace with the flue gases and are then extracted by being passed through a cyclone collector, which removes most of the coarser particles, and then passed over an electrostatic precipitator in series to remove the smaller particles. The fine ash precipitated from the exhaust gases is known as pulverized fuel ash (PFA) in

the United Kingdom and some other European countries, and as fly ash (FA) in USA and many other parts of the world, including the Arabian Gulf region. The properties of PFA will vary depending on the type of coal burnt and the furnace conditions, thus the PFA will vary from plant to plant and will also vary in one plant over a period of time. PFA is relatively chemically consistent but less than the GGBS (Technical Report No. 40, 1991).

PFA consists principally of aluminosulfate glass containing some iron, calcium, magnesium, and alkali metals in the glass structure. The ash particles are coated with calcium sulfate or potassium sulfate. PFA will also contain some residual-burnt coal, which appears as coarse, porous particles (Technical Report No. 40, 1991).

PFA particles are predominantly spherical in shape with about 5% by mass being hollow cenospheres, however, due to the unburnt coal, there will be some irregularly-shaped particles. This spherical shape is able to lubricate a concrete mix and thus increase the workability; this can lead to a smaller requirement of water for a specified workability. The relative density of PFA is between 2.0 and 2.3, being influenced by the amount of porous carbon particles as compared with the relative density of Portland cement is about 3.15. This means that if PFA is used to replace Portland cement on an equal mass basis, the total volume of cementitious materials in a mix will rise.

The color of PFA is usually grey but will be darkened by either the quantity of residual carbon or by its iron content. A PFA with high carbon content may be very dark in color; this means that the color of the ash may form part of the quality control of the PFA (Technical Report No. 40, 1991).

The principal reaction involving PFA in the pozzolanic reaction occurs between the glassy silica phase of PFA and the calcium hydroxide produced during the hydration of cement to produce more binding calcium silicate hydrate. The supplementary

pozzolanic materials bring certain changes in the chemical environment of concrete and bring about a very significant change in the physical structure of the hardened cement paste (Algahtani et al., 1994).

It is interesting to note that PFA has been observed to increase the measured Cl^-/OH^- ratio in concrete with a given chloride ion content get increasing the risk of reinforcement corrosion. However, it has been suggested that this increase is offset by the distinct improvement in the physical characteristics of the cement matrix and substantial reduced permeability of PFA blended cement concrete to chloride ingress, thereby reducing the corrosion risk (Rasheeduzzafar and Hussain, 1993).

2.2.6.4 Role of Blended Cements on Concrete Durability

Concern about the poor durability of OPC-based concretes in recent years has been reflected by the increase in the use of so-called cement `blends` incorporating a range of pozzolanic materials, including PFA, GGBS and silica fume. Pozzolans and slag can play a useful role in enhancing the properties of hydraulic cement concrete. These blended cements, therefore, are being projected as potential materials for usage in harsh environments in general and in the Arabian Gulf States in particular (Hussain and Rasheeduzzafar, 1993). The Middle East, and especially the Gulf region, is the prime example of truly extreme conditions. Here, the temperature of the concrete is high and the insulation is severe (Neville, 1998). Thus, the usage of such blends in concrete construction is becoming more universal (Haque and Kawamura, 1990; Neville, 1995), but is limited to regions where suitable supplies of these materials are available.

A well-cured blended cement mix can be expected to hydrate more slowly than an equivalent Portland cement concrete but for a longer period than a Portland cement, and will eventually have a lower permeability due to the extra cement paste produced. This will help increase the physical barrier afforded by the concrete. However, if proper curing is not achieved on site then the benefits of blended cements will not be achieved in practice (Parrott, 1991). In fresh state, lower rates of stiffening can be expected, which can be an advantage in hot weather but may delay finishing operations and, in winter, may require additional precautions in respect of increased formwork pressures or protection against freezing (Dewar, 1988). It reduces the expansion due to alkali-silica reaction, and minimizes the risk of cracking due to the reducing heat of hydration gradients (Rasheeduzzafar, 1992; Al-Saadoun et al., 1993).

The advantages of blended cements are twofold; firstly they offer the designer, the contractor and the ready-mixed concrete supplier new options for ordinary concreting purposes and also alternatives to solving particular problems. Many countries are actively encouraging the use of these products as cement replacements. This adoptive process is likely to continue since not only do these materials provide improvements to the concrete made with them in the fresh state, but more often in the hardened state. Moreover, they have an ecological contribution by reducing CO_2 emissions resulting from Portland cement manufacture (Malhotra and Mehta, 1997; Turner-Fairbank, 2002**).**

a) Role of Blended Cements on Reinforcement Corrosion

Although during the longer hydration period of cement blends, calcium hydroxide [$Ca(OH)_2$] present in the concrete is consumed, and thus the alkalinity of the cement paste

will decrease; this lower pH caused by a decrease in the $Ca(OH)_2$ content could additionally lead to a reduction in the chemical protection offered to the steel by the concrete (Harrison and Spooner, 1986). Blended cements can be expected to show superior performance in terms of corrosion-initiation time and reduced corrosion rate (Al-Saadoun et al., 1993; Hussain and Rasheeduzzafar, 1993; Rasheeduzzafar et al., 1992 and 1994). Cement blends also generally show lower chloride penetration. In these cements, the porosity was deemed to be reduced and pore size to be refined, which thus hinders the movement of aggressive substances, such as chloride ions.

The chloride content of Portland cement, SF and PFA is typically very low. However, GGBFS may have a significant chloride content if quenched with salt water. These internal "admixed" chlorides may be released into the free water during mixing but they become combined into the reaction products of the hydration process (ACI 201-2R, 1992). As a consequence, cement blends can have significantly lower free chloride ion content than equivalent OPC concretes with the same total chloride ion content. An important source of chloride ions is those arising in the environment.

These cements, while providing resistance against chemical and sulfate attack, also give better protection against chloride-induced reinforcement corrosion than sulfate resisting Portland cement due to the combining effect of the pozzolan additions with the calcium hydroxide produced during the hydration reaction (Page et al., 1981; Hussain and Rasheeduzzafar, 1993; Al-Gahtani et al., 1994; Rasheeduzzafar et al., 1992; Lea, 1983). Partial replacement of cement with PFA reduces the permeability to water and chloride ions, increases electrical resistivity and reduces unbound chlorides (Hussain and Rasheeduzzafar, 1994).

b) Role of Blended Cements on Sulfate Attack

The benefits of pozzolanic reaction in reducing sulfate attack could be categorized in the following scenario (Al-Amoudi, 1998):

- The consumption of $Ca(OH)_2$ reduces the formation of gypsum.
- The replacement of part of the cement by a pozzolanic material entails a reduction in all the aluminate-bearing phases, and as a result the formation of secondary ettringite will be mitigated.
- Since blended cements consume a significant proportion of $Ca(OH)_2$ produced by cement hydration and reduce the pH, ettringite becomes less expansive.
- The formation of secondary C-S-H produces a film or a coating on the alumina-rich and other reactive phases thereby hindering the formation of secondary ettringite.
- The formation of secondary C-S-H results in the densification of the hardened cement paste since it is deposited in the pores thereby making blended cements impermeable and, therefore, sulfate ions cannot easily penetrate through the concrete matrix.

The above statements agree greatly with the case of sodium sulfate attack. In case of magnesium sulfate attack, the magnesium sulfate ions attack directly the cementitious C-S-H and convert it to non-cementitious M-S-H (Al-Amoudi, 1998).

CHAPTER THREE

EXPERIMENTAL PROGRAM

In order to achieve the objectives of this research investigation, the following experimental program was conducted. Figures 3.1 and 3.2 detail the experimental program.

3.1 GEOTECHNICAL EXPERIMENTS

These experiments were carried out to characterize the sabkha and clay soils investigated in this study. Thereafter, the compressibility behavior of the sabkha-clay mixtures and the optimum dosage of clay to sabkha that improved the insulating behavior of the sabkha-clay mixtures were investigated. The dosage of clay was in the range of 0 to 8% by weight of the sabkha soil (i.e., 0, 2%, 5% and 8%).

3.1.1 Soil Materials Preparation

The sabkha soil, from Al-Qurrayah, eastern Saudi Arabia, was brought from all the layers above the groundwater table. The soil was homogenized in the Geotechnical

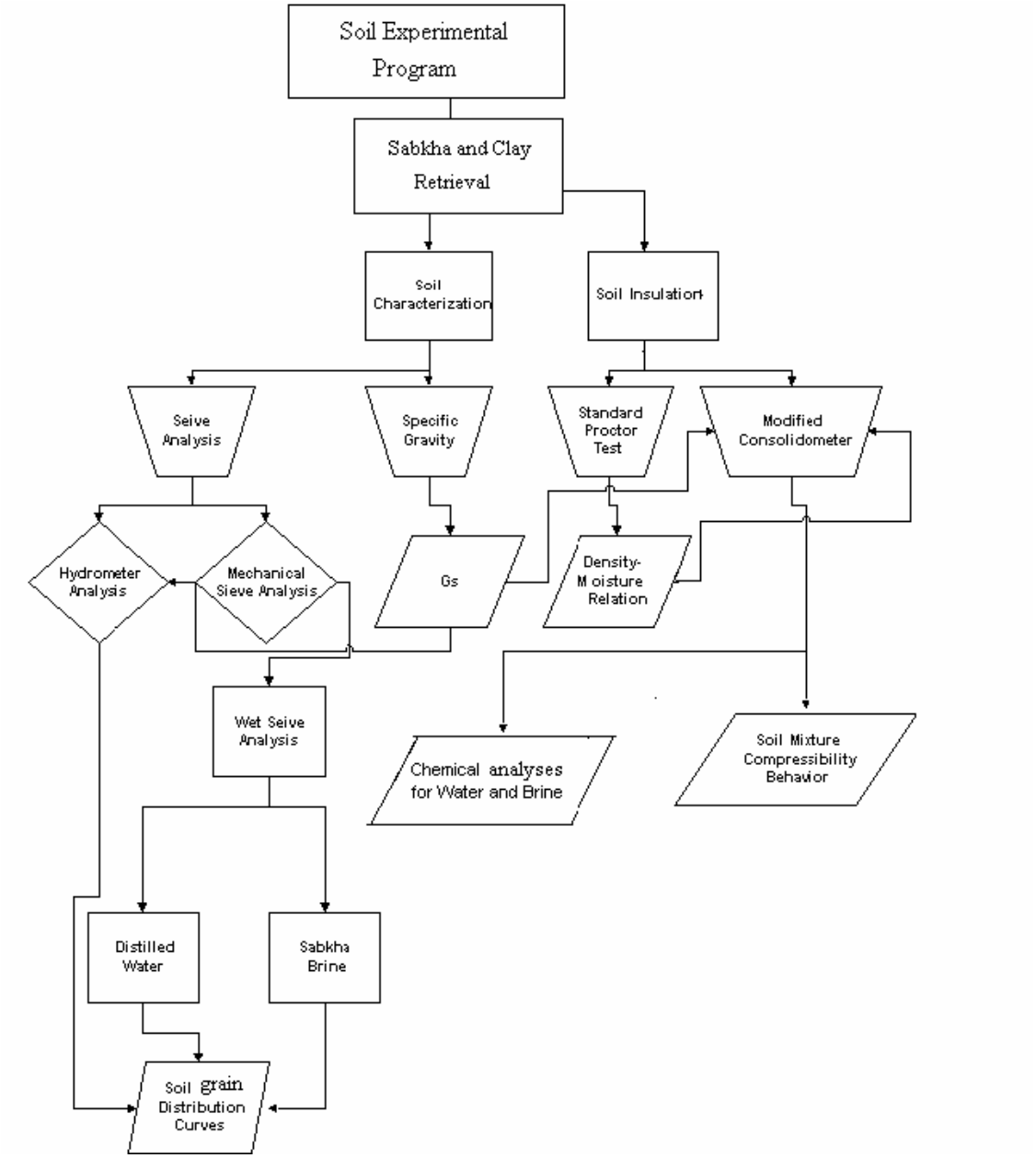

Figure 3.1: Schematic diagram for the soil experimental program

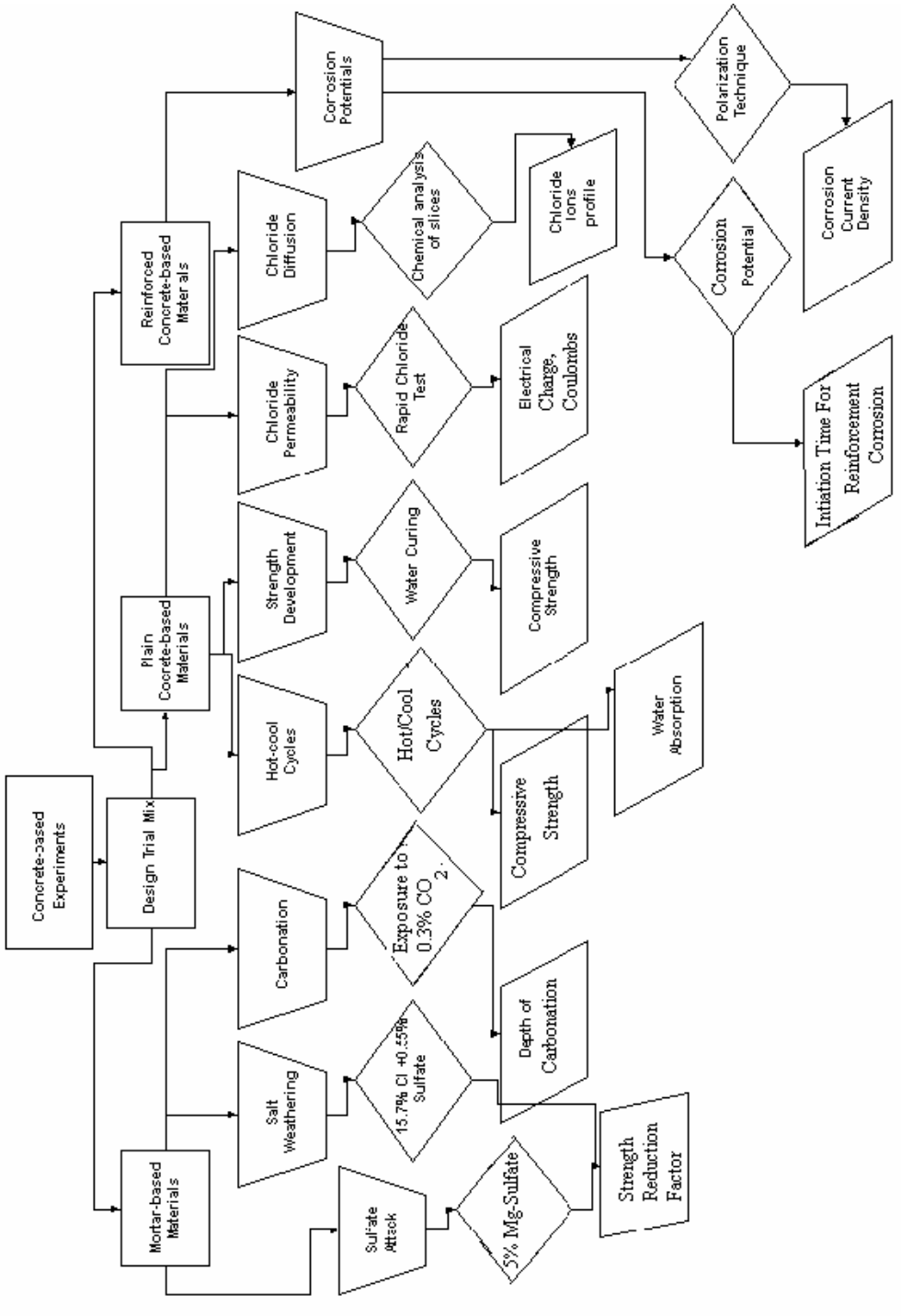

Figure 3.2: Schematic diagram for the concrete experimental program

Laboratory and then spread on plastic sheets to dry up aerially, and left for one month to ensure proper air-drying. Thereafter, the soil material was sieved to pass No. 4 sieve, and stored in dry plastic tanks to avoid contact with atmospheric humidity or external sources of moisture, which could alter the soil chemically or physically.

Sabkha brine was collected from the site and stored in well-sealed barrels, to maintain its initial chemical state.

The clay material was brought from Al-Qatif, and dried up aerially and then grinded to pass sieve No. 200. The grinding process was intended to ensure the breakdown of accumulations and lumps within the clay particles.

3.1.2 Characterization of Sabkha and Clay Soils

Primary geotechnical experiments were conducted to investigate the main characteristics of individual and mixed soil materials.

3.1.2.1 Grain Size Distribution

Grain size distribution is used in most soil classification methods. It can be obtained by using two techniques:

- Mechanical (sieve) analysis; and
- Hydrometer analysis.

Mechanical sieve analysis: Sample preparation for the grain size analysis was conducted according to ASTM D 421. Sieve analyses using both distilled water and sabkha brine were conducted in accordance with ASTM D 422. Sabkha brine was used to avoid dissolution of the salts crusting the soil particles, because the salt itself is part of the soil matrix. Its presence or absence will certainly affect the soil-water behavior of the sabkha strata.

For wet sieving, the sabkha soil was kept in distilled water, to ensure salt dissolution and breakdown of accumulation of the particles. Then, the soil was washed on sieve # 200 using distilled water, where the retained soil was oven-dried and mechanical sieving was performed. The mechanical analysis was accomplished by stacking the sieves, one on top of the other, pouring the soil sample into the top sieve on the stack, and shaking the sieves to allow the soil to fall down through the stack. The soil passing sieve # 200 was collected in a pan to be tested by hydrometer. The same procedure was done for wet sieving using the sabkha brine.

Hydrometer Analysis*:* The hydrometer analysis is based on Stokes' law, which gives the relationship among the velocity of fall of spheres in a fluid, the diameter of the sphere, the specific gravity of the sphere and the fluid, and the fluid viscosity.

According to ASTM D 422, a 50 grams of the oven-dried (70º C) soil passing sieve #200 was mixed with 125 ml of 4% $NaPO_3$ solution in a small evaporating dish and left to be soaked for some time. Then, the mixture was mixed in a dispersion cup and transferred to the sedimentation cylinder, which was agitated to avoid accumulation of soil particles

in the bottom of the cylinder. The readings were taken by 152H type hydrometer, and the grain size distribution was obtained according to the following equations:

$$\% \text{ Finer} = \frac{aR_c}{M_s} * 100\%$$

$$\text{Particle diameter, D} = \sqrt{\frac{30\eta}{980(G_s - G_w)}}\frac{L}{t}$$

$$\text{Where; } a = \frac{1.65G_s}{2.65(G_s - 1)};$$

G_s : specific gravity of soil particles;

G_w : specific gravity of water;

η : viscosity of water;

M_s : mass of original soil in soil-water suspension; and

R_c : grams of soil in suspension after some elapsed time t, where:

$R_c = R_{actual} - \text{zero correction} + C_T$;

C_T : temperature correction factor.

The zero correction was obtained from a control cylinder containing 125 ml of $NaPO_3$ solution as in the sedimentation cylinder, and then distilled water was added to it.

3.1.2.2 Specific Gravity of Soil Solids

According to Archimedes' principle, which states that a body submerged in water will displace a volume of water equal to its own volume, arises the principle of determination of the specific gravity of soil solids. The specific gravity is defined as the ratio of the density of soil solids to that of distilled water at 4ºC. Determining the mass of a known volume of water and then placing the soil solids in the same container and refilling it with the same volume of water can determine the volume of a known mass of soil solids. The specific gravity of the soil solids is used to compute the void ratio in the soil, which would be used in computation of the compressibility characteristics of the soil.

Three representative samples of each of the sabkha and clayey soils were tested according to ASTM D 854. In the deaeration process, both vacuum and heat were used to ensure absence of trapped air within the soil solids. For the sabkha soil, oven heating was raised up to 70ºC only to inhibit the transformation of gypsum-anhydrite phases.

3.1.2.3 Atterberg Limits

In the year 1911, the Swedish agricultural scientist A. Atterberg had proposed the following classification limits:

- Liquid limit: It is the moisture content below which the soil behaves as a plastic material. At this moisture content, the soil is on the verge of becoming a viscous fluid.
- Plastic limit: It is the moisture content below which the soil is non-plastic.

- Shrinkage limit: It is the moisture content below which no further soil volume reduction occurs.

The liquid and plastic limits are used universally for soil identification and classification and for strength correlation. These classification methods are applicable for cohesive soils.

Due to its lack of cohesion, this test was not conducted on the sabkha soil. Only the clay soil was applicable for testing.

An amount of about 250 g of air-dried clay was thoroughly mixed with water in a mixer to achieve homogeneity of the mixture, and then the tests were conducted according to ASTM D 4318.

3.1.3 Insulation of Sabkha Soil

The benefit of mixing sabkha soil with clayey soils to achieve good insulation for soil liners was studied through assessing the compressibility of the sabkha-clay mixtures and penetrability of various ionic species in the sabkha brine through these mixtures. The principal objective of this part of the investigation was to evaluate the role of clay addition on the insulation properties of sabkha soil. The tests conducted to achieve this objective were as follows:

3.1.3.1 Standard Proctor Test

In order to obtain the dry density of the soil used in the compressibility tests, the moisture-density tests were carried out. Standard Proctor test (ASTM D 698) was conducted on the various mixtures needed in the study. The test was done using distilled water and sabkha brine as lubricants.

3.1.3.2 Modified Consolidometer

The standard odometer was modified to allow the liquid (i.e., distilled water or sabkha brine) used in the test to percolate at a constant head. Figure 3.3 shows a schematic diagram of the modified odometer. Two holes were made below the testing specimen with drainage tubes to allow the liquid to percolate through the consolidating specimen. Distilled water and sabkha brine were used in this test in order to assess the collapse potential (Amoudi et al., 1995). The usage of distilled water was intended to assess salt dissolution, while the usage of sabkha brine as the percolating fluid was intended to assess the penetrability of ionic species through sabkha-clay mixtures.

The dry densities and optimum moisture contents of the soil mixtures were determined from the standard Proctor tests, where distilled water and sabkha brine were used to obtain the soil-moisture relationship. The soil mixtures were firstly subjected to free swelling conditions to assess the swelling behavior of different mixtures, then loaded, unloaded and reloaded according to the general test procedures of ASTM D 2435. Each loading cycle was conducted for a duration of 24 hours.

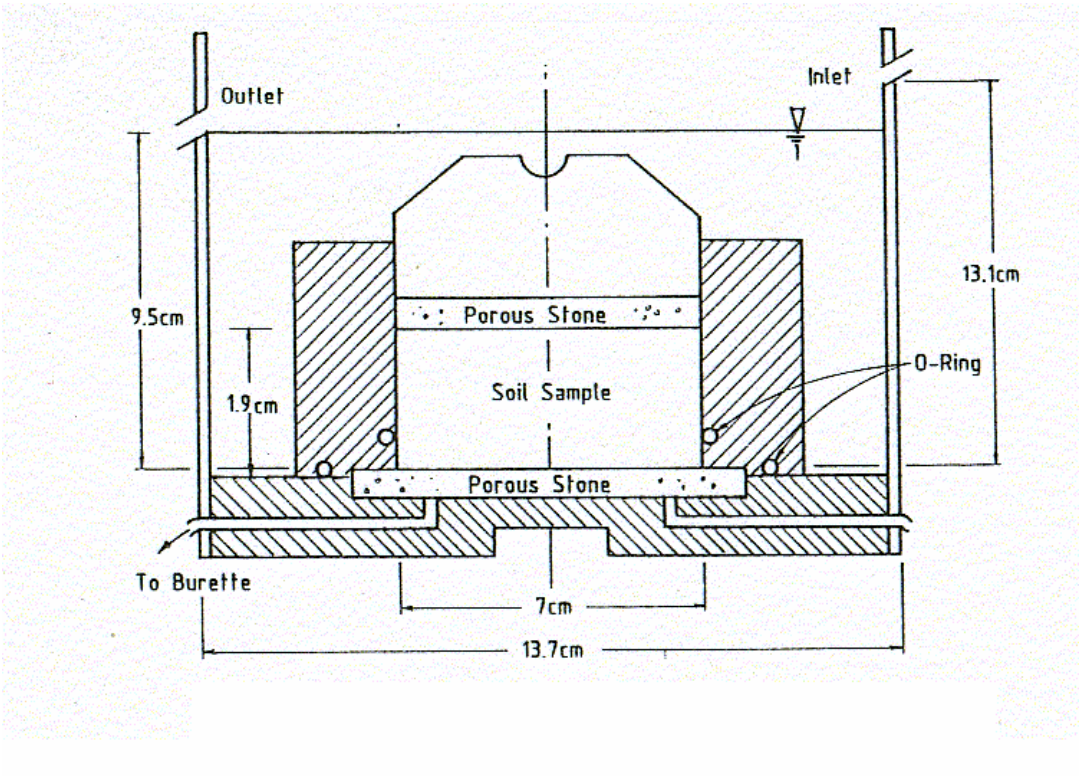

Figure 3.3: Schematic diagram of a modified odometer apparatus (Al-Amoudi et al., 1995)

3.1.3.2 Chemical Analysis

Chemical analyses were carried out through studying the chemistry of the water samples leached from the soil mixtures used in the consolidometer test. Samples of water and brine percolating the consolidating soil were chemically analyzed to get a clear view about the insulation properties due to the addition of clayey soil to the consolidating sabkha in order to assess the leaching of harmful salts. The samples taken were analyzed to determine the chlorides and sulfates in these percolating fluids and the trace metals trapped by the soil.

Ion chromatography technique was used for the determination of the total dissolved salts (TDS), chlorides and sulfates. The filtered trace metals were obtained in reference to the brine used in percolation by using matrix subtraction technique.

3.2 CONCRETE-BASED EXPERIMENTS

In order to have a comprehensive picture of the soil-structure interaction in the sabkha environment, another experimental program was conducted to study the durability performance of blended cements in the aggressive sabkha medium.

3.2.1 Cementitious Materials and Exposure Media

The soil-structure interaction was studied to assess the role of blended cements in improving the durability of reinforced concrete subjected in aggressive sabkha exposures. The dominant salts present in sabkha that are responsible for concrete deterioration are chlorides and sulfates. Table 2.2 shows that the most prevalent ions in the sabkha brine

are chlorides, sulfates, sodium and magnesium ions. The solutions made for the exposure condition for this investigation are:

- **17.5% Cl^- + 0.55% SO_4^{--}**: Sodium chloride was used to provide the chloride ions, while sodium and magnesium sulfates were used to provide the sulfate ions, each of them provided 50% of the sulfates required. This solution was used in detecting the time to initiation of corrosion and the corrosion current density for the reinforcing bars embedded in concrete, measurement of the reduction in compressive strength and determination of chloride diffusion in concrete.
- **5% NaCl**: Sodium chloride was used to provide the chloride ions in this solution which was used to assess the initiation of time of corrosion and the corrosion current density for the steel bars embedded in concrete.
- **5% SO_4^{--}**: Magnesium sulfate was used to provide the sulfate ions to assess the Mg-sulfate attack in the mortar specimens.

The following plain and blended cements were used in this investigation:

- Ordinary Portland (Type I) cement
- Sulfate resisting Portland (Type V) cement
- Densified silica fume (7.5% replacement by weight of Type I cement)
- Undensified silica fume (7.5% replacement by weight of Type I cement)
- Fly ash (30% replacement by weight of Type I cement)
- A highly active pulverized fly ash, known by the trade name "Superpozz®" (10% replacement by weight of Type I cement)
- Blast furnace slag (70% replacement by weight of Type I cement)

All the blended cement replacements were used as a percentage by weight of Type I cement. Chemical analysis of the parent cements and the blending materials is shown in Tables 3.1 through 3.4.

Concrete mix design trials were conducted to maintain a slump of 50 to 75 mm for an effective water to binder (w/b) ratio of 0.45 and a cementitious materials content of 370 kg/m^3.

3.2.2 Mortar-based Experiments

3.2.2.1 Sulfate Attack

Mortar specimens of 50*50*50 mm cubes were cast using plain and blended cements. These specimens were cured in water for 14 days. Thereafter, they were air dried in the laboratory for one day and then exposed to 5% magnesium sulfate solution. The effect of sulfate ions on plain and blended cements was assessed by determining the strength deterioration factor (SDF) after 3, 6 and 9 months of exposure. This factor was obtained as follows:

SDF = (compressive strength of water cured specimens – compressive strength of specimens in the sulfate solution)/ compressive strength of water-cured specimen

The strength values of the mortar specimens were obtained according to ASTM C 109.

Table 3.1: Properties of densified and undensified silica fume

Property	Value		ASTM C 1240 Requirements
	Densified SF	Undensified SF	
Moisture content, %	1.19	1.35	3.0 max.
Loss on ignition, %	2.21	1.62	6.0 max.
SiO_2, %	91.5	98.0	85 min.
Fe_2O_3, %	1.76	2.73	--
Al_2O_3, %	0.56	0.70	--
CaO, %	0.76	0.12	--
MgO, %	1.30	0.67	--
Na_2O, %	0.43	0.39	--
K_2O, %	0.78	0.90	--
SO_3, %	0.55	--	--
Material retained on #325 sieve, %	1.54	2.01	10 max.
Accelerated pozzolanic activity index, % (7 days)	91.0	98	85 (7 days)
Specific surface area, m^2/g	--	16.7	
Shrinkage (Type I cement after 28 days), %	0.069	0.069	--
Shrinkage (Type I +silica fume cement after 28 days), %	0.084	0.099	--
Increase over control, %	0.015	0.030	0.1 max.
Sulfate-resistance expansion (6 months), %	0.028	0.048	0.05 max. (High resistance)

Table 3.2: Properties of fly ash

Property	Value
Moisture content, %	<0.1
Loss on ignition, %	0.8
SiO_2, %	52.8
Fe_2O_3, %	3.5
Al_2O_3, %	34.3
CaO, %	4.4
MgO, %	1.1
Na_2O, %	0.4
K_2O, %	0.5
P_2O_5, %	0.3
SO_3, %	0.1
Material retained on #325 sieve, %	9.5
Water requirement, % of control	90
Reactivity, MPa	10.0

Table 3.3: Properties of superpozz®

Property	Value
Moisture content, %	<0.2
Loss on ignition, %	0.4
SiO_2, %	53.5
Fe_2O_3, %	3.6
Al_2O_3, %	34.3
CaO, %	4.4
MgO, %	1.0

Table 3.4: Chemical composition of cement and BFS materials

Constituent (Weight %)	Type V Cement	Type I Cement	Blast Furnace Slag
SiO_2	22.00	20.52	27.7
Al_2O_3	4.08	5.64	12.8
Fe_2O_3	4.24	3.80	1.2
CaO	64.07	64.35	44.0
MgO	2.21	2.11	8.8
SO_3	1.96	2.10	3.1
Loss on ignition	0.80	0.70	0.9
K_2O	0.31	0.36	0.1
Na_2O	0.21	0.19	0.4
Na_2O equivalent	0.41	0.43	0.5
C_3S	54.57	56.70	-
C_2S	21.75	16.05	-
C_3A	3.50	8.52	-
C_4AF	12.90	11.56	-

3.2.2.2 Salt Weathering

Mortar specimens of 50*50*50 mm cubes were cast using plain and blended cements. These specimens were cured in water for 14 days. They were air dried in the laboratory for one day and thereafter exposed to wet-dry cycles in a sabkha brine solution (15.7% Cl^- + 0.55% SO_4^{2-}). The specimens were wetted for 8 hours and dried for 16 hours in the laboratory environment (23± 3°C). The strength deterioration factor was assessed in a way similar to the specimens exposed to the sulfate solution after 3, 6 and 9 months of exposure.

3.2.2.3 Carbonation

Cylindrical mortar specimens, 37.5 mm in diameter and 75 mm high, were cast and thereafter water-cured for 14 days. These specimens were thereafter air-dried for extra 14 days. They were then placed in a carbonation chamber. The concentration of carbon dioxide in the chamber was maintained at 0.3% through a regulator. The carbonation depth was determined using the phenolphthalein indicator. The cylindrical specimens were cut from the center laterally and the phenolphthalein was sprayed in the inner cut surfaces, and the depth of the carbonated layers was measured.

All the specimens were tested after three, six and nine months of exposure to the accelerated carbonation environment.

3.2.3 Plain Concrete-based Materials

3.2.3.1 Development of Compressive Strength

The development of compressive strength in plain and blended cement concrete specimens was determined on cylindrical concrete specimens of 76 mm in diameter and 152 mm high (3*6 inch). The concrete specimens were cured in water for a period of six months. The compressive strength was determined at different intervals (i.e., 7, 14, 28, 90, and 180 days) according to ASTM C 39-86.

3.2.3.2 Heat-cool Cycles Test

Plain and blended cement concrete specimens, 76 mm in diameter and 152 mm high, were cast and water-cured for 14 days. These specimens were then air-dried for extra 14 days. Thereafter, the concrete specimens were subjected to alternate heat/cool cycles. Each hot-cool cycle composed of 2 hours of heating from the laboratory temperature (23± 3°C) to 70ºC, followed by 6 hours of constant heating at 70ºC, then 2 hours of cooling from 70ºC to the laboratory temperature and followed by constant cooling at the laboratory temperature for 14 hours. After 0, 90 and 180 cycles, the absorption (according to ASTM C 642) and compressive strength (according to ASTM C 39) of these specimens were determined.

3.2.3.3 Chloride Diffusion

Plain and blended cement concrete specimens, 76 mm in diameter and 152 mm high, were cast and then water-cured for 28 days. Thereafter, all the surfaces of the specimens were epoxy-coated except the top surface where the top inch of the concrete was cut off to exclude the weak zone in the concrete due to molding. The specimens were then immersed in a sabkha solution with 15.7% chlorides and 0.55% sulfates. After nine months of exposure, the concrete specimens were sliced laterally every 12.5 mm (0.5 inch) and each slice was crushed and grinded to powder passing sieve #100, the chloride concentration was determined according to ASTM C 1218.

3.2.3.4 Chloride Permeability

Plain and blended cement concrete specimens, 76 mm in diameter and 152 mm high, were cast and cured under water till the time of test. The chloride permeability test was performed after 28, 90 and 180 days according to ASTM C 1202 (AASHTO T-277).

3.2.4 Reinforced Concrete Specimens

Reinforced plain and blended cement concrete specimens, 76 mm in diameter and 152 mm high, were cast and then water cured for 14 days. Prior to casting, the reinforcing steel bars were coated with epoxy at the first lower 25 mm (one inch) and also at the concrete interface to avoid crevice corrosion. After this curing period, they were exposed to either 5% sodium chloride solution or 15.7% chlorides plus 0.55% sulfate solution (similar to eastern Saudi sabkhas), and the reinforced concrete specimens were immersed

to their two-thirds height in the solutions. The effect of chloride and chloride plus sulfate solutions on reinforcement corrosion was evaluated by measuring the corrosion potentials and corrosion current density. The time to initiation of reinforcement corrosion was detected through the use of the half-cell potential. The threshold value, which defines the time of initiation of corrosion, is –270 mV SCE. The corrosion potentials were measured every two weeks according to ASTM C 876.

The corrosion current density was determined using the linear polarization resistance measurement technique. In order to obtain an estimate of the current, it is necessary to shift the potential away from the equilibrium and measure the resultant net current and extrapolate the data to the equilibrium potential. The concrete specimen containing a steel electrode is held at a constant electrochemical potential with respect to the reference calomel electrode. The current flowing between the working electrode and the counter electrode is then measured. The relationship between the applied potential and the current is measured and the slope of this curve gives the resistance to polarization. The corrosion current density is then measured using the Stern and Geary formula:

$$I_{corr} = B/R_P$$

I_{corr} = corrosion current density, $\mu A/cm^2$

R_P = polarization resistance, $Ohms.cm^2$

$$B = (\beta a * \beta c)/2.3(\beta a + \beta c)$$

Where βa and βc are the anodic and cathodic Tafel constants, which are obtained by constructing a Tafel plot. A value of B equal to 52 for steel in the passive condition and equal to 26 for steel in the active condition are normally used.

CHAPTER FOUR

RESULTS AND DISCUSSION

4.1 SOIL PROPERTIES

4.1.1 Soil Characterization

The sabkha and clay soils used in the experimental program were characterized and classified according to the primary geotechnical tests. The results of tests conducted on the soil are discussed in the following subsections.

SPECIFIC GRAVITY

Three representative samples of each of the sabkha and clay soils used in this research were tested to obtain their average specific gravity according to ASTM D 854. Both vacuum and heat treatments were used to remove entrapped air from the soil samples; with extended deaeration process for the samples containing clay portions, where the removal of air adhering to the clay particles needs a continuous process of about 3 to 6 hours. The results obtained from this test are summarized in Table 4.1. These values were used in the hydrometer analysis and consolidation calculations.

Table 4.1: Specific gravity of soil mixtures

Soil Mixture	Specific Gravity
Sabkha	2.67
Clay	3.27
Sabkha + 2% Clay Mixture	2.76
Sabkha + 5% Clay Mixture	2.78
Sabkha + 8% Clay Mixture	2.83

The average specific gravity for the sabkha is marginally less than the values reported in an earlier study (Al-Amoudi, et al., 1991).

GRAIN-SIZE DISTRIBUTION

The grain-size distribution curves were plotted based on the results obtained from sieve and hydrometer analyses. The wet sieve analysis was conducted twice for the sabkha soil, firstly by using the sabkha brine to prevent the dissolution of salts, and secondly by the use of distilled water, according to ASTM D 422. Thereafter, the soil passing sieve No. 200 for the wet sieving using distilled water was collected and further analyzed using hydrometer.

Sieve Analysis: Table 4.2 summarizes the sieve analysis of sabkha soil conducted using sabkha brine. Figure 4.1 displays the wet sieve analysis results for sabkha soil using sabkha brine. From the data in Figure 4.1, the coefficient of uniformity (C_U) is found to be 3.2 and the coefficient of curvature (C_C) is 0.88.

The soil portion passing sieve No. 200 was slightly more than 3%. Therefore, there is no need for further analysis using the hydrometer.

In the second approach, distilled water was used in wet sieving. The grain size distribution by this method is summarized in Table 4.3, while the grain-size distribution curve is plotted in Figure 4.2.

From the grain-size distribution curve in Figure 4.2, it is obvious that the soil passing sieve No. 200 is more than 20%. Therefore, unless the hydrometer analysis was

Table 4.2: Wet sieve analysis for sabkha soil using sabkha brine

Sieve No.	Sieve Opening, mm	% Passing
10	2.000	95.8
20	0.850	88.9
30	0.600	83.5
40	0.425	53.7
60	0.250	29.4
100	0.150	10.6
140	0.106	5.1
200	0.075	3.1

Table 4.3: Wet sieve analysis of sabkha soil using distilled water

Sieve No.	Sieve Opening, mm	% Passing
10	2.000	100.0
20	0.850	99.8
30	0.600	98.5
40	0.425	91.7
60	0.250	68.1
100	0.150	45.5
140	0.106	33.3
200	0.075	27.5
Hydrometer	**Grain Size, µm**	**% Passing**
	0.053	24.1
	0.039	21.9
	0.020	19.2
	0.016	17.5
	0.011	15.4
	0.008	13.7
	0.006	11.5
	0.004	9.9
	0.003	8.8
	0.002	7.1
	0.001	4.9
	0.001	4.4
	0.001	3.3
	0.001	2.7

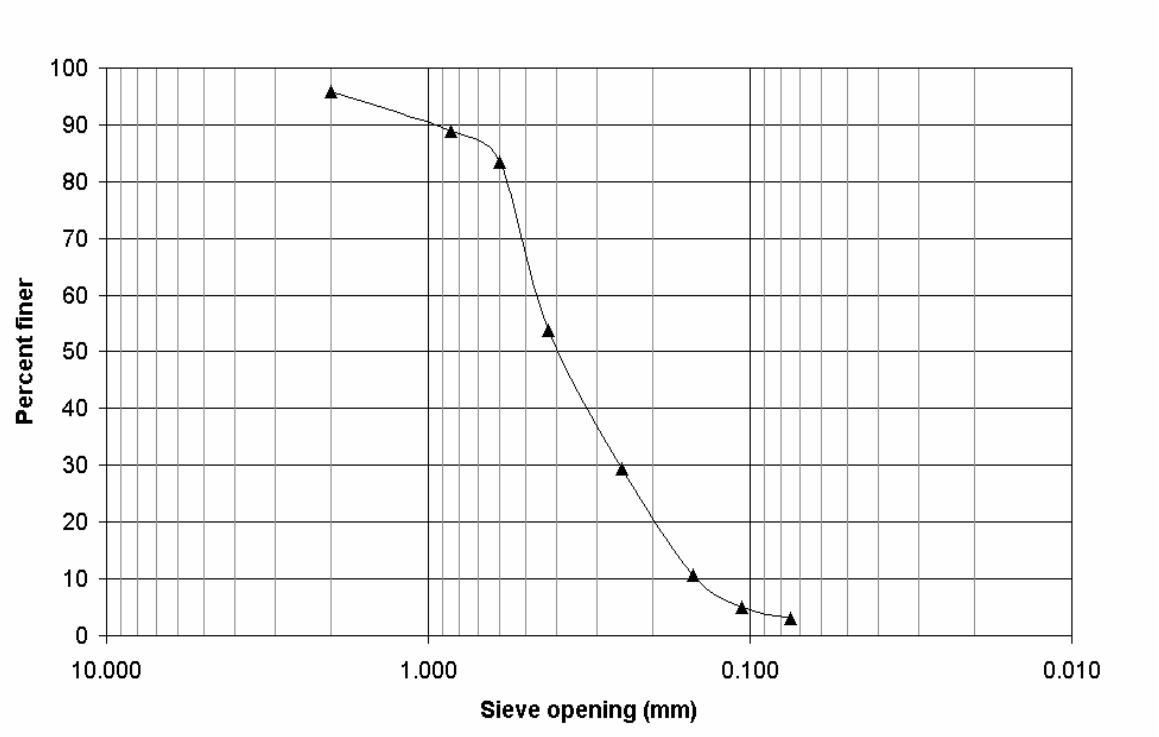

Figure 4.1: Wet sieve analysis for sabkha soil using sabkha brine

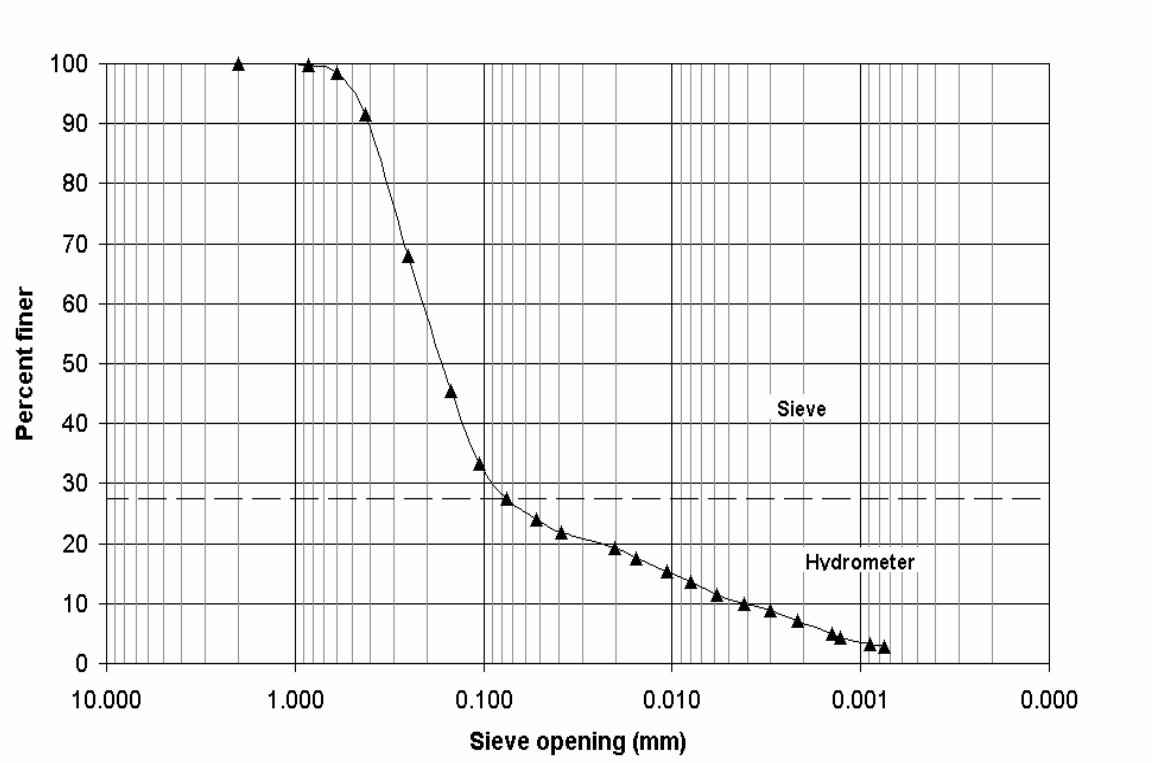

Figure 4.2: Sieve and hydrometer analyses for sabkha soil using distilled water

applied, C_U and C_C could not be determined for the reason that both these coefficients depend on the 10% fine particle diameter.

Hydrometer Analysis: The hydrometer analysis was conducted for the following two soil samples: For the sabkha soil portion that passed sieve No. 200 in the wet sieve using distilled water, and the clayey soil.

(a) Sabkha soil: The results of the hydrometer test are presented as a continuation for the distribution curve obtained from the sieve analysis, as shown in Figure 4.2. From the data therein, the coefficient of uniformity (C_U) is 48, and the coefficient of curvature (C_C) is 12.

(b) Clay soil: All the clay soils were analyzed by hydrometer. The test was conducted in exactly the same manner as for the sabkha soil. The grain size distribution curve for the clay soil is presented in Figure 4.3. The coefficient of uniformity and the coefficient of curvature could not be determined, as the grain size corresponding to 10% finer portion could not be detected.

As shown in Figure 4.4, the distribution curves for the same sabkha soil exhibited different distribution when distilled water or sabkha brine was used. The use of sabkha brine retains the original grain size of sabkha soil, as salts do not dissolve in the brine. When distilled water is used, the salt minerals, which act as cementing agents between the soil particles, get dissolved.

The data in Figure 4.4 indicate that the grain-size curve based on wetting by sabkha brine was shifted to the left side of that based on wetting by distilled water indicating the more coarseness of the former curve.

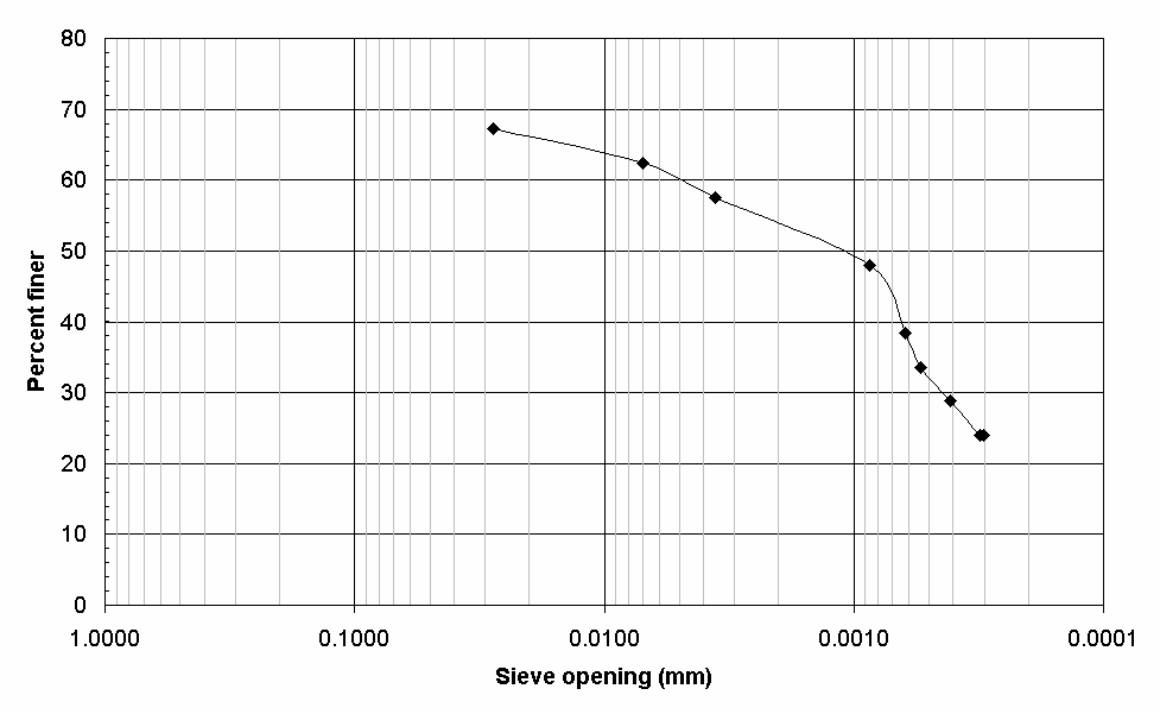

Figure 4.3: Grain size distribution for clayey soil

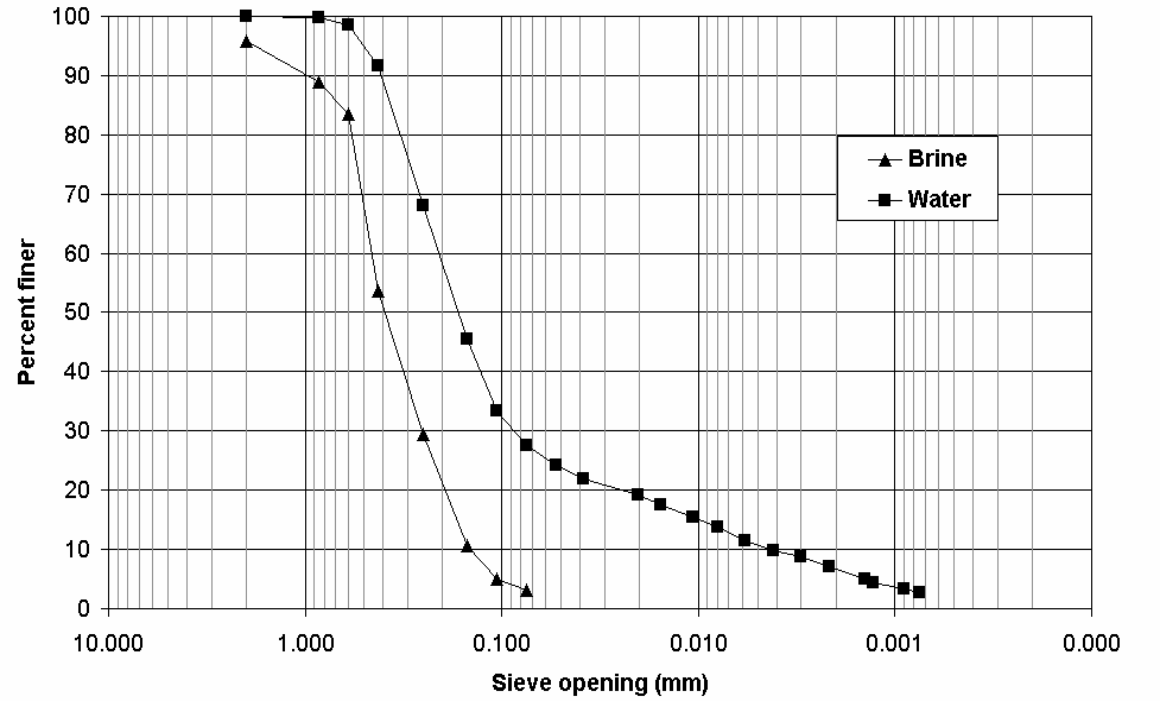

Figure 4.4: Grain size distribution for sabkha soil materials

Table 4.4: Grain size distribution parameters for sabkha soil

Soil (Wetting Liquid)	Coefficient of Uniformity	Coefficient of Curvature
Sabkha soil (distilled water)	0.877	11.99
Sabkha soil (brine)	3.17	6.02

ATTERBERG LIMITS

The sabkha soil used in this investigation was cohesionless and, as a result, the Atterberg limits could not be determined. These limits were determined for the clayey soil only. The results obtained for the clay soil are as follows:

- Liquid limit (L.L) = 140% (Figure 4.5)
- Plastic limit (P.L) = 44%
- Plasticity Index = L.L – P.L = 96%

SOIL CLASSIFICATION

The soil classification was based on the results obtained from the grain size analysis and Atterberg limits. The soil classification based on the Unified Soil Classification System (ASTM D 2487) and the American Association of State Transportation and Highway Officials (AASHTO) are as follows:

1. USCS Classification:

(a) For sabkha soil: There are two approaches to classify the sabkha soil based on the data obtained from either the wet sieve analysis using sabkha brine or the wet sieve analysis using distilled water.

1. The coefficient of uniformity and the coefficient of curvature are 3.2 and 0.88, respectively, and 3% soil was passing sieve # 200 by wet sieving using sabkha brine. Therefore, the sabkha soil sample can be classified as **poorly graded sand (SP).**

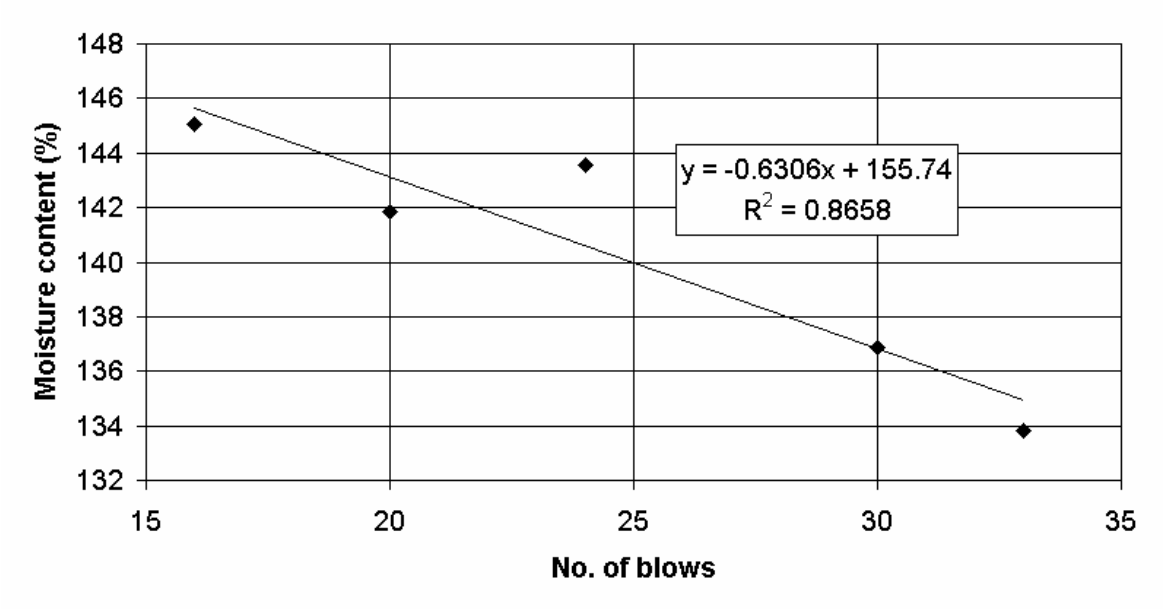

Figure 4.5: Liquid limit for clayey soil

2. The coefficient of uniformity and the coefficient of curvature are 48 and 12, respectively, and 27.5% soil was passing sieve # 200 by wet sieving using distilled water. Therefore, the sabkha soil can be classified as **silty clayey sand (SM-SC)**.

(b) For clayey soil: Since all the soil passed sieve # 200, and based on the liquid limit (140%) and the plasticity index (96%) and according to the requirements of the A-Line equation in the Casagrande's plasticity chart, the clay soil can be classified as **inorganic clay with high plasticity (MH)**.

2. AASTHO Classification:

(a) Sabkha soil: There are two approaches to classify the sabkha soil. These two paths are the data obtained from either the wet sieving using sabkha brine or the wet sieving by the use of distilled water.

1. For wet sieving by using sabkha brine, the soil passing sieves #10, #40 and #200 was 96, 54 and 3%, respectively. Therefore, the soil was classified as **fine sand (A-3).**
2. For wet sieving by using distilled water, the soil passing sieves #10, #40 and #200 was 100, 92 and 28%, respectively. Therefore, the soil was classified as **silty or clayey sand (A-2-4).**

(c) For clay soil: Since all the soil passes sieve # 200, the criteria of classification of the soil depend mainly on the Atterberg limits. As a result, the clay soil can be classified as **clayey soil (A-7-6 (20))**.

4.1.2 Sabkha as an Insulation Material

The main objective of the geotechnical part of this investigation was to assess the behavior of the sabkha-clay mixtures in terms of compressibility, collapse potential and percolation of salts in solution through them.

STANDARD PROCTOR TEST

The standard Proctor test was conducted on the soil-clay mixtures using distilled water and sabkha brine to determine the density-moisture relationship.

Standard Proctor Test using Distilled Water: The test was conducted for four mixtures (sabkha, sabkha plus 2% clay, sabkha plus 5% clay, and sabkha plus 8% clay), and the results obtained are summarized in Table 4.5 and plotted in Figure 4.6.

As depicted in Figure 4.6, an increase in the clay content in sabkha soil decreased marginally the maximum dry density ($\gamma_{d\ max}$) of the soil mixture. However, the optimum moisture content (w_{opt}) increased with increasing the clay content. The decrease in $\gamma_{d\ max}$ may be attributed to the fact that the clay particles adsorb water on their surfaces.

Standard Proctor Test using Sabkha Brine: The Proctor test was also conducted using sabkha brine and the test results are numerically summarized in Table 4.6 and depicted in Figure 4.7.

Table 4.5: Density-moisture relationship using distilled water

Clay, %	Maximum Dry Density (gm/cm^3)	Moisture Content (%)
0	1.8642	10.4
2	1.8640	11.0
5	1.8610	12.4
8	1.8500	13.2

Table 4.6: Density-moisture relationship using sabkha brine

Clay, %	Maximum Dry Density (gm/cm^3)	Moisture Content (%)
0	1.8640	9.9
2	1.8632	11.4
5	1.8348	12.5
8	1.8248	13.2

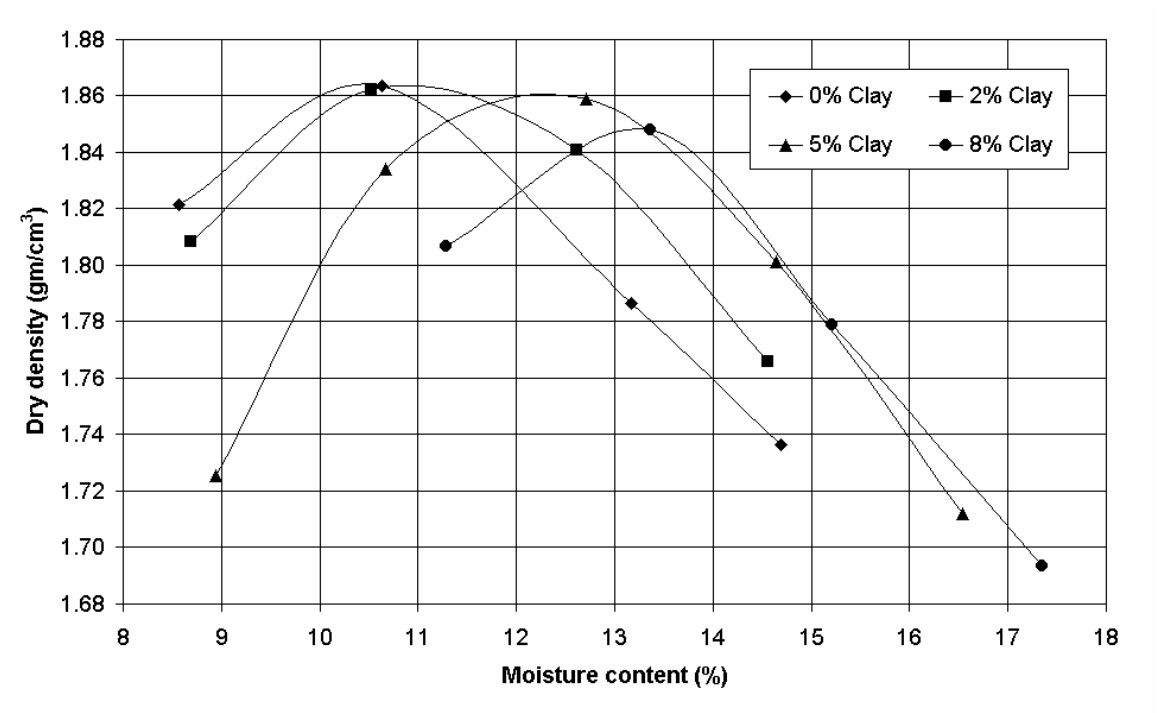

Figure 4.6: Density-moisture relationship using distilled water

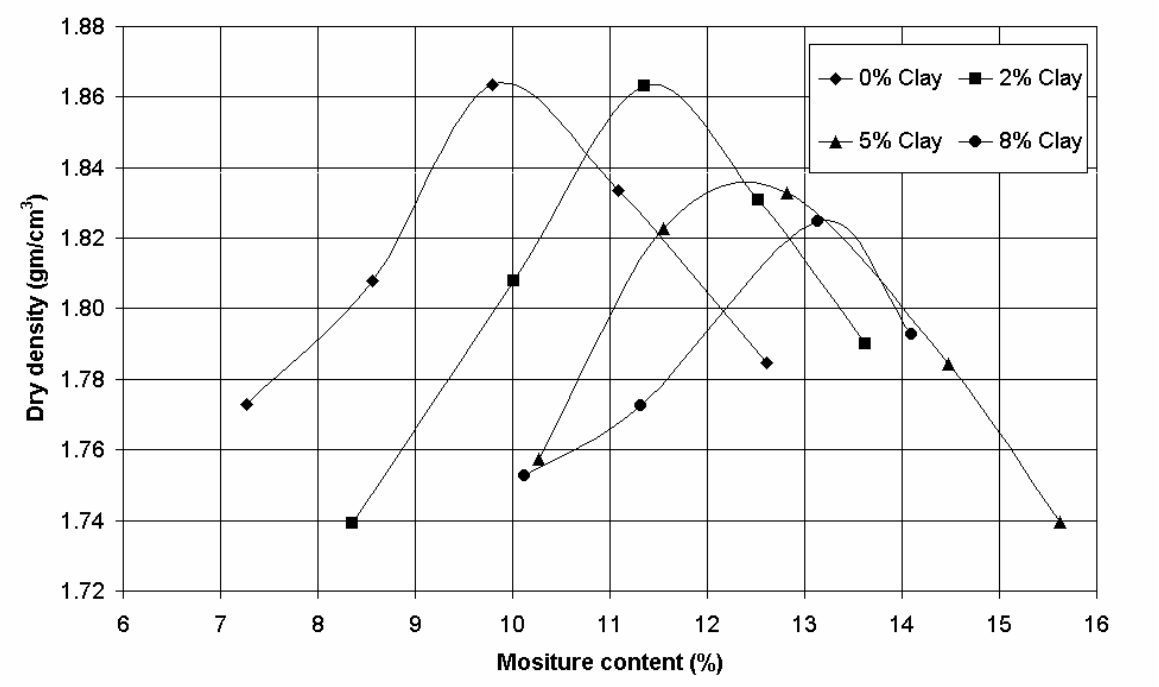

Figure 4.7: Density-moisture relationship using sabkha brine

The trend of data in Figure 4.7 is similar to that noted in the previous figure (Figure 4.6) whereby the increase in the clay addition reduced the $\gamma_{d\ max}$ and increased the w_{opt}.

The effect of distilled water and sabkha brine on $\gamma_{d\ max}$ and $w_{opt,}$ is compared in Table 4.7. No significant difference was noted between the two sets of results for sabkha soil and sabkha soil with 2% clay. However, for sabkha soil with 5% and 8% clay additions, there was some difference in terms of the maximum dry density only whereby the usage of sabkha brine reduced $\gamma_{d\ max}$. These differences could be ascribed to the electrolytic effect of the sabkha brine on the clay particles. Though both the distilled water and sabkha brine tend to cause flocculation of the clay particles resulting in expansion and swelling of the clay, the increase in the salt concentration in the sabkha brine raises the swelling pressures in the clay soil leading to higher volumetric change (Mitchell, 1993), thereby reducing the density.

4.1.2.1 Modified Consolidometer Tests

The results obtained from the density-moisture tests ($\gamma_{d\ max}$ and w_{opt}) for the various sabkha-clay mixtures were used to prepare the specimens for the consolidation tests that were conducted on two groups of specimens. Firstly, the test was conducted with distilled water as the percolating solution. In the other group, the test was conducted with sabkha brine.

Table 4.7: Summary of the density-moisture relationships determined using distilled water and sabkha brine

Clay, %	Dry density, gm/cm^3		Moisture content, %	
	Distilled water	Sabkha brine	Distilled water	Sabkha brine
0	1.8642	1.8640	10.4	9.9
2	1.8640	1.8632	11.0	11.4
5	1.8610	1.8348	12.4	12.5
8	1.8500	1.8248	13.2	13.2

MODIFIED CONSOLIDOMETER USING DISTILLED WATER

This test was conducted on four soil samples with different clay additions (i.e. 0%, 2%, 5% and 8%). The samples were left damp under a water head of 10 cm for free swelling for 24 hours and then the loads were applied as specified in ASTM D 2435.

(a) Sabkha soil: The sample was first prepared at $\gamma_{d\ max}$, then wetted with a water head of 10 cm for 24 hours. Thereafter, the sample was percolated with distilled water, and the percolated water was collected for chemical analysis. Then, the sample was subjected to loading, unloading, and reloading. The free deformation at first stage (seating load during the first 24 hours) is shown in Figure 4.8.

The data in Figure 4.8 indicate that the soil sample exhibited a settlement behavior (i.e., reduction in volume). The collapse behavior in terms of settlement could be ascribed to the dissolution of the salts by the percolating water. The dissolved salts formerly made barriers to the soil grains and enveloped them and, after dissolution those salts, experienced reduction in volume resulting in settlement. The large settlement observed happened at the time when the percolating fluid began to flow through the consolidated sample, which took place immediately after flooding.

The consolidation behavior of the sabkha sample is shown in Figure 4.9. The soil compression characteristics are summarized in Table 4.8. Due to the percolation of water through the consolidating specimen throughout the testing period, the salt content would reduce leaving only the silty clayey sand (i.e., mineral grains) without any soluble salts. The compression index (shown in Table 4.8) was found to be 0.16, indicating low compressibility soil (Mitchell, 1993). The swell index was 0.02, which is about 12.5% of the compression index. The ratio of the compression index to the swell index was about 8

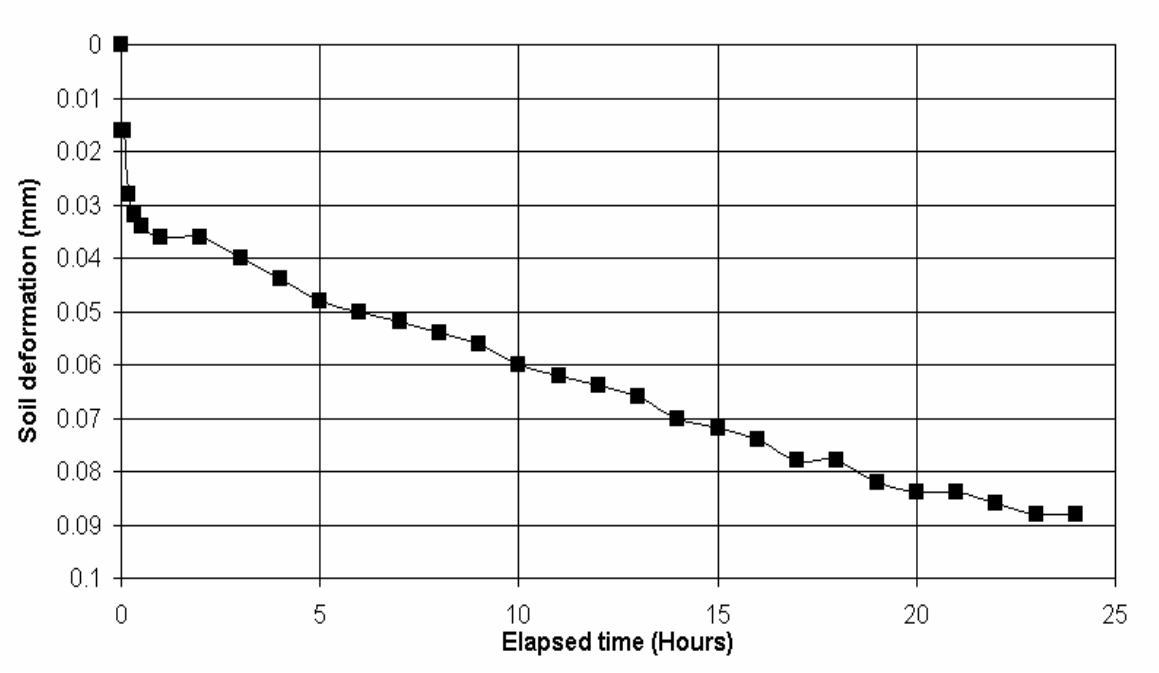

Figure 4.8: Free deformation of sabkha soil under seating load

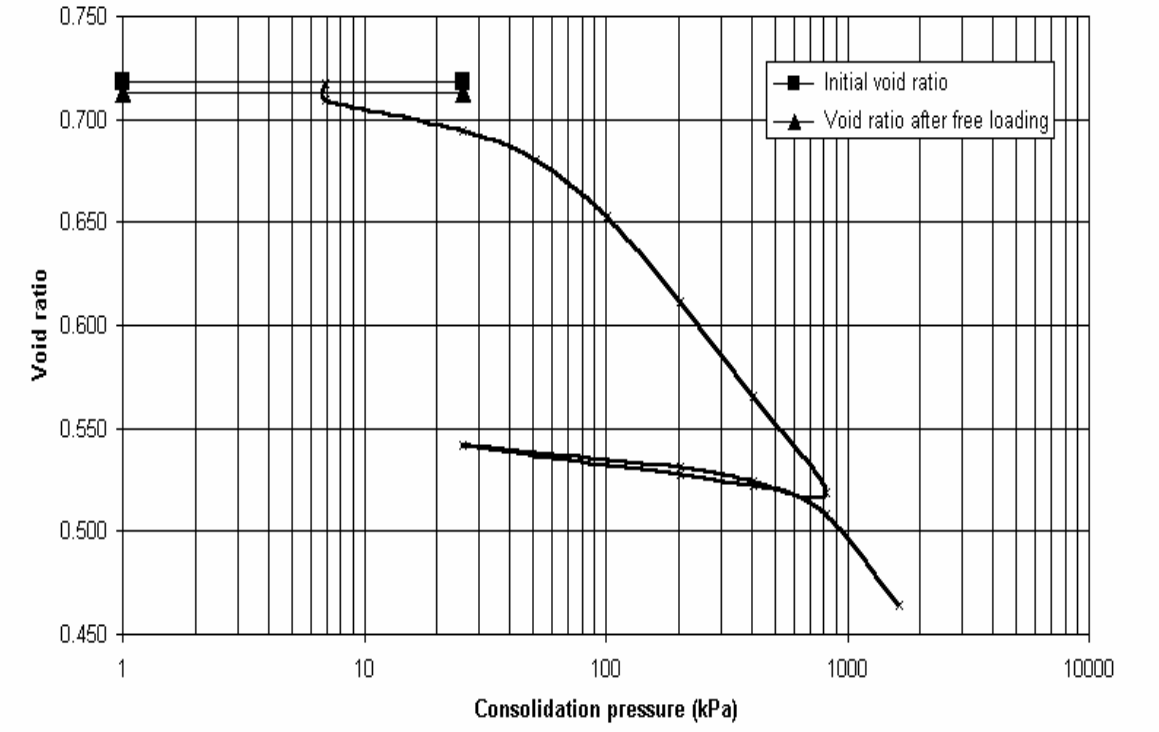

Figure 4.9: Consolidation curve for sabkha soil (Distilled water)

Table 4.8: Sabkha soil consolidation characteristics (Distilled water)

Soil characteristics	Value
Overconsolidation pressure, kPa	55
Compression index	0.16
Swell index	0.02
Recompression index	0.02
Initial void ratio	0.72
Void ratio after free loading	0.71
Initial water content, %	10.4
Final water content, %	19.88
Final void ratio	0.46

to classify the sabkha with low to moderate compressibility (Al-Amoudi, 1992). Further, the increase in the final water content from 10.4% up to 19.9%, and the decrease in the final void ratio from 0.718 to 0.464 is ascribed to the mechanism of the consolidation test. This behavior was observed for all consolidating specimens regardless of the soil type.

(b) Sabkha soil plus clay: The results of consolidation test on the sabkha-clay mixtures are presented in Figure 4.10 through 4.15 and summarized in Table 4.9. As observed in Figure 4.10, the sabkha soil with 2% clay addition exhibited settlement immediately after flooding as percolation also occurred. For the specimens mixed with 5% and 8% of clay, the free loading stage was somewhat different from that of the sabkha and sabkha soil plus 2% clay. The difference arises from the application of vacuum pressure beneath the soil samples in the consolidometer to enhance the permeation of the water through the soil specimens. Initially, these two mixes (sabkha with 5% and 8% clay additions) had been freely-loaded, as shown in Figure 4.11, whereby they experienced settlement without any percolation of the water. As a result of the non-percolation pattern, the pressure was applied with a pressure head of 10 kPa for the sabkha soil with 5% clay and sabkha with 8% clay, respectively, to enhance the percolation of water, as shown in Figure 4.12. The increase in the clay addition needs increased vacuum pressure for percolation of water. Without the vacuum pressure, the water would not permeate through the soil strata, which was ascribed to the increased clay content in the soil specimen leading to blockage of the flow channels through the sabkha-clay mixtures.

All the clay-mixed samples displayed initially some settlement behavior, as shown in Figures 4.10 and 4.11, where sabkha with 2% clay addition had a net settlement of 0.05 mm, same as sabkha with 5% clay addition, while the sabkha with 8% clay addition had a settlement of about 0.02 mm. This is due to the fact that the collapse potential in the

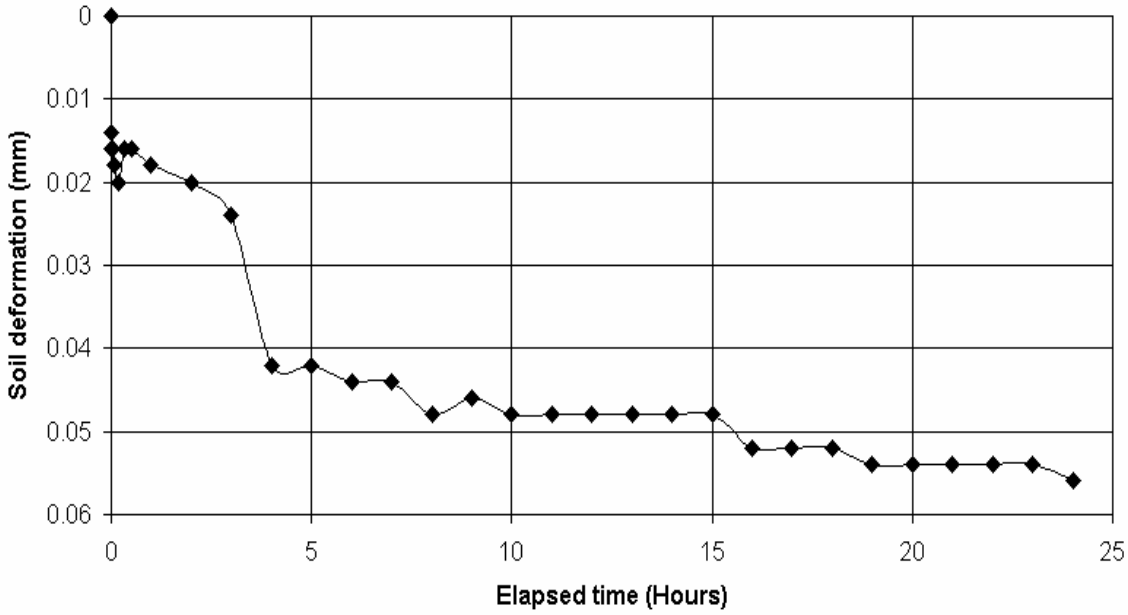

Figure 4.10: Free deformation for sabkha soil mixed with 2% clay under seating load

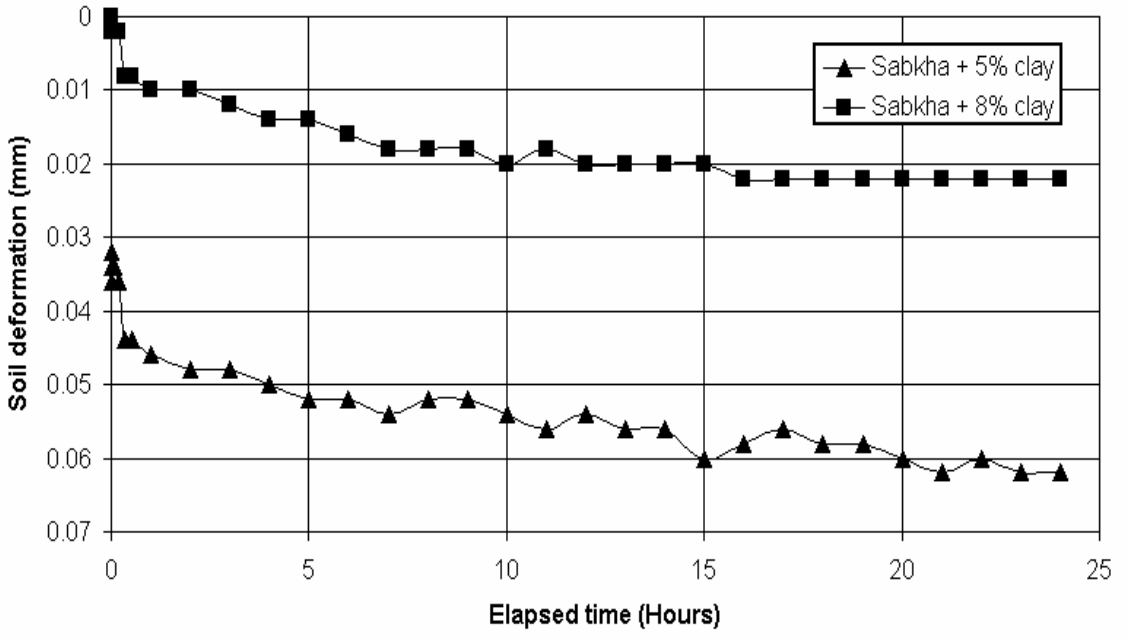

Figure 4.11: Free deformation for sabkha soil mixed with 5% and 8% clay under seating load

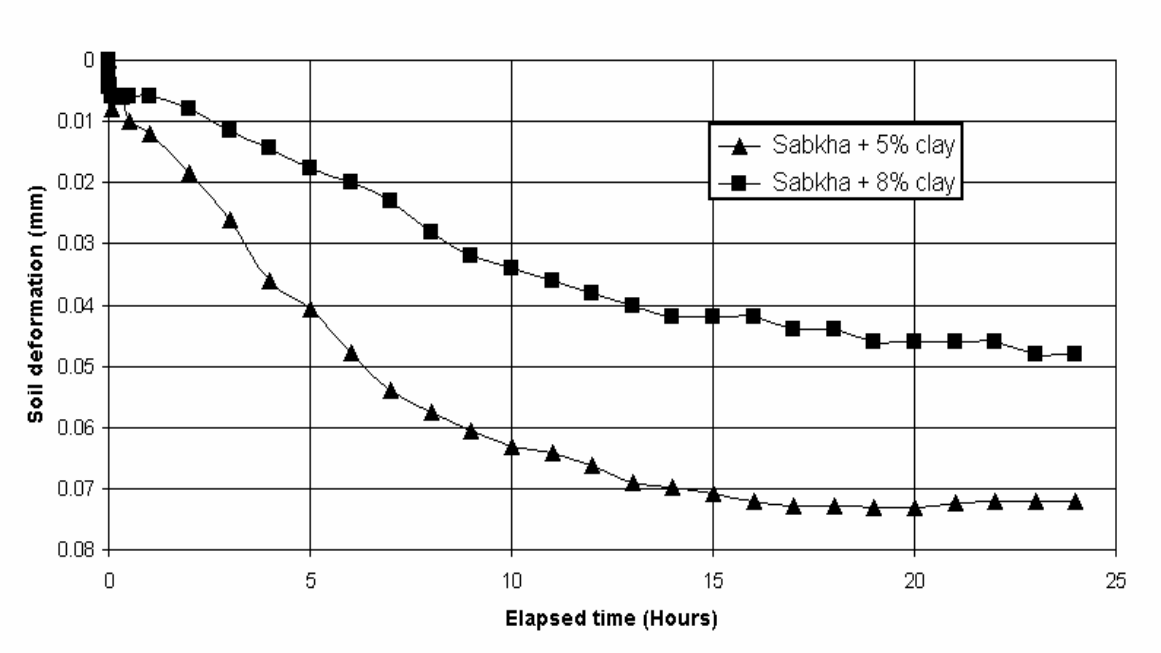

Figure 4.12: Free deformation for Sabkha soil mixed with 5% and 8% clay under seating load and vacuum pressure

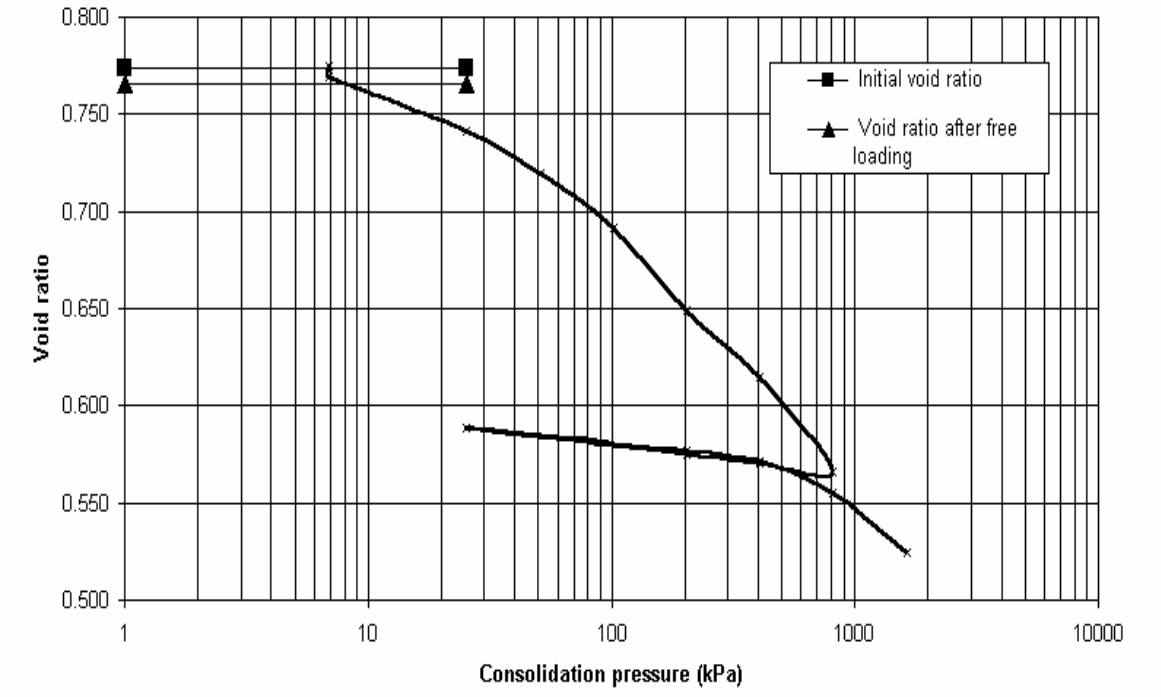

Figure 4.13: Consolidation curve for sabkha soil mixed with 2% clay under constant water head

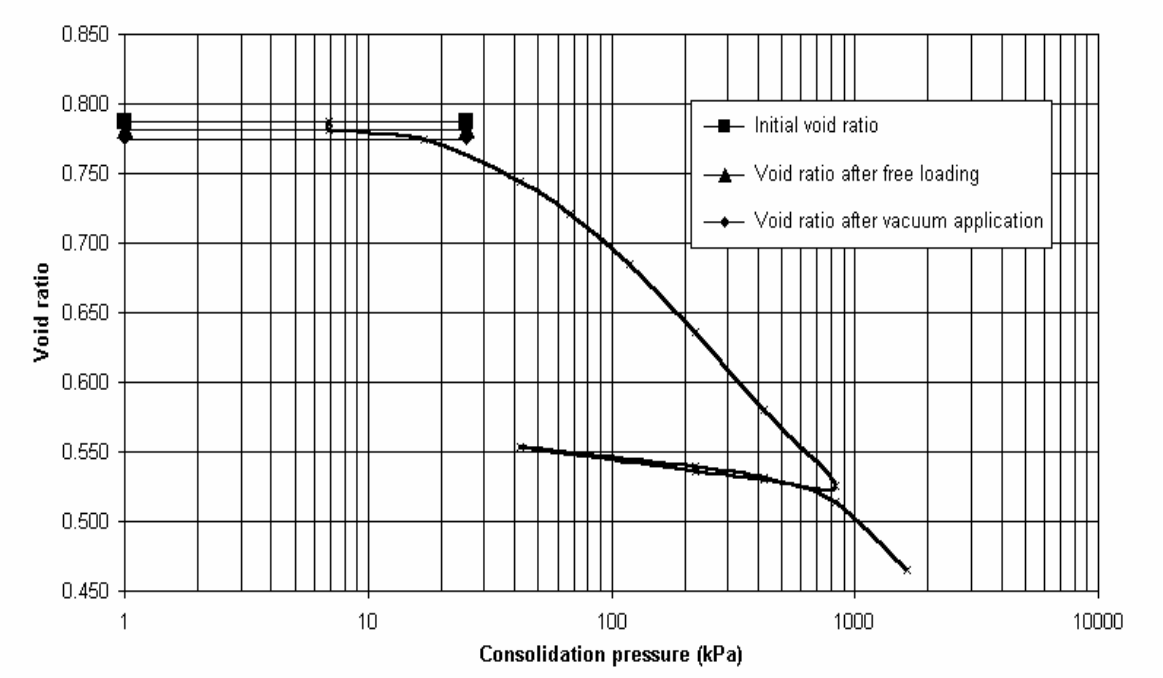

Figure 4.14: Consolidation curve for sabkha soil mixed with 5% clay under constant water head and vacuum pressure

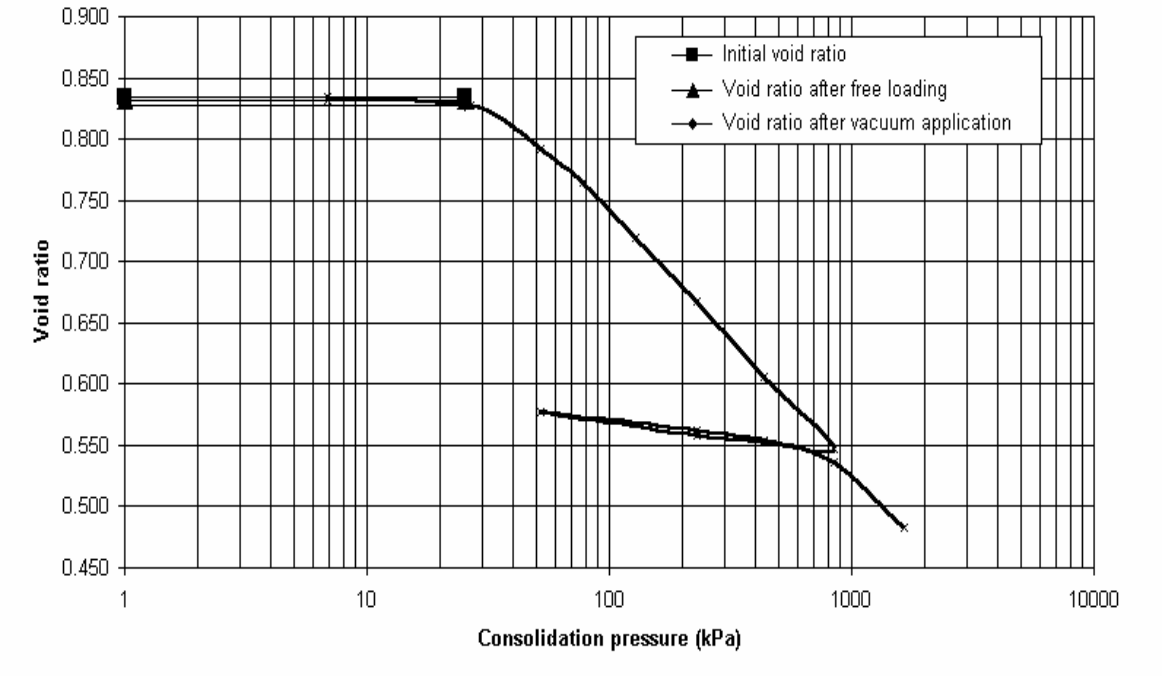

Figure 4.15: Consolidation curve for sabkha soil mixed with 8% clay under constant water head and vacuum pressure

Table 4.9: Consolidation test results for sabkha-clay mixtures (Distilled water)

Soil Characteristics	Clay Content		
	2%	5%	8%
Overconsolidation Pressure, kPa	55	68	82
Compression index	0.15	0.19	0.22
Swell index	0.01	0.02	0.03
Recompression index	0.01	0.02	0.03
Initial void ratio	0.77	0.79	0.83
Void ratio after free loading	0.77	0.78	0.83
Final void ratio	0.52	0.47	0.48
Initial water content, %	11.0	12.4	13.2
Final water content, %	17.6	18.5	18.5

sabkha soil is larger than the swell potential in the clay soil resulting in a net settlement behavior. For the soil mixed with clay, the increase in the clay addition reduces the settlement behavior of the soil, and for the same applied vacuum pressure, as shown in Figure 4.12.

The geotechnical characteristics of the clay-sabkha soil specimens were improved in terms of overconsolidation pressure (as shown in Table 4.9). For sabkha with 2% clay addition, there was no improvement in the overconsolidation pressure which was the same as recorded in the case of sabkha soil (about 55 kPa), and with an increase in the clay addition to 5% the pressure was 68 kPa, and 82 kPa for 8% clay addition. The increase in the overconsolidation pressure is directly related to the increase in the clay content in the soil mixture. Moreover, the compressibility behavior of the soil increased with the clay addition. The compression indices were 0.15, 0.19, and 0.22 for sabkha with 2%, 5% and 8% clay additions, respectively, indicating that the sabkha with 2% and 5% possessed low compressibility, while the sabkha with 8% clay addition possessed moderate to intermediate compressibility, according to Mitchell (1993). The compression index to swell index ratios were 15, 9.5, and 0.7 for sabkha with 2%, 5%, and 8% clay additions, respectively, which indicates a decrease in this ratio with an increase in the clay addition. Also, there were volumetric changes within the soil associated with an increase in the clay content, which was related to an increase in the initial void ratio. The net change in the void ratios as a result of consolidation was found to be 0.25, 0.32 and 0.35 for the sabkha with 2%, 5%, and 8% clay additions, respectively. The clay particles in the presence of salts flocculate causing high pore voids, but not enough open structure to create flow channels for the percolating fluids to flow.

The results in Table 4.9 indicate that the difference between the initial water content and the final water content tends to reduce as the clay addition increased. The increase in the final water content relative to the initial water content was found as 6.6, 6.2 and 5.3 for the sabkha with 2%, 5%, and 8% clay additions, respectively. The addition of clay increases the surface area of the soil allowing more moisture to be adsorbed on the surface area of the soil grains.

In general, the addition of clay to soil increases its compressiblity with increased void ratio within the soil specimens. Further, the addition of 5 and 8% clay to the sabkha soil inhibited the permeation of water through the soil under normal seating conditions.

MODIFIED CONSOLIDATION USING SABKHA BRINE

The modified consolidation test was repeated using sabkha brine, which was obtained from the same location as the sabkha soil. The test results can be categorized into the following two sections:

(a) Sabkha soil: The test results on the sabkha soil are shown in Figures 4.16 to 4.18 as well as in Table 4.10. Initially, when the soil was flooded with sabkha brine, the soil had some settlement but the brine could not flow through the consolidating soil under normal seating load. To overcome this situation, a vacuum pressure of 10 kPa was applied, which was kept all over the consolidation stages to maintain the percolation of the brine. The non-flow pattern of the soil could be related to the high viscosity of the brine, which needed a suction pressure in order to permeate through the soil specimen.

In comparison with the sabkha soil percolated with distilled water, there was significant change in the overconsolidation pressure in both the tests. The value obtained

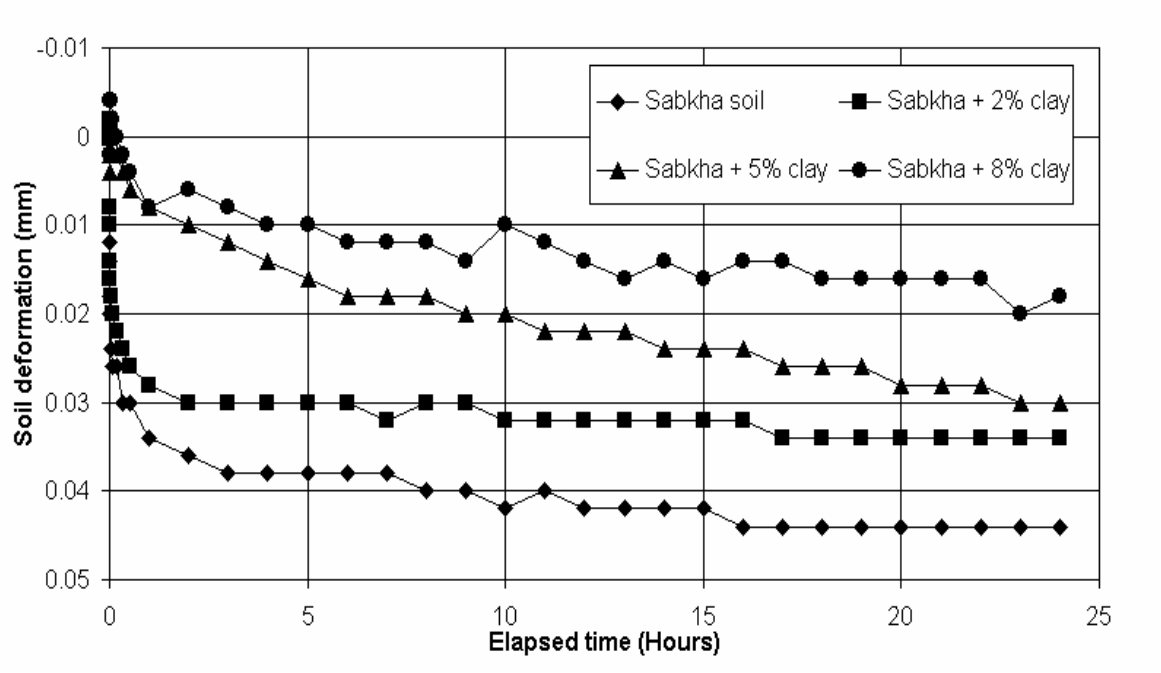

Figure 4.16: Free loading for sabkha-clay mixtures under seating load

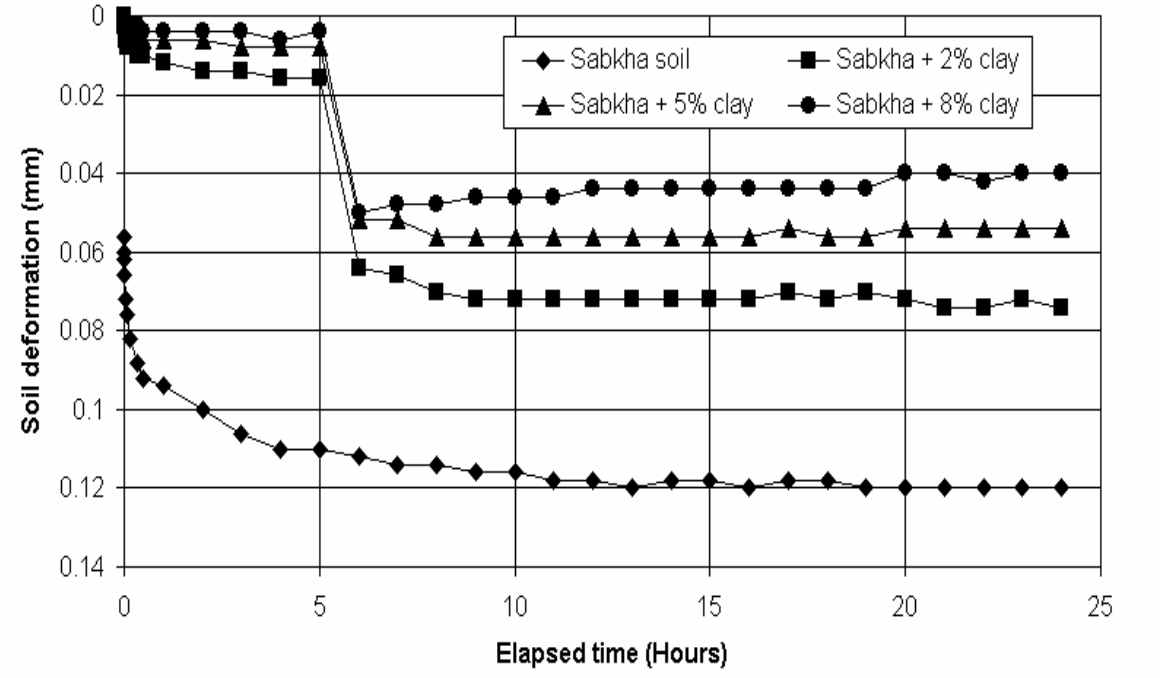

Figure 4.17: Free loading for sabkha-clay mixtures under seating load and vacuum pressure

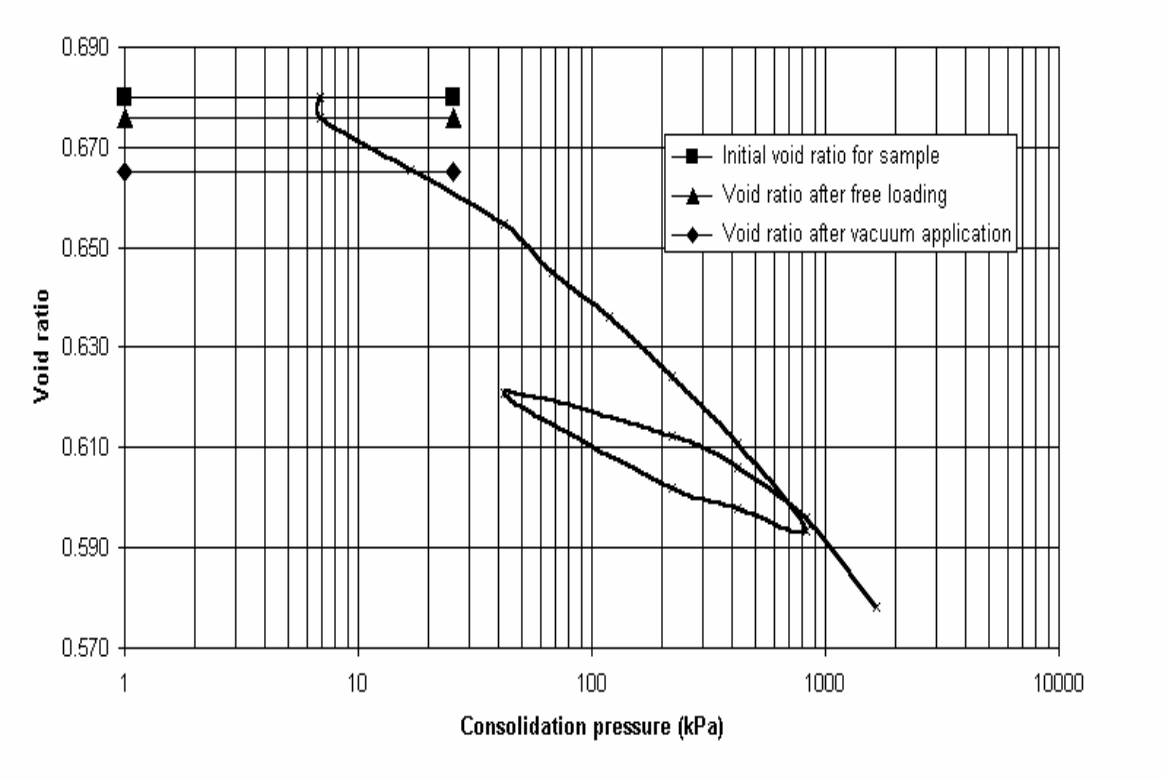

Figure 4.18: Consolidation curve for sabkha soil under constant brine head and constant vacuum pressure

Table 4.10: Consolidation characteristics for sabkha soil (Brine)

Soil Characteristics	Value
Overconsolidation pressure, kPa	80
Compression index	0.05
Swell index	0.02
Recompression index	0.02
Initial void ratio	0.68
Void ratio after free loading	0.68
Initial water content, %	10.4
Final water content, %	9.7
Final void ratio	0.58

when distilled water was used is 55 kPa while the obtained value when the brine was the percolating fluid is 80 kPa. The increase in the overconsolidation pressure when brine was used could be attributed to the fact that when brine is used, the soil is retaining its natural structure. However, the usage of water causes dissolution of the salt accumulated within the soil grains. As brine was used, the compression index was found to be lower than that obtained when water was used, it had a value of 0.05 compared to 0.16, and the compression index to swell index ratio was lowered from a value of 8 to 2 only. Furthermore, another difference is clearly on the initial and final water contents; they were 10.4% and 19.8% for the soil leached with distilled water as compared to 10.4% and 9.7% for those treated with sabkha brine. The narrow gap between the initial and final water content in the case of brine was due to the partial chemical inactivity of the brine in changing the chemistry of the soil leading to a negligible loss of moisture only as a result of consolidation of the soil specimen. The change in the void ratio was just 0.10 as compared to 0.26 for the sabkha treated with distilled water, and associated with a percolation with no significant salt dissolution, leading to slight change in the water content through the consolidation process.

(b) Sabkha soil plus clay: The results of consolidation tests on sabkha-clay mixtures are shown in Figures 4.16 and 4.17 and Figures 4.19 to 4.21 and Tables 4.11 and 4.12. Initially, as shown in Figure 4.16, all the mixtures were exposed to a seating load under flooding, and as a result all the soil specimens exhibited settlement. The settlement potential had been reduced with an increase in the clay addition whereby the sabkha-clay mixtures had settlement values of 0.044, 0.033, 0.030 and 0.018 mm for sabkha soil, sabkha with 2%, 5%, and 8% clay additions, respectively. At this stage, no percolation of brine had been shown, therefore, vacuum pressure of about 10 kPa was applied to the soil

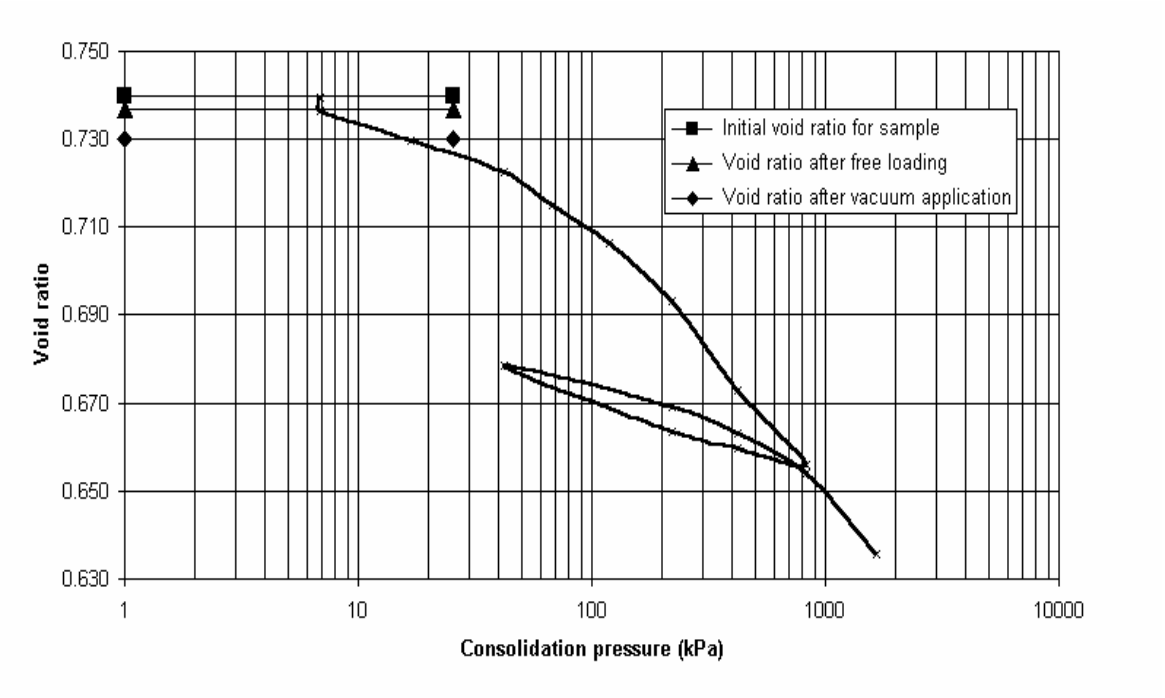

Figure 4.19: Consolidation curve for sabkha soil mixed with 2% clay under brine head and constant vacuum pressure

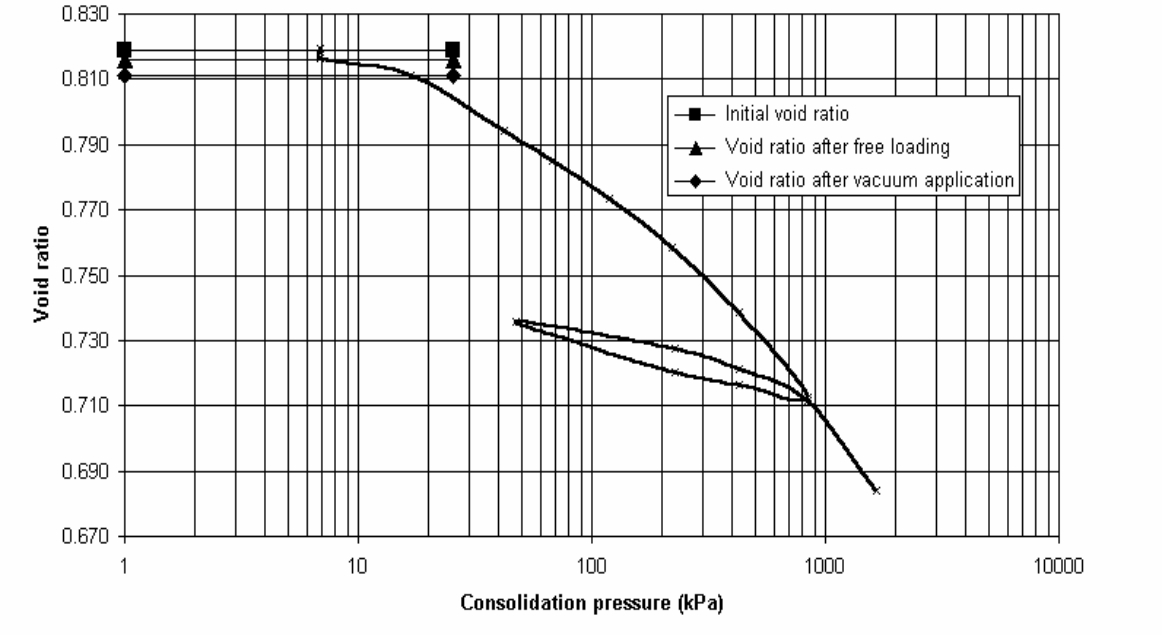

Figure 4.20: Consolidation curve for sabkha soil mixed with 5% clay under brine head and increased vacuum pressure

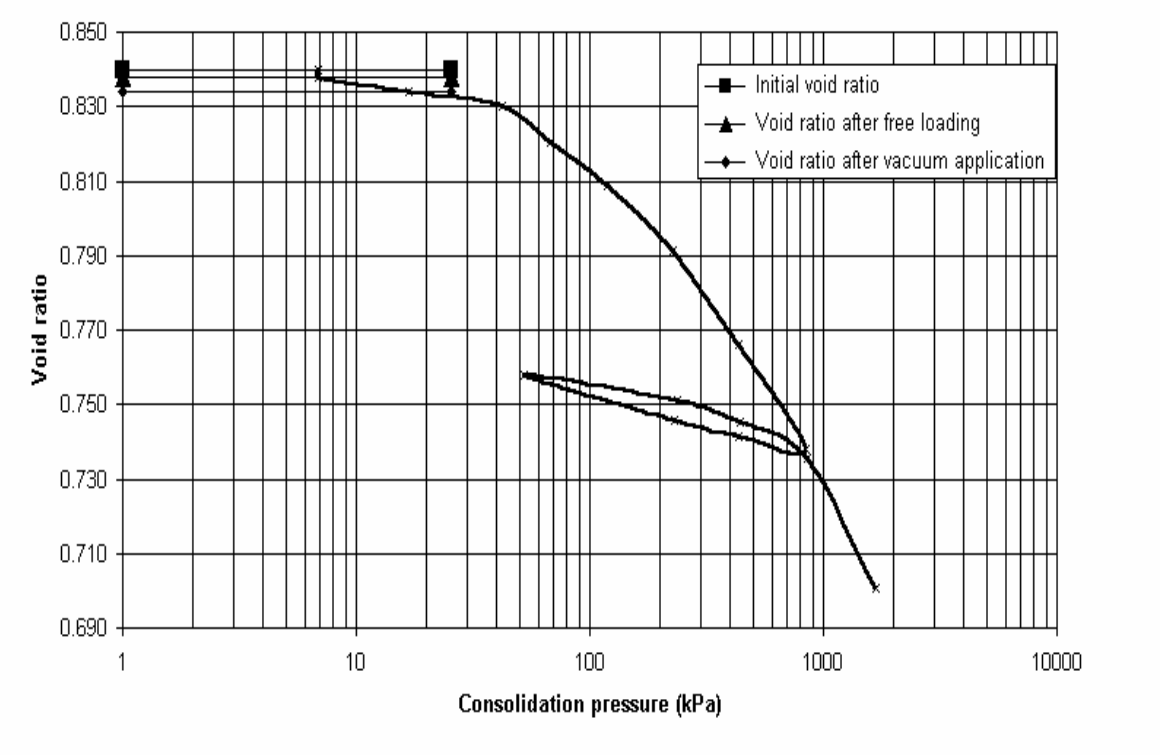

Figure 4.21: Consolidation curve for sabkha soil mixed with 8% clay under constant brine head and increased vacuum pressure

Table 4.11: Vacuum pressures applied to consolidated sabkha-clay mixtures (Brine)

Sabkha-clay Mixture	**Applied Vacuum Pressure**			
	10 kPa	**15 kPa**	**20 kPa**	**30 kPa**
Sabkha with 2% clay addition	Initial	_*	_*	_*
Sabkha with 5% clay addition	Initial	At reload of 827.03 kPa	At reload of 1637.15 kPa	_*
Sabkha with 8% clay addition	Initial	At load of 215 kPa	At load of 404 kPa	At reload of 1637.15 kPa

* No vacuum pressure was applied

Table 4.12: Consolidation test results for sabkha-clay mixtures (Brine)

Soil Characteristics	Clay Content		
	2%	**5%**	**8%**
Overconsolidation pressure, kPa	90	100	107
Compression index	0.06	0.07	0.08
Swell index	0.02	0.02	0.02
Recompression index	0.02	0.02	0.01
Initial void ratio	0.74	0.82	0.84
Void ratio after free loading	0.74	0.82	0.84
Final void ratio	0.64	0.68	0.70
Initial water content, %	11.0	12.4	13.2
Final water content, %	10.9	12.0	11.8

specimens to enhance percolation of the brine, as shown in Figure 4.17. After application of vacuum pressure and the brine was percolated, the soil specimens still showed settlement potential, with reduced potential as the clay addition was increased. Figure 4.17 showed an instant settlement in the sabkha soil associated by percolation of brine, while in the sabkha-clay mixtures, the specimens exhibited primary settlement followed by a sharp increase in the settlement value due to the percolation of brine which took place after approximately one hour after flooding. Then, the consolidation test continued with an increase in the rate of vacuum pressure for sabkha soil with 5% and 8% clay additions to maintain the percolation of brine, as summarized in Table 4.11.

The results indicate that the overconsolidation pressure increased with an increase in the clay addition whereby the values obtained were 90, 100 and 107 kPa for sabkha with 2%, 5% and 8% clay additions, respectively (Table 4.12). The compression index showed a slight increase proportional to the clay addition; its values were 0.06, 0.07 and 0.08 for sabkha with 2%, 5% and 8% clay additions, respectively, which reveals that all the three mixes are in the category of low compressibility soil as reported by Mitchell (1993). The compression to swell index ratios were 3, 3.5 and 4 for the sabkha with 2%, 5% and 8% clay additions, respectively, the change being negligible. The change in the void ratio due to consolidation were found to be 0.1, 0.14 and 0.14 for sabkha with 2%, 5% and 8% clay additions, respectively, indicating a marginal effect due to the addition of clay to the sabkha soil. Also, it was observed that the change in the moisture content during consolidation could be neglected indicating that the brine did not induce any chemical activity within the soil specimens.

In general, the changes in the soil compressibility when brine was used were less than that recorded when distilled water was used, although the use of brine with the

specimens inhibited the percolation of fluid. The marginal effect due to brine percolation could be ascribed to the fact that the swellability of the clay had been reduced by the high salinity of the brine (Mitchell, 1993).

CHEMICAL ANALYSIS

For better understanding of the insulation and leakage of trace metals in consolidating sabkha soil, some samples of the percolated liquid were collected from the consolidometer outlets and analyzed. These samples from the percolated water and brine were collected at different intervals during the first 24 hours of leaching (after 1 hour, 4 hours, 8 hours and 16 hours). These liquid samples were taken after percolation through the sabkha soil mixed with 8% clay. The percolated liquids were chemically analyzed and the results are numerically summarized in Tables 4.13 to 4.15 and depicted in Figures 4.22 to 4.30.

The analysis of the brine itself (shown in Table 4.13) reveals a high concentration of chlorides, however, the sulfate concentration was low indicating that the brine was chloride-rich and hypersaline.

When analyzing the leached fluids for the total dissolved salts, it was found that the chloride content was generally about half the quantity of the total dissolved salts determined through the ion chromatography technique (Table 4.14).

In the samples percolated with distilled water, it was observed that the leached water from the sabkha soil had marginally less chloride concentration than the sabkha soil mixed with 8% clay (Figure 4.22). For the soil percolated with brine, the sabkha soil had almost the same concentration as the parent brine. Chlorides did not show a significant

Table 4.13: Chemical analysis for brine

Brine	Concentration, ppm
TDS	350,000
Cl^-	191,000
SO_4^{2-}	3,570

Table 4.14: Ion chromatographic analysis for percolated fluid samples

Percolated Soil Samples			Concentration, ppm		
			TDS	Chloride	Sulfate
Water Percolation	Sabkha soil	After 1 Hour	50,700	22,900	2,110
		After 4 Hours	60,000	24,600	2,200
		After 8 Hours	22,800	10,200	1,720
		After 16 Hours	3,010	123	1,570
	Sabkha soil + 8% clay	After 1 Hour	100,000	51,000	2,220
		After 4 Hours	48,800	25,600	2,010
		After 8 Hours	30,500	15,300	1,690
		After 16 Hours	8,210	3,690	1,110
Brine Percolation	Sabkha soil	After 1 Hour	358,000	191,000	3,540
		After 4 Hours	355,000	195,000	3,560
		After 8 Hours	355,000	194,000	3,940
		After 16 Hours	351,000	188,000	4,050
	Sabkha soil + 8% clay	After 1 Hour	357,000	190,000	3,140
		After 4 Hours	354,000	193,000	3,260
		After 8 Hours	349,000	179,000	3,260
		After 16 Hours	350,000	197,000	3,580

Table 4.15: Trace metals filtered from the brine by the soil specimens

Percolated Soil Samples		Concentration, ppm		
		Mn	Pb	Zn
Sabkha soil	After 1 Hour	n.d	2.13	2.17
	After 4 Hours	0.36	2.97	7.34
	After 8 Hours	0.17	0.84	4.40
	After 16 Hours	0.24	1.63	9.66
Sabkha soil + 8% clay	After 1 Hour	0.49	12.8	36.8
	After 4 Hours	0.49	7.58	27.6
	After 8 Hours	0.19	5.77	13.7
	After 16 Hours	0.31	5.72	16.1

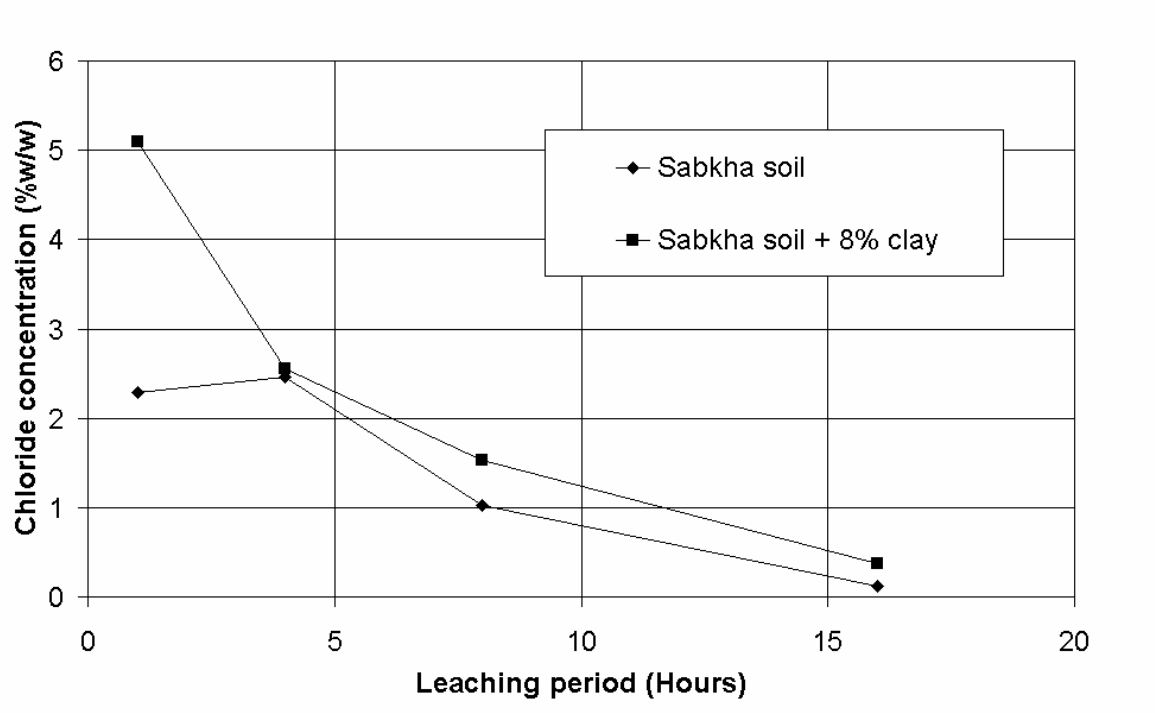

Figure 4.22: Chloride ions in soil specimens leached with distilled water

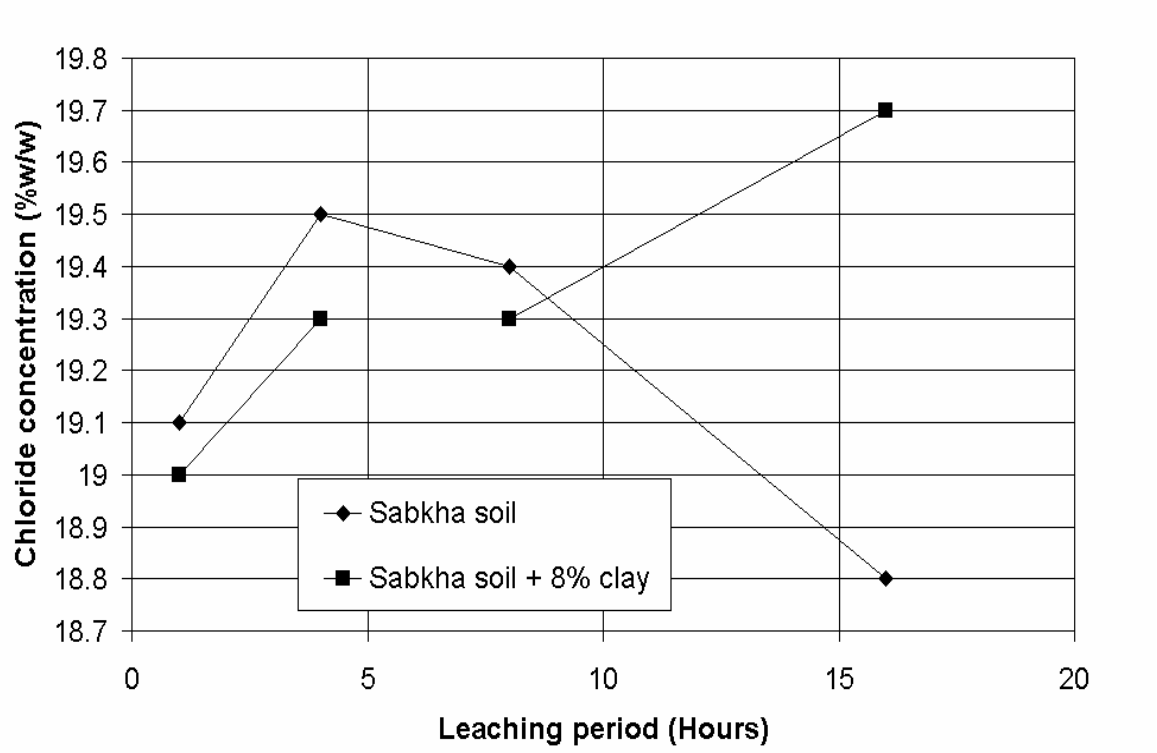

Figure 4.23: Chloride ions in soil specimens leached with brine

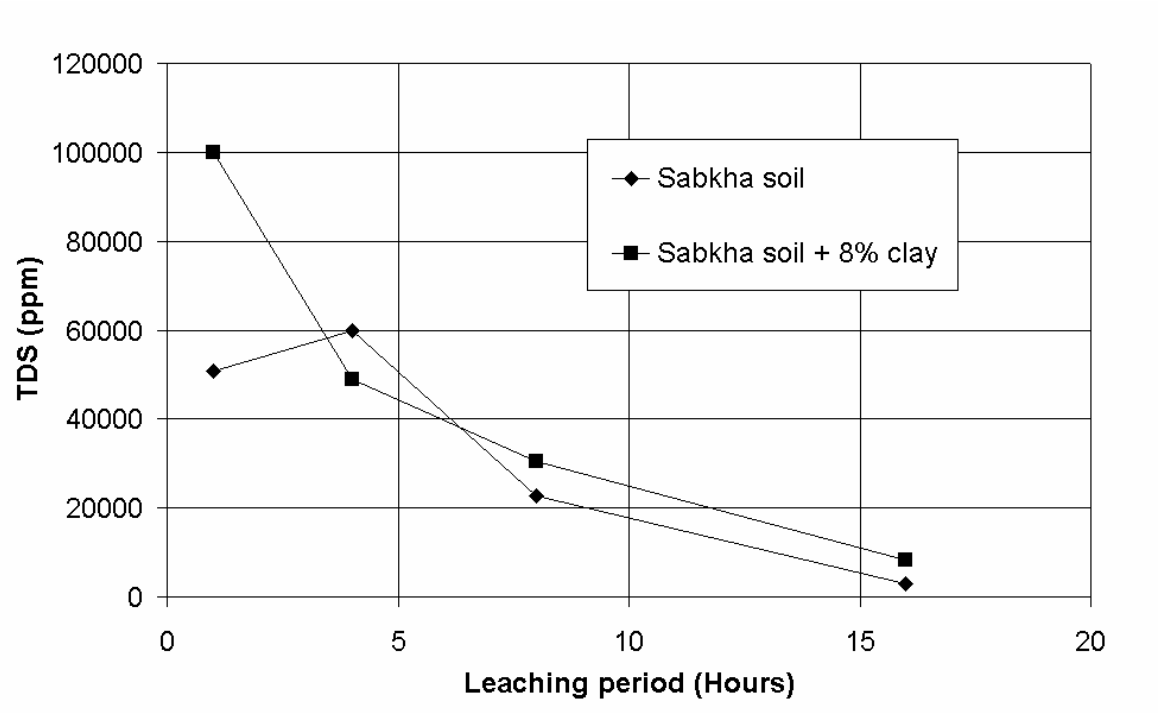

Figure 4.24: TDS in soil specimens leached with distilled water

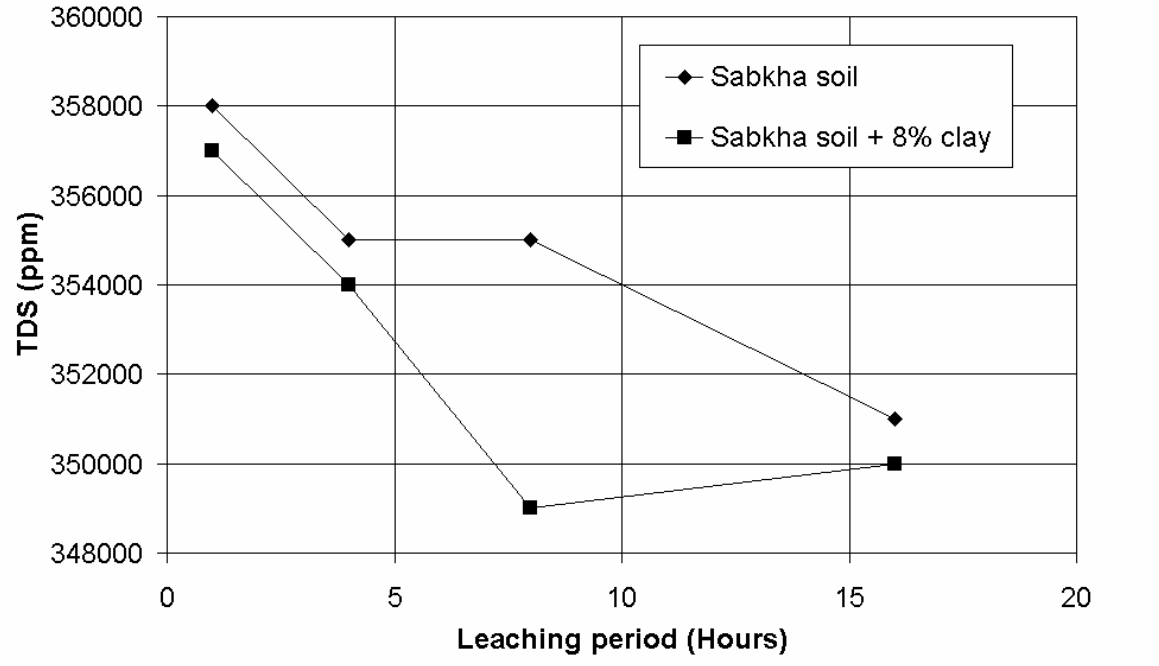

Figure 4.25: TDS in soil specimens leached with brine

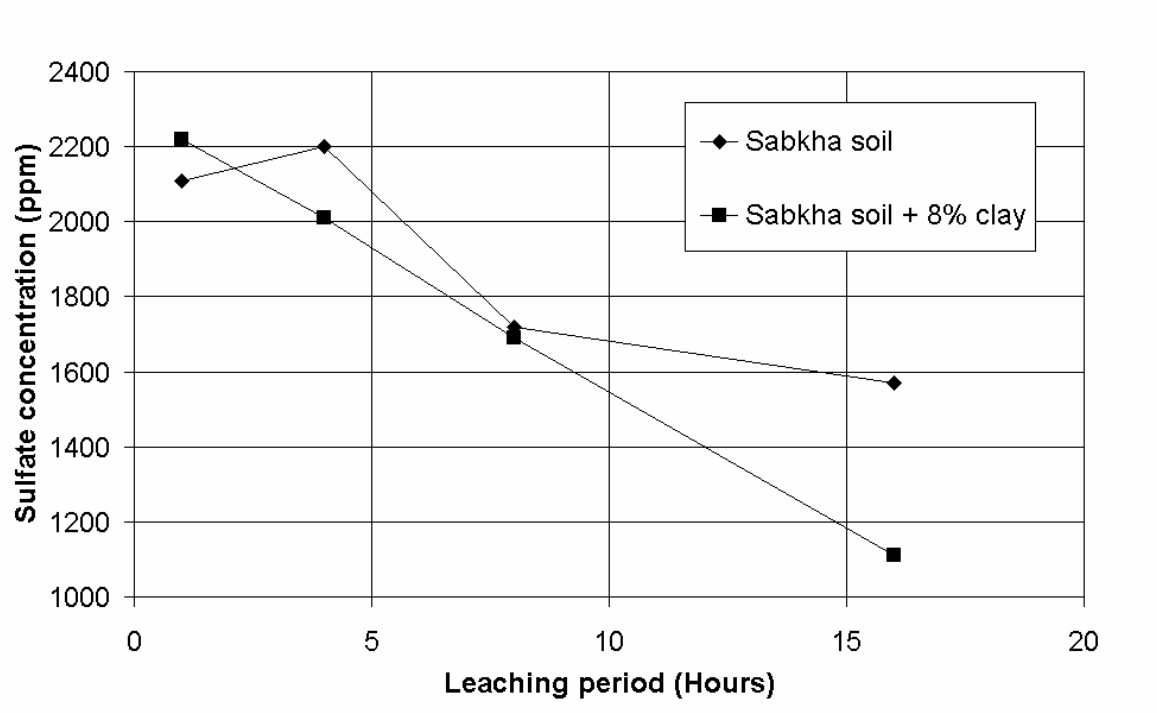

Figure 4.26: Sulfate ions in soil specimens leached with distilled water

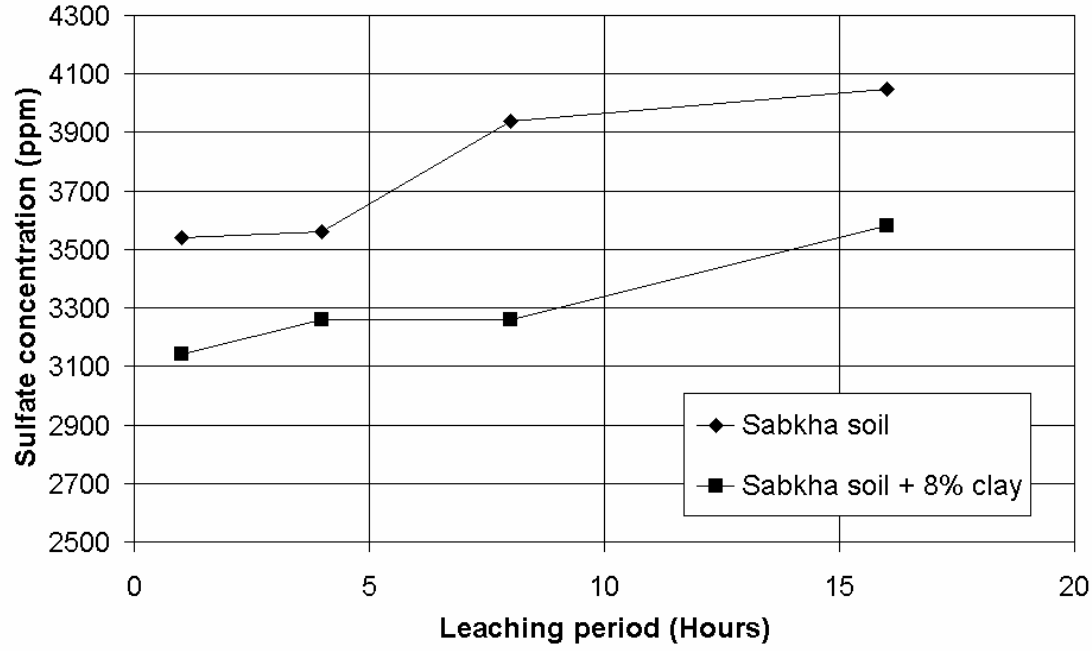

Figure 4.27: Sulfate ions in soil specimens leached with brine

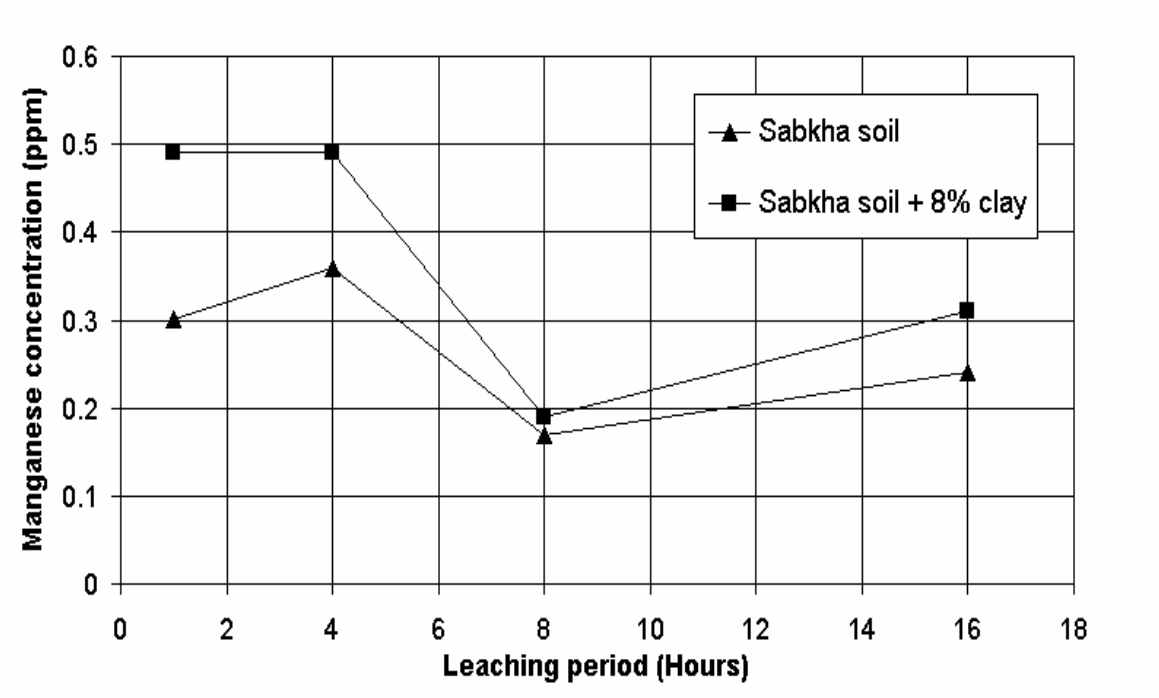

Figure 4.28: Manganese filtered in soil leached with brine

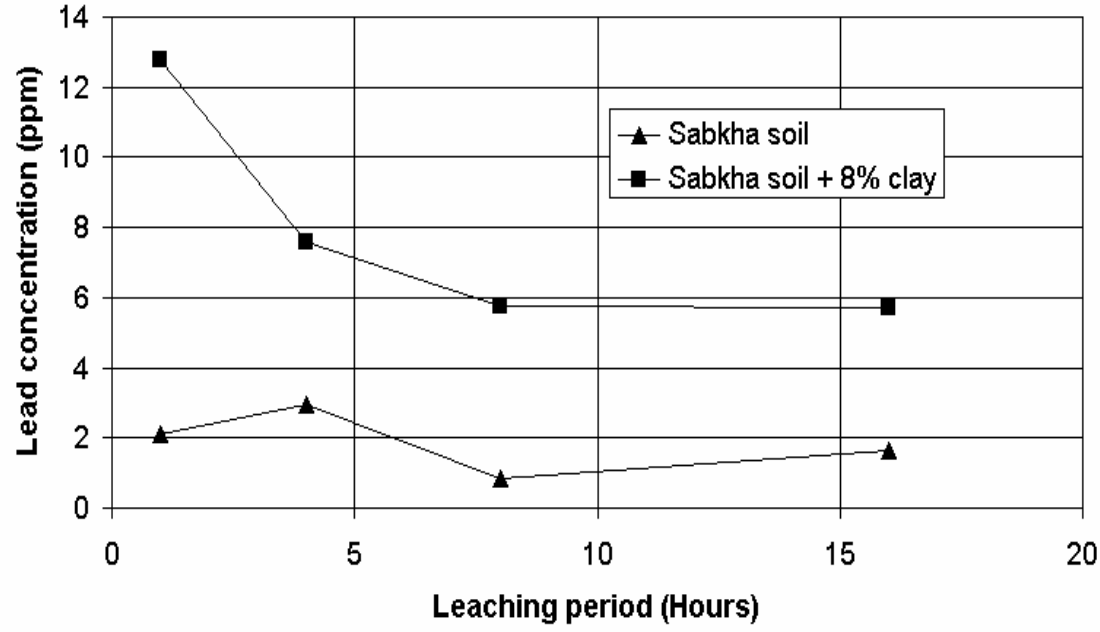

Figure 4.29: Lead filtered in soil leached with brine

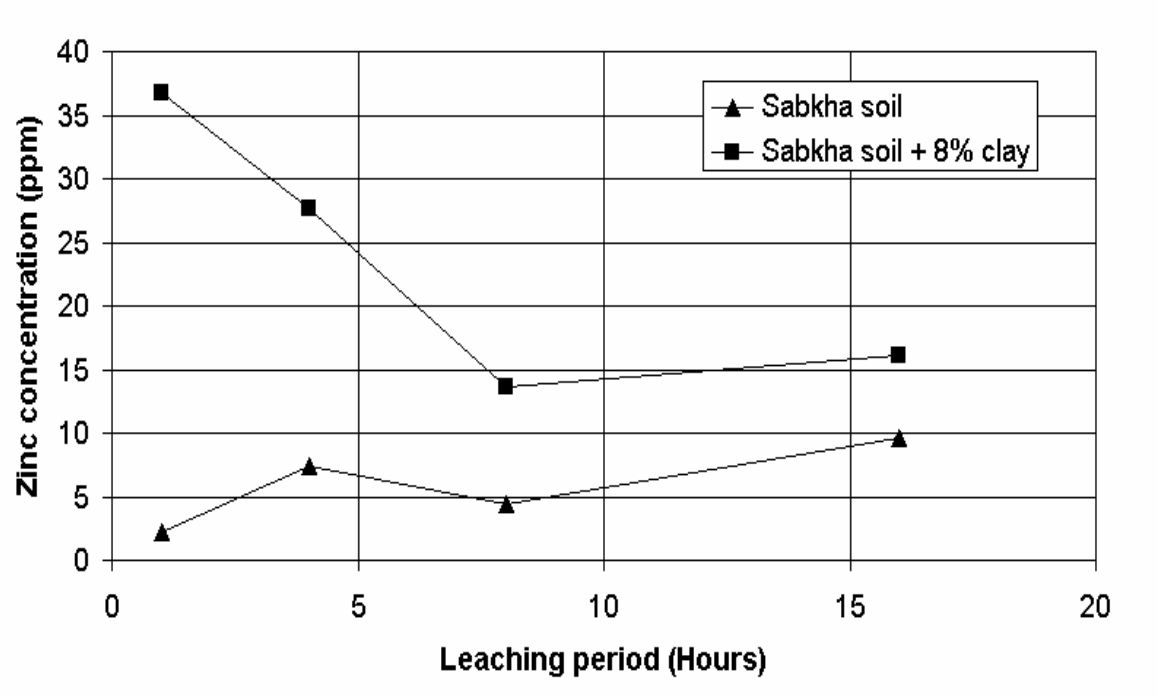

Figure 30: 4.Zinc filtered in soil leached with brine

reduction in the concentration due to the addition of clay to the sabkha soil, as shown in Figure 4.23. The chloride concentration leached from sabkha when distilled water was used was governed by the dissolution of the salts, while the interference of clay in the soil tends to increase the volume of the soil specimen leading to higher porosity of the soil which allows water to dissolve more salts that enveloped the soil grains.

As shown in Figures 4.24 and 4.25 and summarized in Table 4.14, the profiles for the TDS when clay was added to sabkha soil indicate an increase in the TDS when distilled water was the percolating fluid. When the brine was used, the reverse trend was observed when adding clay to the sabkha soil. The TDS profiles exhibited the same trend as the chloride profiles. This is due to the fact that chlorides were the major constituents in the brine and the TDS followed the chloride trend.

The sulfate concentration in the soil mixed with clay is a bit lower than that in the sabkha soil leached with water, as shown in Figure 4.26. The same trend was noted when the brine was used, as shown in Figure 4.27. When sabkha was used alone, the sulfate concentration was a result of salt dissolution. The addition of clay was believed to create an electrolyte media, which in the presence of chlorides, reduced the sulfates solubility (Mitchell, 1993).

The addition of clay was found to have significant effect in removing the sulfates although the use of distilled water might increase the chloride concentration within the percolated water due to its ability to dissolve the chloride salts.

The filtered trace metals were obtained with reference to the brine used in percolation, as summarized in Table 4.15 and shown in Figures 4.28 through 4.30. A subtraction process was performed for the leached brine relative to the parent brine. It was found that the quantity of zinc, manganese and lead trapped by the sabkha soil with 8%

clay addition was greater than that trapped by the sabkha soil only. In the sabkha soil, the filtered base metals were due to the adsorption of these metals onto the soil particles, in the presence of chlorides (Barrow et al., 1981). While in the case of sabkha soil mixed with clay, the concentration of lead, zinc and manganese exhibited an increase in the filtered metals from solution due to the sorption of the trace metals on the surface of the clay, rather than experiencing ion exchange. At high concentrations of sodium chloride, adsorption was dominant (LeDred and Wey, 1965).

4.2 PERFORMANCE OF PLAIN AND BLENDED CEMENTS IN CHLORIDE-SULFATE ENVIRONMENTS

Experiments were conducted to investigate the performance of plain and blended cements in the aggressive environment of the sabkha. The experimental program was conducted on:

1. Cement mortar specimens;
2. Plain cement concrete specimens; and
3. Reinforced cement concrete specimens.

4.2.1 Results of Tests Conducted on Mortar Specimens

SULFATE ATTACK

Two sets of 50x50x50 mm mortar specimens were cast. The first set was water-cured for all the test duration, while the other set was water-cured for 14 days at first, and thereafter immersed in a 5% magnesium sulfate solution for the remaining test period.

The compressive strength for the two sets was determined using an automatic compression machine with a rate of loading of 1.1 kN/s. From the compressive strength of water-cured specimens and those immersed in the 5% Mg-sulfate solution, summarized in Table 4.16, the strength deterioration factors were calculated. The compressive strength development of the water-cured specimens is shown in Figure 4.31.

The water-cured mortar specimens were used as control for the sulfate attack and salt weathering experiments. As shown in Figure 4.31, the compressive strength increased with the curing period in all the specimens. It is also clear that blast furnace slag cement had the lowest compressive strength among all the cements. This could be ascribed to the large replacement of the cement in this mix; BFS was 70% of the total cementitious materials content. Also, it is observed that the rate of the strength development in the undensified silica fume cement was very small as compared to the other cements. After 14 days of water curing, the undensified silica fume and superpozz cements exhibited better compressive strength than Type I cement mortar. At later ages, densified silica fume and superpozz cements were the only two cements that had compressive strength values similar to that of Type I cement mortar.

Figure 4.32 depicts the compressive strength of plain and blended cements mortar specimens immersed in the 5% magnesium sulfate solution. From the data in Figure 4.32, it is noted that the compressive strength of almost all the blended cements exhibited some reduction due to the progress of sulfate attack. Silica fume cements had the worst trends in behavior, while blast furnace slag was the only cement that displayed strength development, even in the presence of the aggressive Mg-sulfate environment. The decrease in strength of the densified silica fume was due to the surficial deterioration effect of the magnesium sulfate attack with time (Al-Amoudi, 1998).

Table 4.16: Compressive strength of specimens exposed to water and sulfate solution.

Cement	Parameter	Exposure Period, Days			
		14	**90**	**180**	**270**
Type I	Water cured, MPa	49.61	70.29	74.03	77.19
	Sulfate exposed, MPa	49.61	60.30	62.78	60.37
	SDF*, %	**0.00**	**14.22**	**15.21**	**21.79**
Type V	Water cured, MPa	48.09	57.71	67.00	68.98
	Sulfate exposed, MPa	48.09	54.82	58.00	55.26
	SDF, %	**0.00**	**5.01**	**13.43**	**19.89**
Densified Silica	Water cured, MPa	46.24	65.84	76.92	78.07
	Sulfate exposed, MPa	46.24	59.24	68.12	62.93
	SDF, %	**0.00**	**10.03**	**11.44**	**19.39**
Undensified Silica	Water cured, MPa	57.63	59.19	61.85	62.54
	Sulfate exposed, MPa	57.63	48.83	45.39	42.78
	SDF, %	**0.00**	**17.51**	**26.61**	**31.60**
Fly Ash	Water cured, MPa	42.47	64.75	67.23	68.17
	Sulfate exposed, MPa	42.47	57.69	54.48	52.41
	SDF, %	**0.00**	**10.91**	**18.96**	**23.12**
Superpozz	Water cured, MPa	59.37	71.15	74.25	77.83
	Sulfate exposed, MPa	59.37	65.63	65.45	64.33
	SDF, %	**0.00**	**7.75**	**11.85**	**17.35**
Blast Furnace Slag	Water cured, MPa	35.93	53.84	57.25	63.51
	Sulfate exposed, MPa	35.93	51.45	54.24	57.62
	SDF, %	**0.00**	**4.44**	**5.27**	**9.27**

* Strength deterioration factor

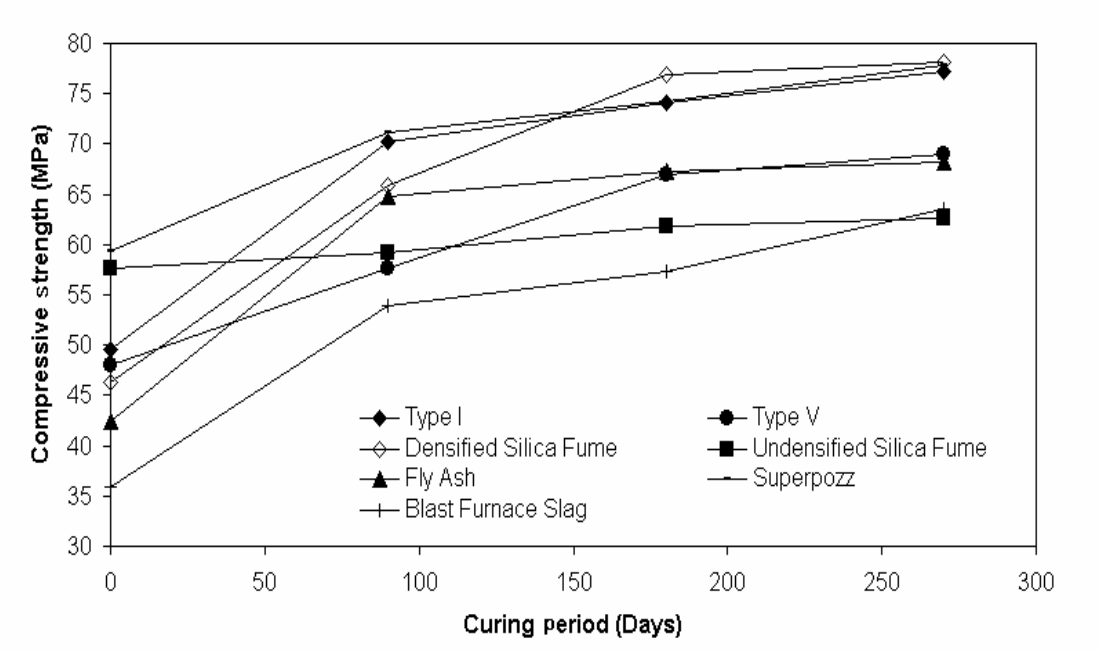

Figure 4.31: Compressive strength of water-cured plain and blended cement mortar specimens

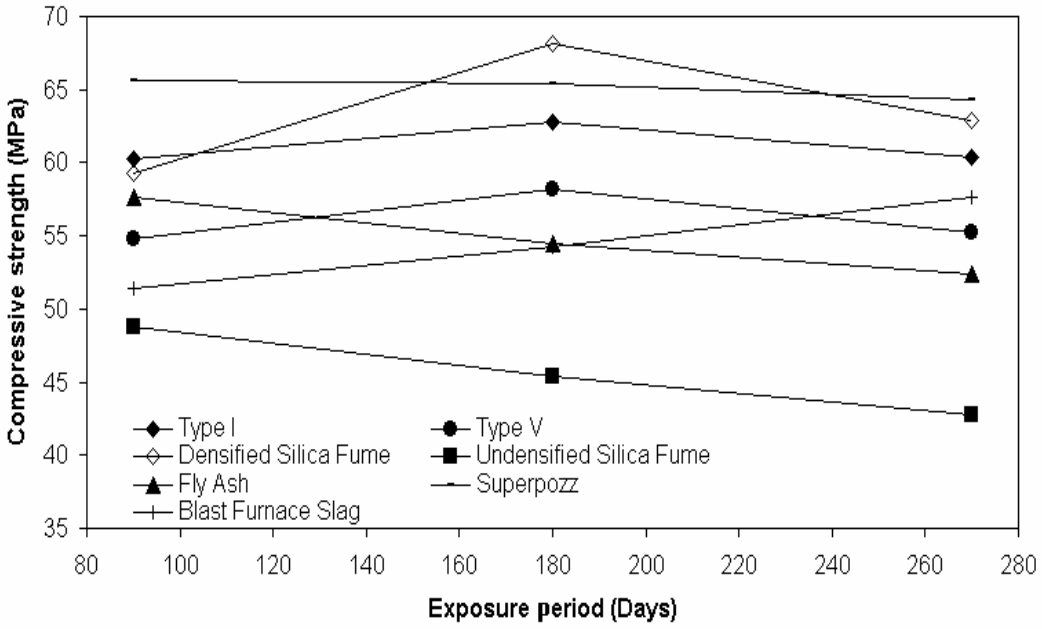

Figure 4.32: Compressive strength of mortar specimens immersed in 5% magnesium sulfate solution

The mechanism of sulfate attack in Mg-sulfate exposure for Portland cements can be explained as follows: Magnesium sulfate reacts with portlandite present as a result of cement hydration, forming gypsum and insoluble magnesium hydroxide (brucite). This insoluble hydroxide has a pH of 10.5. At this low pH, calcium silicate hydrate and ettringite become unstable. As a result of this low pH condition, secondary ettringite will not form and magnesium sulfate will react with calcium silicate hydrate forming gypsum, brucite, and silica gel ($SiO_2.H_2O$) (Al-Amoudi, 1998). As the pH is lowered by the evolution of this further brucite, calcium silicate hydrate will liberate lime to raise the pH and to establish its equilibrium. The liberated lime reacts with magnesium sulfate in the solution producing more brucite, resulting in more and more concentration of gypsum and brucite. As a result, calcium silicate hydrate loses its lime and becomes less cementitious. The excess magnesium hydroxide reacts with the silica gel produced formerly, and produces magnesium silicate hydrate, which is a non-cementitious, fibrous material.

The Type I cement used in this study had a C_3A content of 8.52% and a C_3S/C_2S ratio of 3.53, while Type V cement had a C_3A content of 3.5% and C_3S/C_2S ratio of 2.51. The inferior performance of Type I cement may be ascribed to the high C_3A and C_3S/C_2S ratio that aggravated the sulfate attack, while the cause for the relatively low deterioration observed in Type V cement, as shown in Figure 4.33, could be attributed to the lower C_3S/C_2S ratio, which resulted in a low deterioration compared to Type I cement mortar.

Blended cements experienced severe Mg-sulfate attack due to the lack of portlandite causing dense silicates formation that were attacked directly by the magnesium sulfate (Al-Amoudi, 1998), particularly in the case of undensified silica fume, which exhibited the highest degree of deterioration, as shown in Figure 4.33. The data also

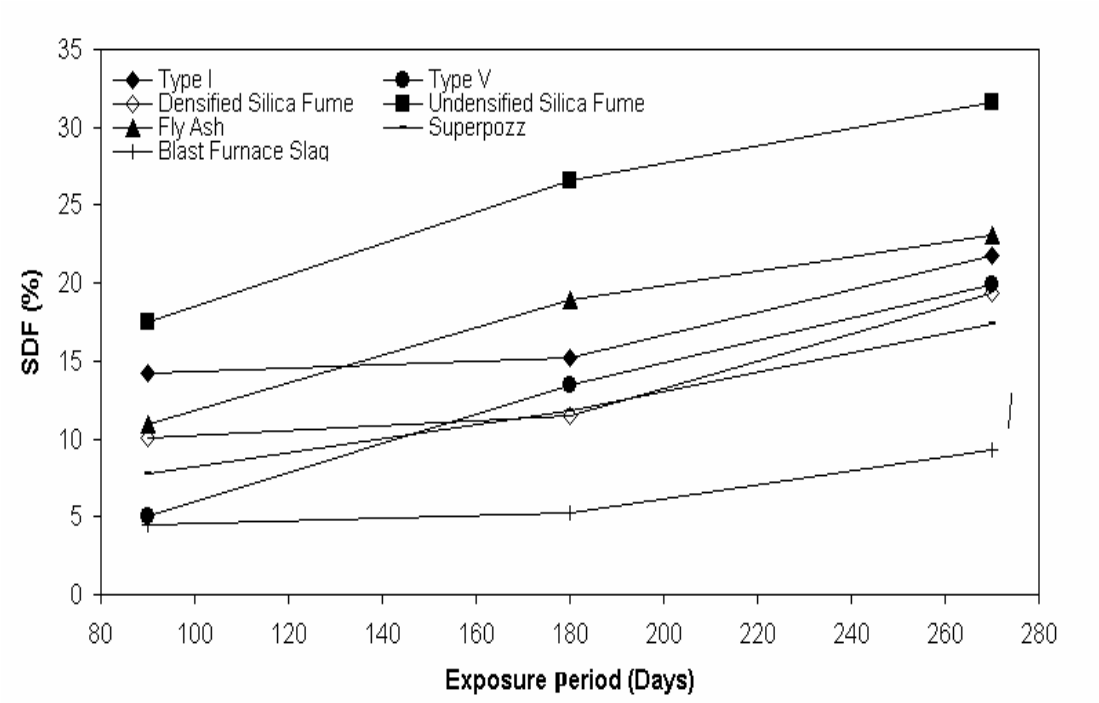

Figure 4.33: Strength deterioration factor due to sulfate attack

strengthens the evidence of the good performance of blast furnace slag in Mg-sulfate medium. This was perhaps caused by the reduction in the C_3A content of this cement.

SALT WEATHERING

The water-cured specimens were used as control for detecting the deterioration due to salt weathering. The results obtained from these experiments are summarized in Table 4.17.

Figure 4.34 shows the compressive strength of plain and blended cements mortar specimens exposed to salt weathering. The compressive strength of all the specimens decreased with the period of exposure to the salt solution, except that of blast furnace slag, superpozz and densified silica fume cements. The compressive strength of densified silica fume cement mortar specimens increased up to the 180 days and a reduction in strength was noted thereafter.

Figure 4.35 shows the strength deterioration factors for plain and blended cements. The trend shown by the blended cements in Figure 4.35 was similar to that of the specimens exposed to the sulfate solution. However, the undensified silica fume specimens exhibited the worst situation due to salt weathering. Both Type I and Type V cement mortar specimens exhibited a high degree of deterioration, which could be ascribed to the conjoint effect of salts on the pore structure that might lead to scaling and softening of the specimens (Hervey, 2000). Type I cement mortar exhibited a uniform increase in deterioration, however, Type V cement mortar displayed sharp increase in deterioration after 6 months of exposure.

Table 4.17: Strength deterioration factor for specimens exposed to salt weathering

Cement Type	Parameter	Exposure Period, Day			
		14	**90**	**180**	**270**
Type I	Water cured, MPa	49.61	70.29	74.03	77.19
	Salt weathering, MPa	49.61	53.73	50.94	48.32
	SDF*, %	**0.00**	**23.56**	**31.19**	**37.40**
Type V	Water cured, MPa	48.09	57.71	67.00	68.98
	Salt weathering, MPa	48.09	49.47	41.85	39.11
	SDF, %	**0.00**	**14.28**	**37.54**	**43.30**
Densified Silica	Water cured, MPa	46.24	65.84	76.92	78.07
	Salt weathering, MPa	46.24	58.20	66.44	63.45
	SDF, %	**0.00**	**11.60**	**13.62**	**18.73**
Undensified Silica	Water cured, MPa	57.63	59.19	61.85	62.54
	Salt weathering, MPa	57.63	42.70	42.16	35.36
	SDF, %	**0.00**	**27.86**	**31.83**	**43.46**
Fly Ash	Water cured, MPa	42.47	64.75	67.23	68.17
	Salt weathering, MPa	42.47	56.59	57.25	53.73
	SDF, %	**0.00**	**12.61**	**14.85**	**21.18**
Superpozz	Water cured, MPa	59.37	71.15	74.25	77.83
	Salt weathering, MPa	59.37	60.70	61.65	63.10
	SDF, %	**0.00**	**14.68**	**16.96**	**18.93**
Blast Furnace Slag	Water cured, MPa	35.93	53.84	57.25	63.51
	Salt weathering, MPa	35.93	49.91	52.98	55.10
	SDF, %	**0.00**	**7.29**	**7.46**	**13.24**

* Strength deterioration factor

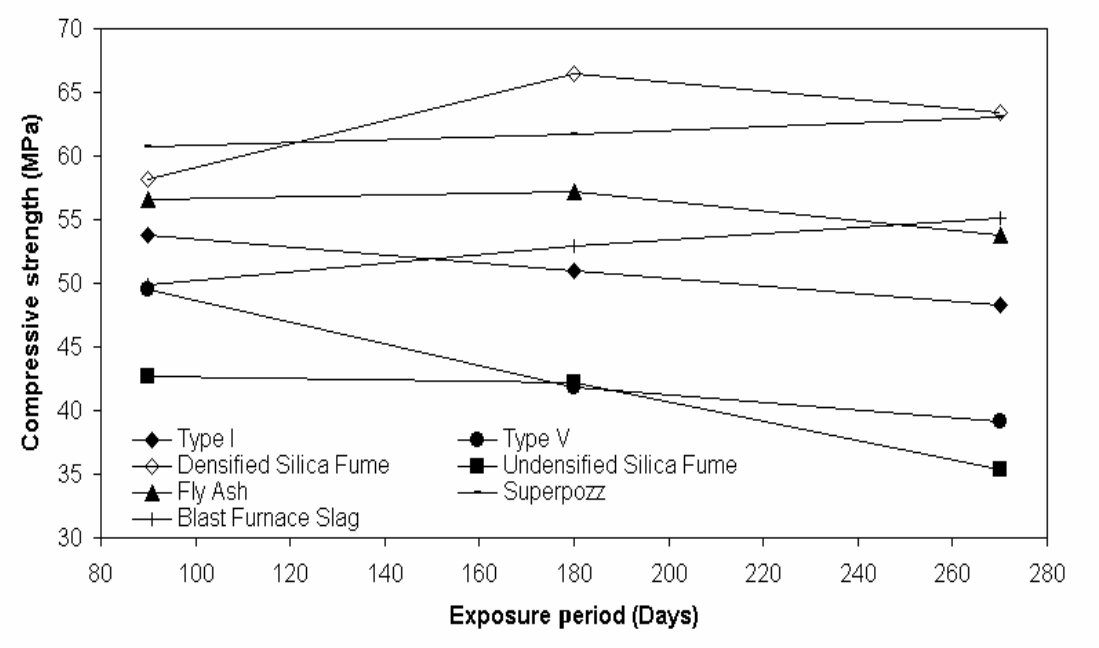

Figure 4.34: Compressive strength of specimens exposed to salt solution

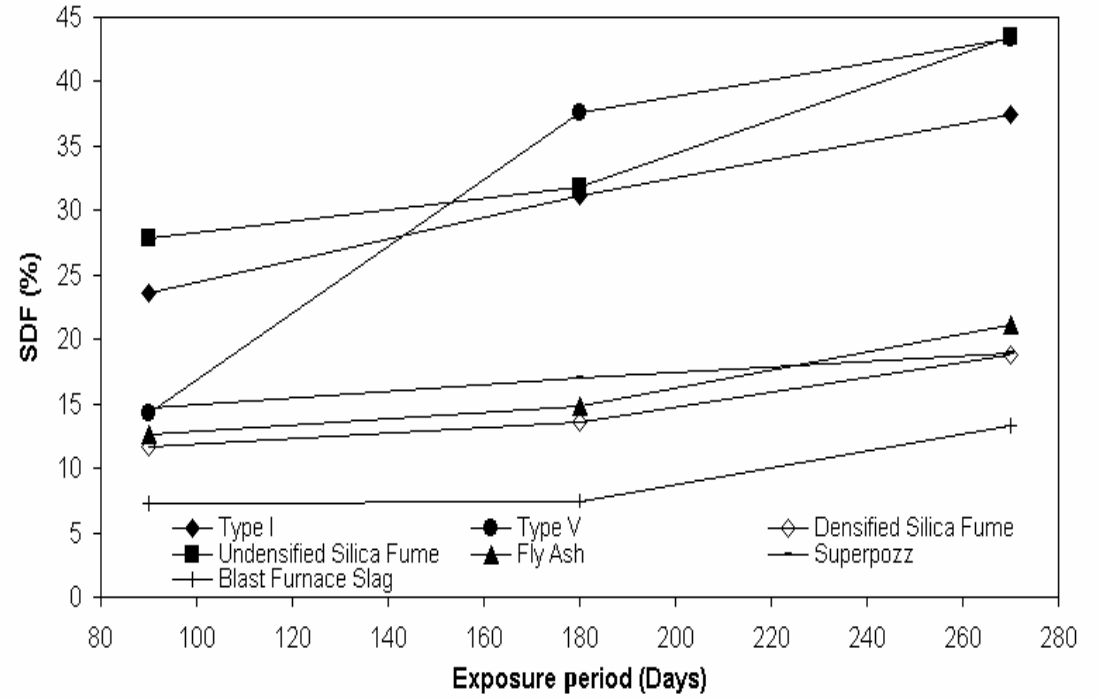

Figure 4.35: Strength deterioration factor due to salt weathering

The strength deterioration in the blended cement mortar specimens may be ascribed to the salt crystallization that occurs in their fine pores causing expansion, flaking and spalling (Mehta, 2000).

A comparison of the strength deterioration factors due to sulfate attack and salt weathering, as presented in Table 4.18, indicates that the undensified silica fume cement exhibited the worst performance when exposed to both media, while the best performance was shown by the blast furnace slag cement. This supports the use of the blast furnace slag in marine structures and in structures in contact with groundwater.

The surprising result is the behavior shown by Type V cement when exposed to salt weathering, which had a very high strength deterioration factor. However, its performance in the sulfate solution was better than Type I cement.

CARBONATION

Cylindrical mortar specimens, 37.5 mm in diameter and 75 mm high, were cast and water cured for 14 days. They were then left to dry in air for extra 14 days. Thereafter, they were kept in a carbonation chamber with 3.0 % carbon dioxide concentration.

The depth of carbonation in the plain and blended cement mortar specimens is presented in Table 4.19 and Figure 4.36. After 3 months of exposure, maximum carbonation was noted in the BFS cement, which could be related to the high replacement of the cement by slag, which reduces the portlandite content in the mortar thereby making it more susceptible to carbonation. Further, the high cement replacement exacerbates the inferior properties of this cement at the initial stages of curing, as evidenced by the slow

Table 4.18: Comparison of strength deterioration factors due to sulfate attack and salt weathering

Cement Type	SDF (Salt weathering)			SDF (Sulfate attack)		
	90 Days	180 Days	270 Days	90 Days	180 Days	270 Days
Type I	23.56	31.19	37.40	14.22	15.21	21.79
Type V	14.28	37.54	43.30	5.01	16.16	19.89
Densified Silica	11.60	13.62	18.73	10.03	11.44	19.39
Undensified Silica	27.86	31.83	43.46	17.51	26.61	31.60
Fly Ash	12.61	14.85	21.18	10.91	18.96	23.12
Superpozz	14.68	16.96	18.93	7.75	11.85	17.35
Blast Furnace Slag	7.29	7.46	13.24	4.44	5.27	9.27

Table 4.19: Depth of carbonation in the mortar specimens

Cement Type	Carbonation Depth (mm) at:		
	3 Months	6 Months	9 Months
Type I	1.20	1.60	2.05
TypeV	1.80	2.05	2.45
Superpozz	1.00	1.25	1.30
Blast Furnace Slag	2.15	2.20	2.30
Fly Ash	1.75	2.10	2.20
Densified Silica	0.60	0.75	0.90
Undensified Silica	0.65	0.80	0.90

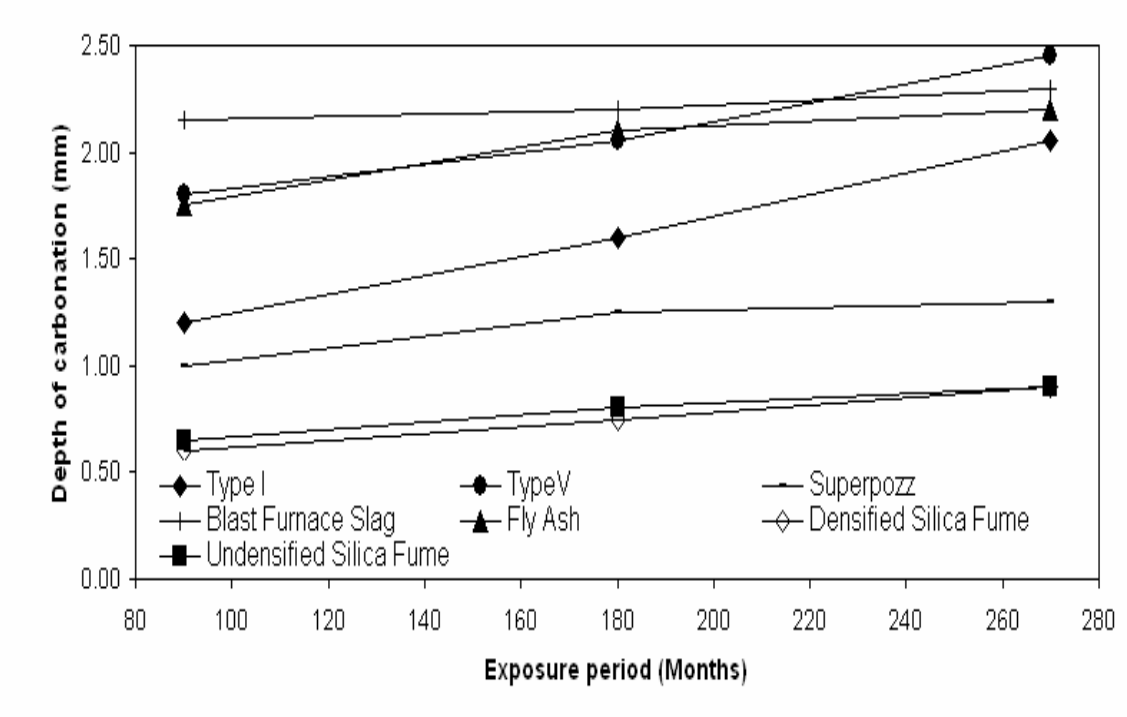

Figure 4.36: Carbonation profiles in mortar specimens

compressive strength development (Table 4.16), which tends to increase the carbonation depth. The depth of carbonation in the silica fume cements was less than that in the plain and other blended cements. The pore refinement through the use of silica fume prevents the diffusion of carbon dioxide through the mortar paste. After 9 months of exposure, the depth of carbonation in all the plain, BFS and FA cements was almost similar, around 2.20 mm. The depth of carbonation in the SF cements was the minimum followed by the superpozz cement.

4.2.2. Plain Concrete Specimens

STRENGTH DEVELOPMENT

The strength development of concrete specimens, 75 mm in diameter and 150 mm high, was assessed by applying a compressive load at a rate of 3.3 kN/s. Pulse velocity was determined on the air dried specimens through the use of ultrasonic pulse-velocity technique.

The data on strength development and pulse velocity of the plain and blended cement concretes is summarized in Tables 4.20 and 4.21 and Figures 4.37 and 4.38. Among plain cements, Type I cement concrete exhibited the highest rate of strength development in the first 7 days followed by a gradual increase in strength between 7 days and 6 months wherein no significant increase in the compressive strength was observed. A similar trend in strength development was noted in Type V cement concrete specimens. Kosmatka et. al. (2002) stated that the high initial compressive strength of Type I cement concrete may be ascribed to the greater C_3S content as compared with that in Type V

Table 4.19: Compressive strength development in plain and blended cement concretes

Cement Type	Compressive strength, MPa				
	7 days	14 days	28 days	90 days	180 days
Type I	33.36	35.91	37.55	38.11	40.77
Type V	26.09	33.11	34.76	35.18	40.79
Superpozz	24.86	31.45	36.08	36.25	39.90
Blast Furnace Slag	22.12	25.33	29.80	34.54	37.04
Fly Ash	29.43	32.02	35.21	37.25	41.84
Densified Silica	31.70	32.77	36.28	40.59	41.76
Undensified Silica	30.90	32.24	32.84	39.16	42.93

Table 4.20: Pulse velocity in plain and blended cement concretes

Cement Type	Pulse Velocity, m/s				
	7 days	14 days	28 days	90 days	180 days
Type I	4555	4718	4758	4818	4953
Type V	4545	4689	4753	4864	4922
Superpozz	4743	4808	4815	4908	4964
Blast Furnace Slag	4572	4591	4763	4819	4909
Fly Ash	4278	4758	4803	4818	4932
Densified Silica	4000	4632	4637	4670	4818
Undensified Silica	4229	4600	4723	4817	4880

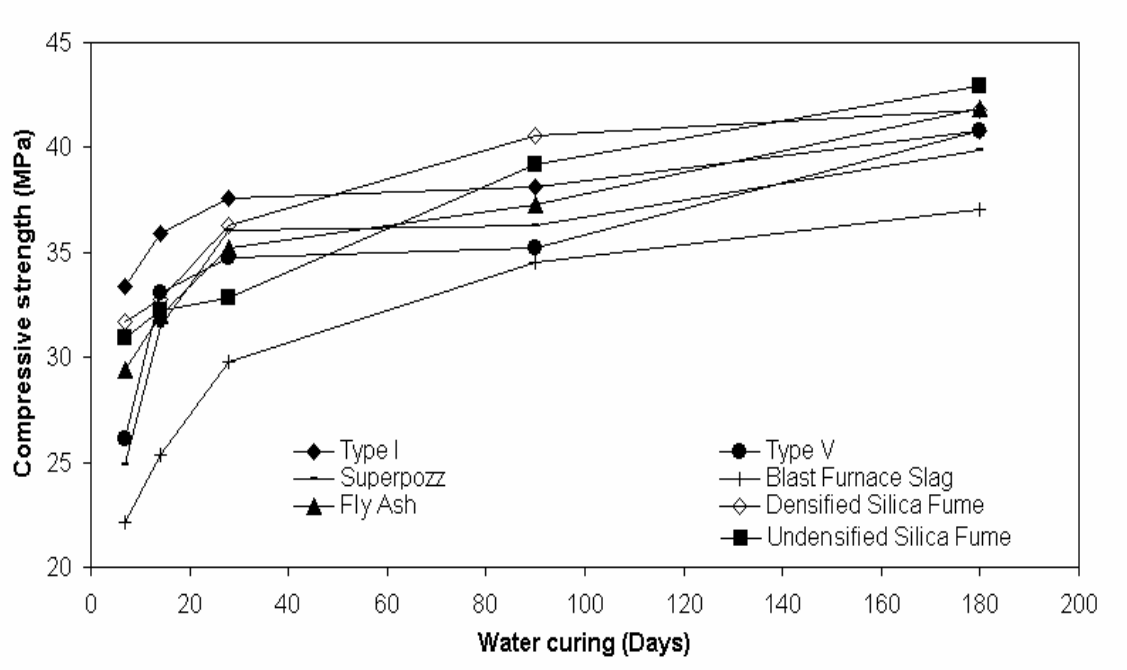

Figure 4.37: Strength development in water-cured concrete specimens

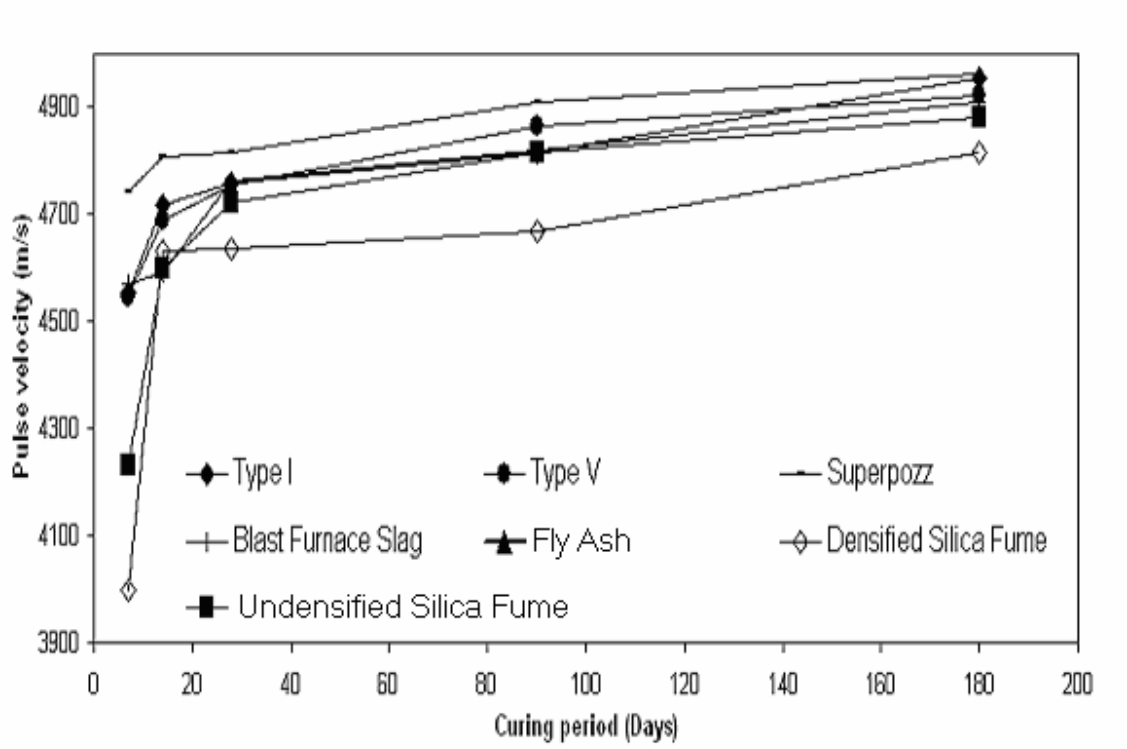

Figure 4.38: Pulse velocity in water-cured concrete specimens

cement. Kosmatka et. al. (2002) also reported that the delayed strength gain in Type V cement concrete might be attributed to the higher C_2S, which hydrates slowly and contributes largely to the strength increase at later ages beyond two weeks.

The compressive strength of all the blended cements concrete specimens used in this research was less than that of Type I cement concrete specimens in the first 28 days. This may be attributed to the low pozzolanic activity of these materials. Even after 3 months of curing, the compressive strength of blended cements was less than that of Type I cement with the exception of densified silica fume cement concrete, which exhibited higher strength than Type I cement concrete.

The compressive strength of fly ash and undensified silica fume cement concrete specimens was more than that of Type I cement concrete specimens after 6 months. On the other hand, the compressive strength of blast furnace slag cement was the lowest among all plain and blended cements. The large replacement of cement by the slag may be the reason for the low strength of that cement.

For most of the concrete specimens tested, it is clear that the intense acceleration in pore densification occurs in the first 28 days, and after that the rate of pore refinement becomes slow. The rate of acceleration in pore refinement decreased with time, except in Type V and supperpozz cement concretes, which show more acceleration after 3 months of water curing (Figure 4.38). After 28 days of curing, the pulse velocity in all the blended cement concrete specimens was more than that in the plain cement concrete specimens with the exception of the silica fume cement concrete specimens which exhibited the lowest pulse velocity.

HEAT-COOL EXPOSURE

Plain concrete specimens were exposed to alternate heating (70º C) and cooling (room temperature) for 8 hours and 16 hours, respectively. Tables 4.22 through 4.24 and Figures 4.39 through 4.41 show the compressive strength, pulse velocity and water absorption in the concrete specimens exposed to heat-cool cycles. The compressive strength of all the concrete specimens increased with increasing heat-cool cycles. The increase in the compressive strength with increasing heat-cool cycles might be attributed to the acceleration of the hydration reactions by heating (Figure 4.39). A tremendous increase in the compressive strength was noted in the densified silica fume cement concrete specimens after 90 heat-cool cycles. Blast furnace slag cement concrete showed uniform increase in strength throughout the test duration, which could be attributed to the minimal content of cement in this concrete and the delayed pozzolanic reaction. The fly ash cement concrete exhibited a sharp increase in strength initially followed by a reduced rate of strength gain. This behavior of fly ash cement concrete may be justified due to the low water content within this concrete. Upon continued heating, the water within the pores may evaporate leading to retarded hydration reaction due to the loss of water needed to complete the process.

The pulse velocity in all the concrete specimens decreased with the extended exposure to heat-cool cycles (Figure 4.40). This may be attributed to the formation of micro cracks in the concrete. Another point to note is that the pulse velocity of blast furnace slag and fly ash cement concretes was more that that of plain cements while the pulse velocity of the two silica fumes and superpozz® cement concretes is less. This trend indicates that some

Table 4.22: Compressive strength of concrete specimens exposed to heat-cool cycles

Cement Type	Compressive strength, MPa		
	0 Cycles	90 Cycles	180 Cycles
Type I	38.9	40.5	44.2
Type V	38.8	41.5	47.7
Superpozz	35.7	37.2	44.5
Blast Furnace Slag	29.2	36.6	43.4
Fly Ash	33.8	43.2	45.7
Densified Silica	35.0	44.2	49.6
Undensified Silica	38.2	44.2	47.3

Table 4.23: Pulse velocity of concrete specimens exposed to heat-cool cycles

Cement Type	Pulse Velocity, m/s		
	0 Cycles	90 Cycles	180 Cycles
Type I	4618	4563	3945
Type V	4733	4380	3762
Superpozz	4685	4476	3928
Blast Furnace Slag	4331	4237	4014
Fly Ash	4744	4549	4253
Densified Silica	4465	4180	3868
Undensified Silica	4632	4172	3744

Table 4.24: Water absorption in the concrete specimens exposed to heat-cool cycles

Cement Type	Water Absorption, %		
	0 Cycles	90 Cycles	180 Cycles
Type I	5.07	5.58	5.73
Type V	4.78	5.37	5.61
Superpozz	4.20	5.37	5.45
Blast Furnace Slag	4.95	5.73	5.90
Fly Ash	4.37	5.22	5.36
Densified Silica	5.51	6.71	6.86
Undensified Silica	5.03	5.61	5.93

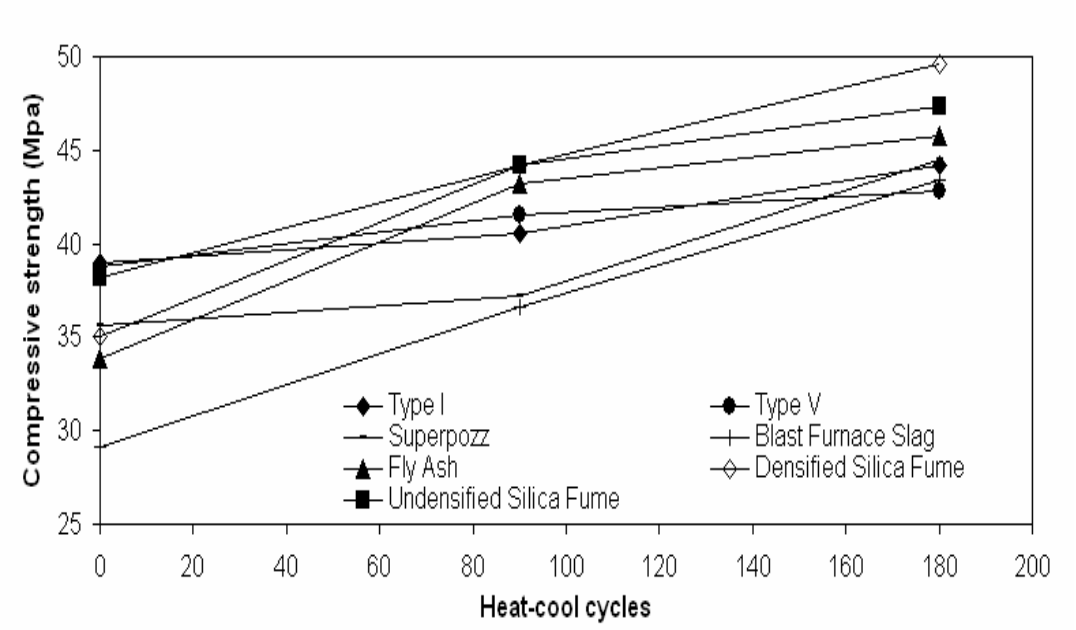

Figure 4.39: Compressive strength of the concrete specimens exposed to heat-cool cycles

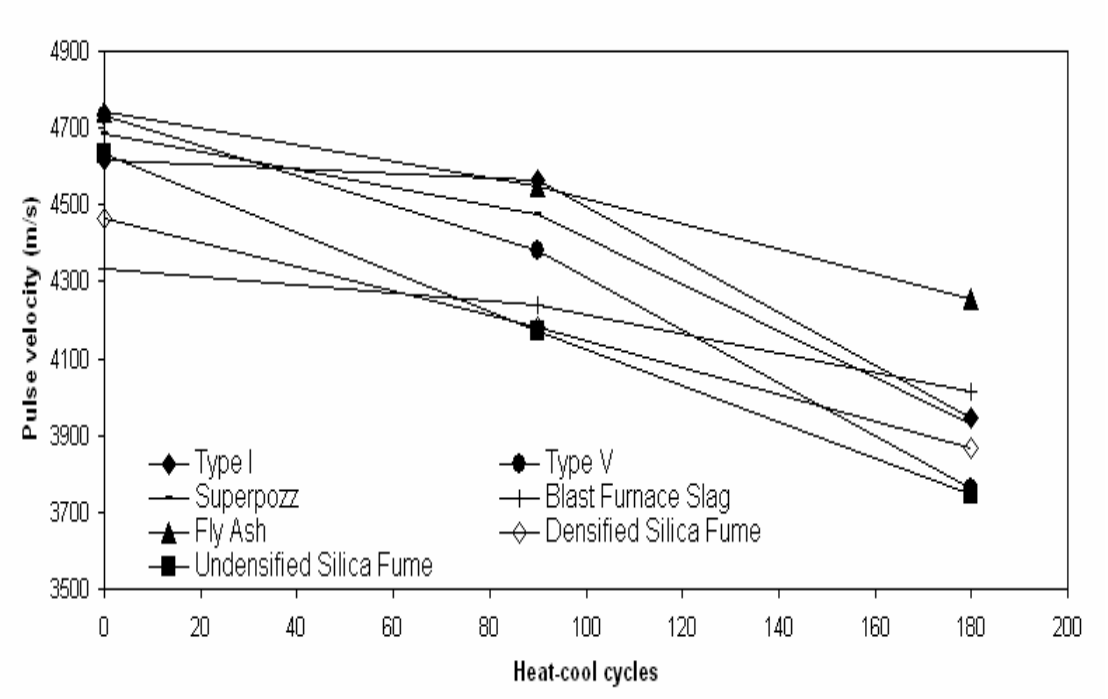

Figure 4.40: Pulse velocity in the concrete specimens exposed to hot-cool cycles

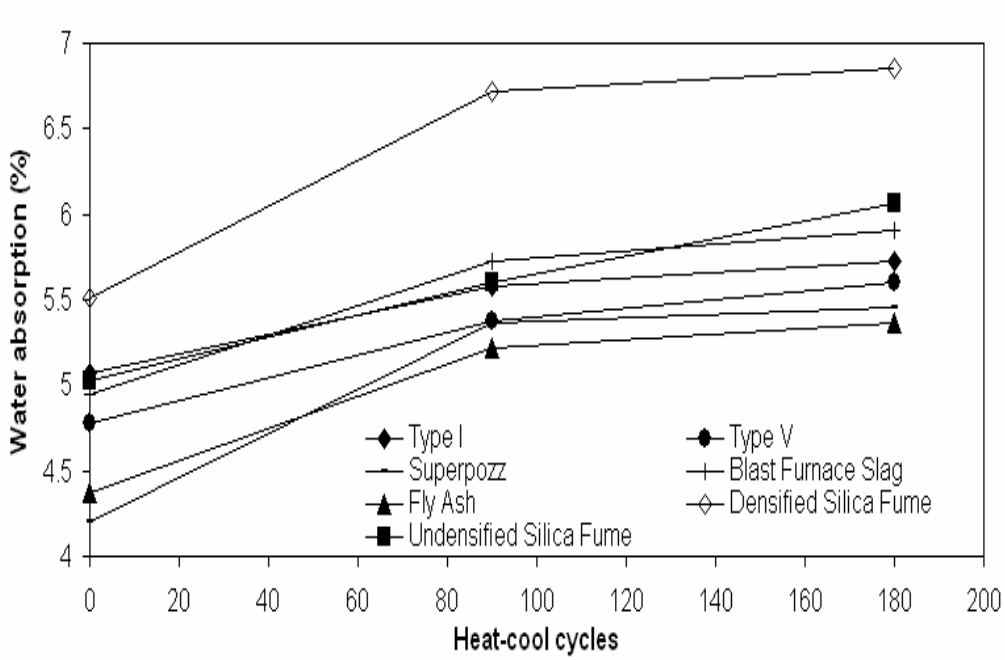

Figure 4.41: Water absorption in the concrete specimens exposed to hot-cool cycles

blended cements may be prone to cracking due to the extended exposure to heat-cool cycles.

The water absorption in all the concrete specimens increased with the number of heat-cool cycles, as shown in Figure 4.41. Both fly ash and supperpozz concretes exhibited the best performance in terms of water absorption compared to plain cements. The water absorption in the silica fume and blast furnace slag cement concrete specimens was more than that of plain cements. These data also show that silica fume cements were affected by the exposure to thermal cycles more than other cements.

CHLORIDE PERMEABILITY

The ingress of the chloride ions into concrete was evaluated by measuring the current passing through the speciemen for six hours according to AASHTO T-277 (ASTM C 1202). The results, obtained in Table 4.25 and Figure 4.42, are rated according to the AASHTO T-277 standard in Table 4.26. The general observation from this experiment is that the penetrability of the chloride ions in both the plain and blended cement concretes decreased with increasing the curing period, which was ascribed to the denser matrix and less pore voids due to the continuing hydration.

According to the ranges suggested by AASHTO T-277, after 28 days of water curing, the chloride permeability in the Type I and V cement concretes was low and moderate, respectively. The chloride permeability in Type I cement as compared to that of Type V cement may be ascribed to the higher C_3A content in the Type I cement that complexes with the chloride ions thereby reducing the free chloride content in the

Table 4.25: Chloride permeability in plain and blended cement concrete specimens

Cement Type	Chloride Permeability, Coulombs		
	28 DAYS	3 MONTHS	6 MONTHS
Type I	1815	1409	1192
Type V	2322	1538	1488
Superpozz	679	653	636
Blast Furnace Slag	427	426	414
Fly Ash	597	519	430
Densified Silica	782	689	580
Undensified Silica	486	459	429

Table 4.26: Chloride ion penetrability based on the charge passed according to AASHTO T-277

Charge Passed (Coulombs)	Chloride Ion Penetrability
> 4,000	High
2,000-4,000	Moderate
1,000-2,000	Low
100-1,000	Very low
< 100	Negligible

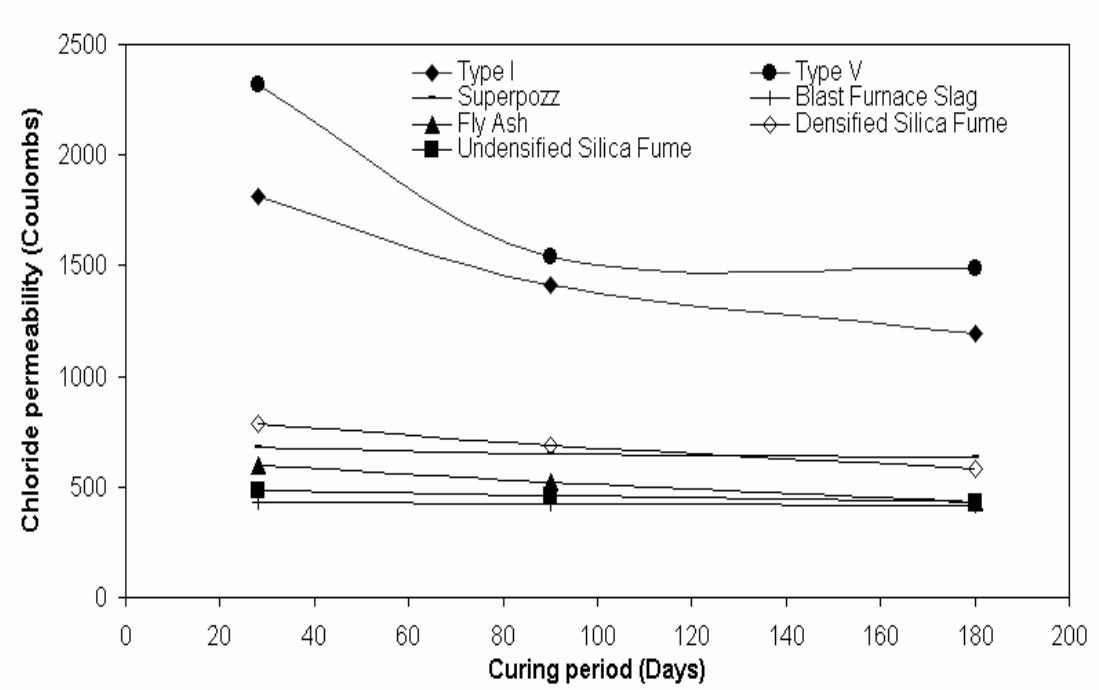

Figure 4.42: Chloride permeability of plain and blended cement concrete specimens

concrete matrix. This trend was noted at all ages of curing by Özturan and Güneyisi (2000) as well.

The chloride ion permeability of all the blended cement concrete specimens was low. The enhanced densification of the concrete matrix by the addition of mineral admixtures decreased the rate of permeation of chloride ions through concrete. Blast furnace slag, undensified silica fume and supperpozz exhibited no big variation in the chloride permeability with the curing period, while densified silica fume and fly ash showed marked decrease in the chloride permeability at 28 and 90 days of curing. Such a trend was reported by Özturan and Güneyisi (2000).

Among the blended cements investigated, blast furnace slag and undensified silica fume cements exhibited the lowest chloride ion penetration values.

CHLORIDE DIFFUSION

Cylindrical concrete specimens were water-cured for 14 days and thereafter air dried in the laboratory for another 14 days. Then, they were conditioned by cutting the top 25 mm using a saw and the circumferential and bottom surfaces of the concrete specimens were coated with epoxy resin leaving only the top surface uncoated. Thereafter, the concrete specimens were immersed in 15.7 % Cl^- plus 0.55% SO_4^{2-} (i.e., sabkha brine) solution for 9 months. After this, the concrete specimens were sliced in ten equal parts and pulverized into powder. The powder samples were chemically analyzed to determine the water-soluble chloride concentration.

The chloride concentration profiles for the plain and blended cement concrete specimens are plotted in Figure 4.43. The high chloride diffusion profile obtained in plain cements may be attributed to the relatively large pores in the concrete matrix, which allow easy diffusion of chloride ions. As expected, the chloride ion concentration is very high initially and decreases with the depth. However, at a depth of 50 mm, the chloride ion concentration is fairly similar in almost all the concrete specimens regardless of the type of cement.

The refinement of the pore structure of the concrete matrix due to the addition of pozzolanic materials mitigates to some extent the diffusion of harmful chloride ions into the concrete. In ordinary Portland cements, the C_3A complexes with the chloride ions to form Friedel's salts. This is true in the case of chlorides present at the stage of mixing, while for external chlorides, a small amount of chloroaluminates is formed and, at later stage, they may become dissociated (Neville, 1995). In the case of blended cements, concretes prepared with either densified silica fume or blast furnace slag exhibited high concentrations of chlorides at the top surface layers and low diffusion profiles inwards. Despite the pore refinement, the presence of Mg-sulfate ions in the solution might have caused softening of the surficial layer thereby providing more access to the chloride ions (Al-Amoudi, 1998). While in the case of fly ash and superpozz, the stable chloride profiles were reached after 45 and 60 mm depth, respectively. This could be ascribed to the presence of high Al_2O_3 in the two minerals; 25.3% in fly ash and 34.3% in the superpozz.

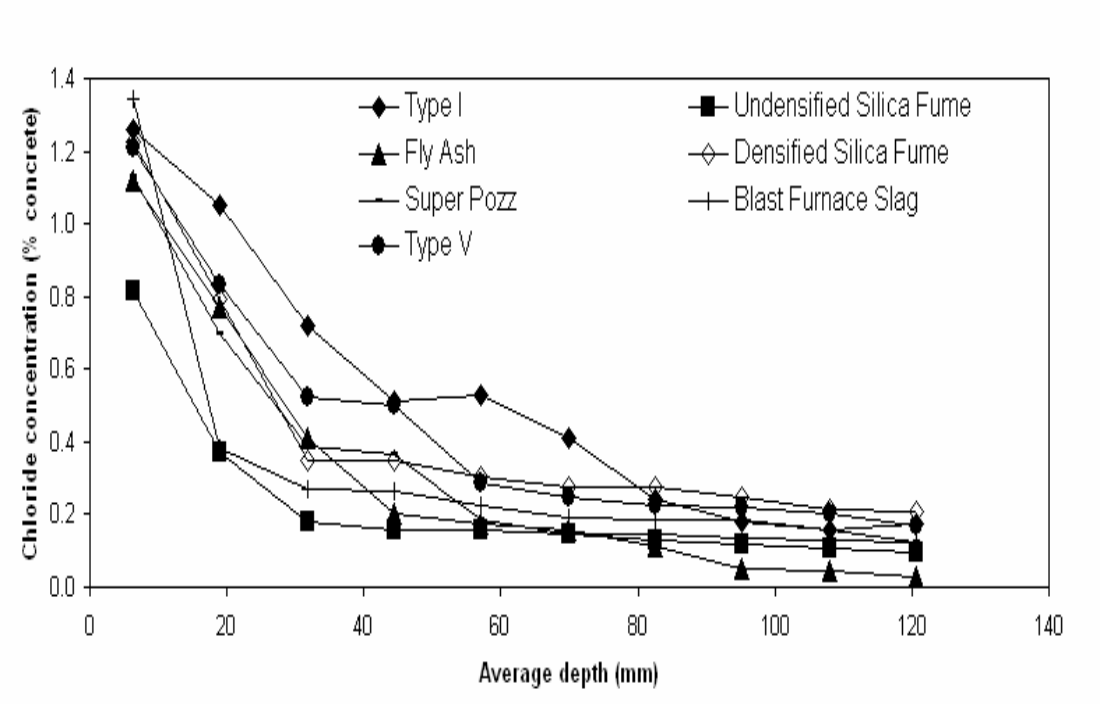

Figure 4.43: Chloride diffusion profiles for plain and blended cement concretes

4.2.3 Reinforcement Corrosion

TIME TO INITIATION OF REINFORCEMENT CORROSION

The corrosion potentials on steel in the concrete specimens immersed in the 5% NaCl and 15.7% Cl^- + 0.55% SO_4^{2-} solutions are shown in Figures 4.44 and 4.45, respectively.

The time to initiation of reinforcement corrosion was taken as the one corresponding to a corrosion potential of –270 mV SCE, according to ASTM C 876. These data are summarized in Table 4.27.

From the results reported in Table 4.27, it is clear that the time to initiation of reinforcement corrosion in the specimens immersed in sabkha solution (i.e., 15.7% Cl^- + 0.55% SO_4^{2-}) is much less than that of the specimens exposed to 5% NaCl solution. This may be attributed to the high concentration of the chloride ions present in the chloride plus sulfate solution. Secondly, the concomitant presence of sulfate ions accelerates the corrosion process. The presence of sulfate ions may help in diffusing more chloride ions through the concrete matrix to the concrete-steel interface by causing scaling and/or softening of the concrete matrix.

The time to initiation of corrosion in the Type I cement concrete exposed to the chloride solution was 32 days compared to 30 days for the steel in Type V cement concrete. The time to initiation of reinforcement corrosion in the blended cement concretes was more than that in the plain cement concrete. The time of initiation of reinforcement corrosion in the silica fume cement concrete specimens was more than that in the other blended cement concretes. This may be attributed to the extensive pore

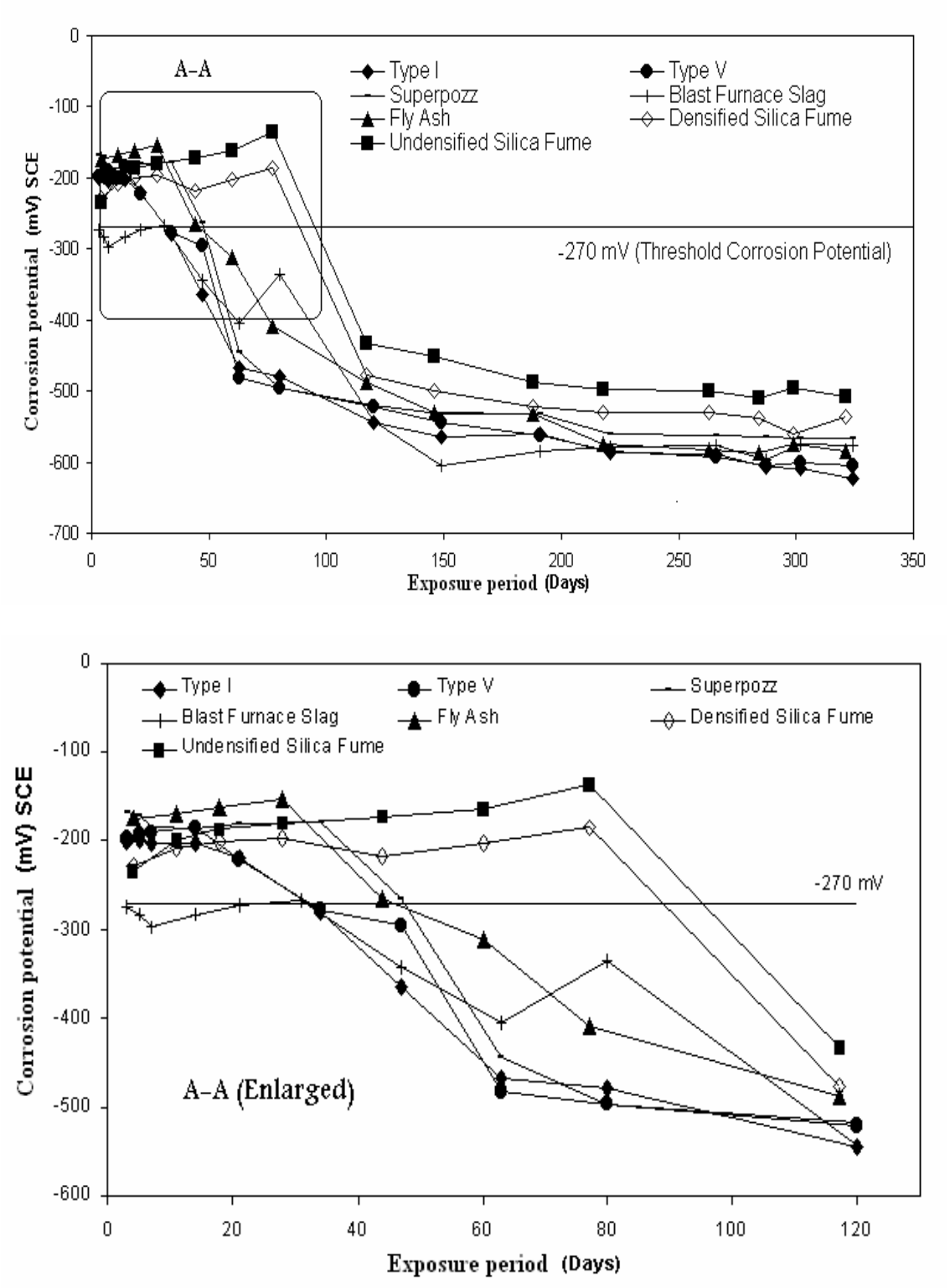

Figure 4.44: Corrosion potentials on steel in the concrete specimens exposed to chloride solution

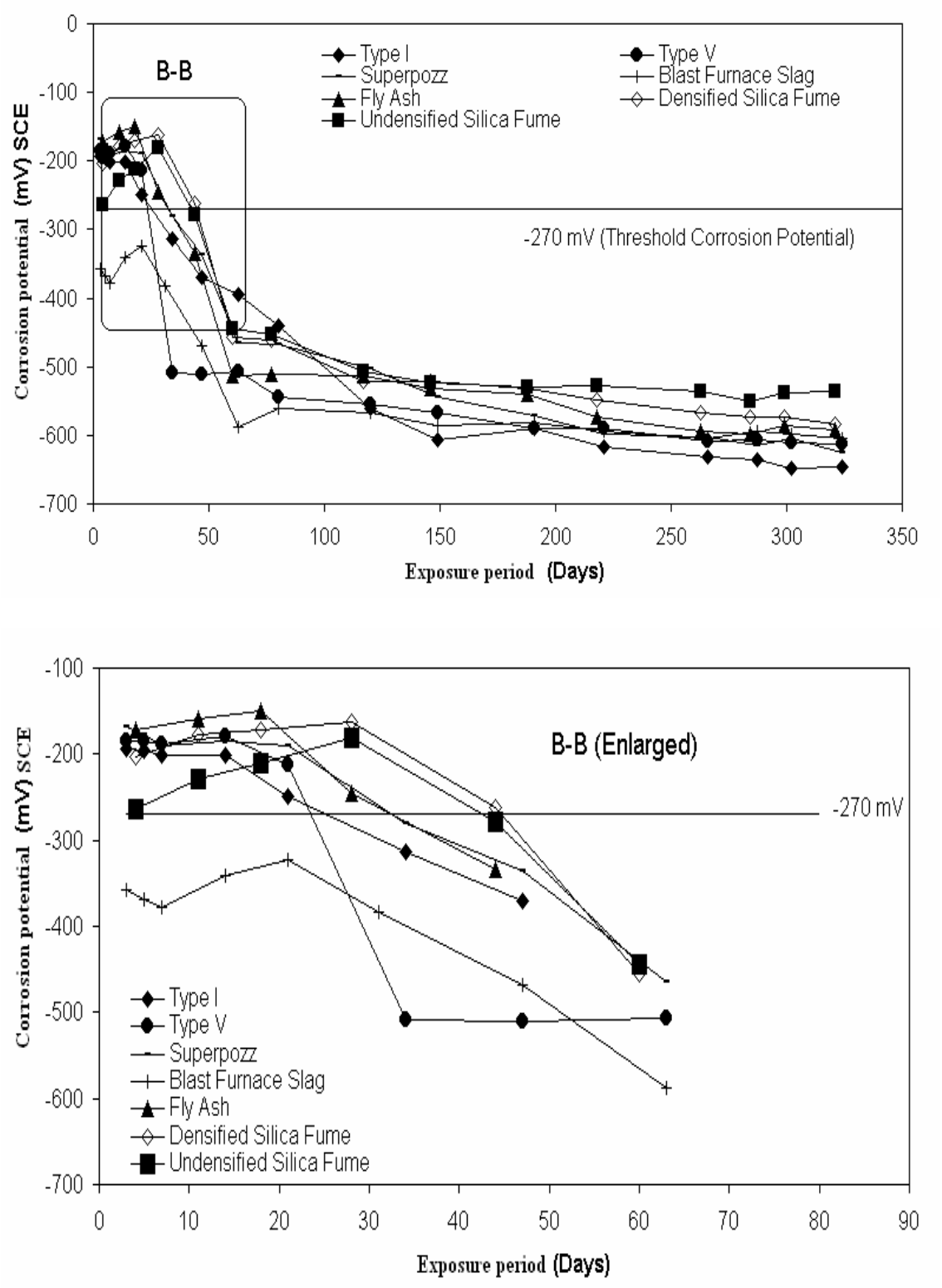

Figure 4.45: Corrosion potentials on steel in the concrete specimens exposed to chloride-sulfate solution

Table 4.27: Time to initiation of reinforcement corrosion

Cement Type	Time to Initiation of Reinforcement Corrosion, Days	
	Chloride Solution (5%Chloride)	Sabkha Solution (15.7%Chloride + 0.55% Sulfate)
Type I	**32**	**25**
Type V	**30**	**24**
Superpozz	**48**	**33**
Blast Furnace Slag	**N.A**	**N.A**
Fly Ash	**49**	**38**
Densified Silica Fume	**89**	**45**
Undensified Silica Fume	**95**	**42**

refinement in the hardened cement paste matrix due to the addition of silica fume that decreases the difussion of the chloride ions to the steel surface.

In the case of sabkha solution, the presence of the sulfate ions in the solution accelerates the corrosion process in the plain cements. The sulfate ions present in the solution weaken the concrete thereby accelerating the diffusion of chloride ions to the steel surface.

In the case of blended cements, there is a marginal difference in the time to initiation of reinforcement corrosion for the concretes made with superpozz or fly ash when exposed to the two solutions. However, there is great reduction in the time to initiation of reinforcement corrosion in the two types of silica fume cements. These silica fume concretes displayed the best performance for the initiation time in the sabkha solution. However, the sabkha solution is much more aggressive than that of the chloride solution. This aggressivity is reflected by the reduced time to initiation of reinforcement corrosion of the steel in all the concrete specimens when exposed to the sabkha solution. This aggressivity is due to the high chloride concentration (157,000 ppm compared to 50,000 ppm). Further, the concomitant presence of Mg-sulfate in the sabkha solution degrades the concrete matrix thereby allowing more chloride ions to diffuse to the steel surface.

The corrosion potentials on steel in the blast furnace slag cement concrete specimens were more than –270 mV SCE from the earlier stages of exposure. This indicates that the ASTM C 876 criteria of –270 mV SCE is not applicable to this type of cement (Maslehuddin et. al., 1990).

CORROSION CURRENT DENSITY

The corrosion current density (I_{corr}) on steel in the plain and blended cement concrete specimens is shown in Tables 4.28 and 4.29 and plotted in Figures 4.46 and 4.47. For the specimens immersed in the chloride solution, the I_{corr} on steel in Type I cement concrete was less than that on Type V cement. After more than 13 months of exposure to the chloride solution, the I_{corr} on steel in Type I cement concrete specimens was 1.045 $\mu A/cm^2$ compared to 1.084 $\mu A/cm^2$ on steel in Type V cement concrete specimens.

The better performance of Type I cement is mainly ascribed to its high C_3A content of 8.52% in comparison with 3.5% in Type V cement. The C_3A reacts with the intruding chloride ions forming Friedel's salts thereby mitigating the free chloride ions in the pore solution and reducing the corrosion activity.

Blended cements displayed superior performance in resisting reinforcement corrosion due to the pore refinement, which inhibits the ingress of the harmful chloride ions to the steel surface. Among the blended cements used, both the densified and undensified silica fume exhibited the best resistance to reinforcement corrosion, with corrosion current density of 0.241 and 0.207 $\mu A/cm^2$, respectively, after more than 13 months of exposure. From the data in Table 4.46, it is clear that the steel reinforcement in silica fume concrete specimens was the only one that did not reach the active state, defined as 0.3 $\mu A/cm^2$ (Andrade et. al., 1986), and still in the passive state after about 13 months of exposure to the chloride solution.

Table 4.28: Corrosion current density on steel in the concrete specimens exposed to chloride solution

Cement Type	I_{corr} (μA/cm^2) after									
	40 days	78 days	120 days	150 days	175 days	207 days	252 days	303 days	359 days	408 days
Type I	0.178	0.338	0.354	0.620	0.659	0.676	0.704	0.844	0.960	1.045
Type V	0.121	0.225	0.452	0.676	0.716	0.735	0.816	0.877	1.016	1.084
Superpozz	0.037	0.256	0.323	0.368	0.381	0.396	0.412	0.489	0.530	0.546
Blast Furnace Slag	0.043	0.066	0.241	0.468	0.518	0.546	0.625	0.626	0.656	0.679
Fly Ash	0.089	0.167	0.285	0.305	0.317	0.333	0.368	0.453	0.485	0.555
Densified Silica	0.021	0.024	0.127	0.171	0.199	0.217	0.187	0.199	0.231	0.241
Undensified Silica	0.021	0.016	0.127	0.212	0.229	0.238	0.170	0.187	0.201	0.207

Table 4.29: Corrosion current density on steel in the concrete specimens exposed to chloride-sulfate solution

Cement Type	I_{corr} (μA/cm^2) after									
	40 days	78 days	120 days	150 days	175 days	207 days	252 days	303 days	359 days	408 days
Type I	0.131	0.386	0.583	0.584	0.579	0.605	0.883	1.080	1.269	1.402
Type V	0.155	0.443	0.685	0.719	0.744	0.761	0.932	1.020	1.273	1.433
Superpozz	0.105	0.200	0.305	0.301	0.303	0.328	0.501	0.522	0.553	0.578
Blast Furnace Slag	0.251	0.274	0.284	0.464	0.547	0.529	0.636	0.653	0.673	0.698
Fly Ash	0.078	0.272	0.296	0.336	0.329	0.342	0.414	0.448	0.459	0.481
Densified Silica	0.079	0.147	0.191	0.205	0.207	0.215	0.273	0.274	0.288	0.303
Undensified Silica	0.025	0.109	0.195	0.226	0.221	0.237	0.189	0.194	0.204	0.215

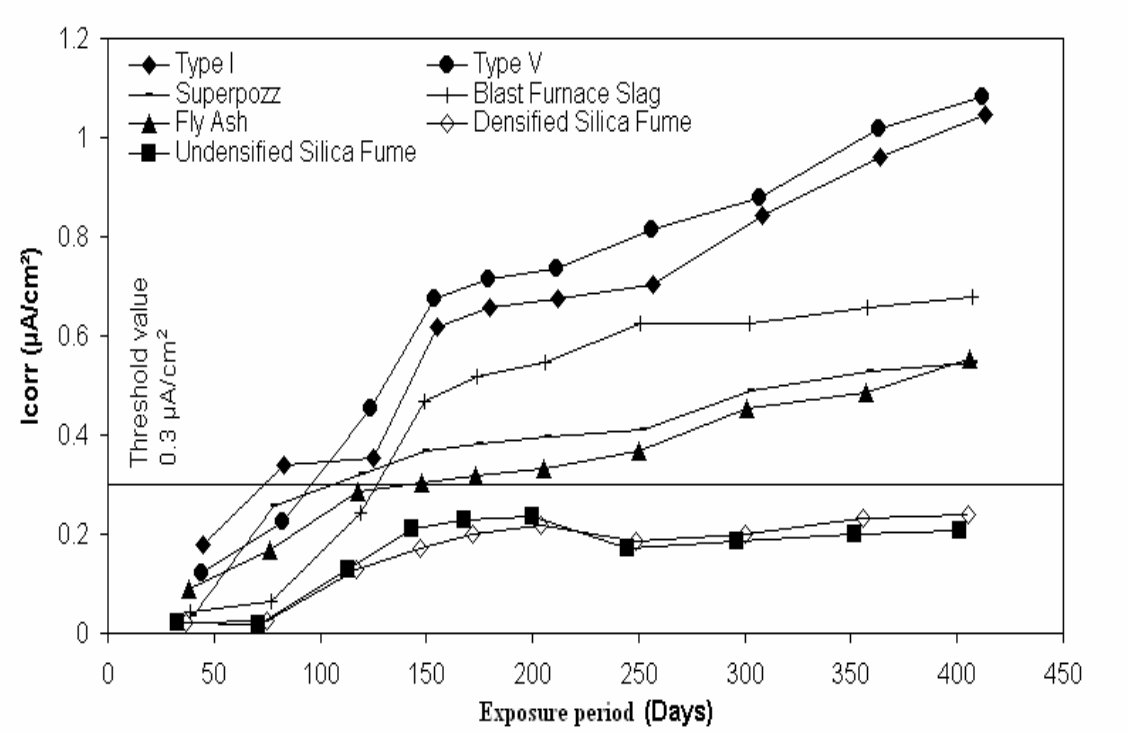

Figure 4.46: Corrosion current density on the steel in the concrete specimens exposed to the chloride solution

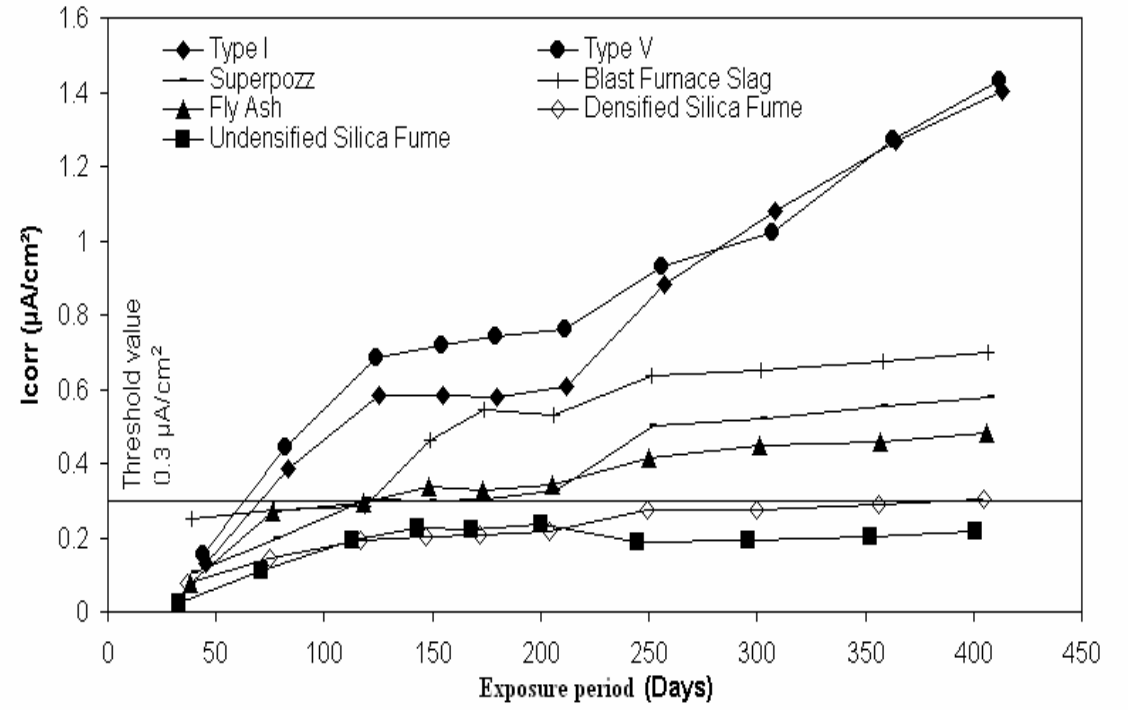

Figure 4.47: Corrosion current density on the steel in the concrete specimens exposed to the chloride-sulfate solution

The performance of ordinary Portland Type I cement reinforced concrete specimens placed in both the sabkha solution (i.e., 15.7% Cl^- plus 0.55% SO_4^{2-}) and the chloride solution were better than those made of Type V cement concrete. The presence of sulfate ions in the solution accelerates the rate of corrosion in these specimens and the corrosion current density was 1.402 $\mu A/cm^2$, as compared to 1.433 $\mu A/cm^2$ in Type V cement. The sulfate ions react with the Friedel's salt formed due to the reaction of C_3A with the chlorides, resulting in the liberation of the bound chlorides and increasing the chloride concentration within the reinforced concrete.

Fly ash cement concrete exhibited better performance than blast furnace slag and superpozz cement in terms of I_{corr}, as shown in Table 4.29. Furthermore, both types of silica fume cement reinforced concretes did not display any significant change in the corrosion current density value in the chloride solution. However, for the sabkha solution and after about 13 months of exposure, the I_{corr} was 0.303 $\mu A/cm^2$ and 0.215 $\mu A/cm^2$, for the densified and undensified silica fume cements, respectively, and the steel reinforcement in both types of concrete was still in a passive state of corrosion (I_{corr} is less than 0.3 $\mu A/cm^2$). This superiority of both types of silica fume in mitigating corrosion of reinforcing steel is a vivid manifestation of the ability of silica fume to improve the quality of concrete and serve well in both types of the aggressive exposures of pure chloride and sulfate plus chloride.

CHAPTER FIVE

CONCLUSIONS AND RECOMMENDATIONS

5.1 CONCLUSIONS

Based on the experimental work conducted in this investigation and the analysis of results, the following conclusions could be drawn:

5.1.1. Soil Properties

1. The sabkha soil was characterized as silty clayey sand (SM-SC) and silty or clayey sand (A-2-4) according to the USCS and AASHTO systems, respectively, when distilled water was used in the wet sieve analysis. When sabkha brine was used, the sabkha soil was classified as poorly-graded sand (SP) and fine sand (A-3) using the same classification systems. On the other, the clay soil was classified as inorganic clay with high plasticity (MH) and clayey soil (A-7-6 (20)) according to the same systems, respectively.
2. The sabkha brine used in the consolidation test was highly concentrated with a chloride ion concentration of 19% (as compared with 15.7% for the Ras Al-Ghar sabkha brine) indicating the hypersaline nature of the groundwater in Al-Qurrayah sabkha terrain.

3. The addition of clay to the sabkha soil increased the compressibility, particularly when distilled water was used. Generally, the addition of clay to the sabkha increased the preconsolidation pressure, swell index, void ratio and optimum water content of the sabkha soil.
4. The concentrated brine had a negative effect on the swelling behavior of the clay; probably due to ion exchange between the brine and the clay minerals.
5. The addition of clay to the sabkha soil reduced the percolation of sulfates through the soil layer, while there was an opposite action for the chlorides ions. The chlorides were found to be higher in the presence of the clay when distilled water was used as the percolation liquid.
6. The clay helped in removal of trace metals, mainly lead, zinc and manganese, from the percolating brine. The use of clay with the sabkha to act as a soil liner can help in the mitigation of the disposal of the trace metals to the ground water.

5.1.2. Concrete Properties

7. Blast furnace slag cement mortar exhibited the best resistance to Mg-based sulfate attack and salt weathering in chloride-sulfate solution. However, the undensified silica fume mortars exhibited the worst performance in these exposures.
8. Blast furnace slag and fly ash blended cement mortars exhibited the worst performance against carbonation among all the blended cements used in this investigation. The superior performance was noted in the densified and undensified silica fume cements.

9. The strength development was observed to be very sharp in the densified silica fume cement concrete specimens leading to a 28-day strength of 20% more than that of Type I cement concrete. The densified silica fume had the lowest values in terms of pulse velocity obtained among all the mixes. Both types of ordinary Portland cement concretes displayed no great variation in the pulse velocity test results.
10. The densified silica fume cement concrete exhibited a significant increase in strength upon hot-cool exposure. However, the undensified silica fume cement exhibited maximum reduction in the pulse velocity, while fly ash cement concrete showed better behavior than the other cements. Both fly ash and supperpozz cement concretes displayed the best performance in terms of water absorption. Densified silica fume displayed the worst situation upon surface drying; it had the highest value of water absorption.
11. After 28 days of water curing, Type V cement concrete had a moderate penetrability of chloride ions as compared with the low penetrability in Type I cement concrete. All the blended cement concrete specimens displayed very low chloride ion permeability at all ages. Among the blended cements investigated, blast furnace slag cement had the lowest chloride permeability.
12. The lowest time to initiation of reinforcement corrosion was noted in the ordinary Portland cement reinforced concrete specimens exposed to the chloride solution. The best performance among the blended cements was noted in the undensified silica fume cement. The high concentration of chloride ions and the presence of sulfate ions in the sabkha solution helped decreased the time to initiation of reinforcement corrosion in all the reinforced concrete specimens.

13. The corrosion current density on steel in Type I cement concrete exposed to the chloride and sulfate-chloride solutions was less than that in Type V cement concrete. Further, all blended cements performed better than plain cements. Among blended cements, the undensified and densified silica fume cements displayed distinctly superior performance in terms of corrosion resistance in both solutions. The undensified silica fume cement exhibited better performance than the densified silica fume cement.

5.2 RECOMMENDATIONS

The recommendations outlined from this study can be summarized in the following:

- Clay could be used as additive in liners of sabkha soil. The addition of clay decreased the trace metals percolating the soil liner as well as the TDS and sulfate ions.
- The sabkha-clay liner is a good barrier between the underneath groundwater and the contaminated fluids flooded on the soil.
- Care should be taken when using the soil liner as a foundation material under concrete sub-structures; an increase in the chloride ions concentration was noted in the percolating fluid when clay was added to the sabkha.
- In the Gulf region, the main deteriorating factor is the chloride-induced corrosion of reinforcing steel. As a result, it is recommended to use blended cements, specially silica fume, to mitigate the concrete deterioration.

- When using silica fume as a partial replacement for cement in foundations, care should be taken regarding the surface treatment of concrete to minimize the sulfate attack.
- Curing should be given good attention since blended cements are affected very much by the curing conditions.

5.3 FURTHER SUGGESTIONS

In order to further understand the behavior of the clay-sabkha mixtures, the following studies should be conducted:

(i) Filtering mechanisms of trace metals and anions. Samples of leached water and brine should be analyzed through various stages of the soil consolidation.

(ii) Effect of sabkha brine on the swelling characteristics of clay in order to assess the effect of the brine concentration on the swelling and compressibility.

(iii) Study the soil structure and mineralogy before and after water or brine percolation.

For better understanding of the durability of ordinary Portland and blended cements, the following studies are suggested:

(i) The chloride diffusion after prolonged exposure periods, much longer than the 9-month exposure conducted in the present study.

(ii) The corrosion behavior of reinforcing steel embedded in blended cement concretes should be studied at elevated temperatures.

(iii) The effect of cation type associated with the sulfate anions on reinforcement corrosion separately.

REFERENCES

Abduljawad, S.N., Bayomy, F., Al-Shaikh, A.M. and Al-Amoudi, O.S.B. (1994). Influence of Geotextiles on Performance of Saline Sebkha Soils. *ASCE Journal of Geotechnical Engineering*, v. 120, n. 11, pp. 1939-1960.

Abu-Taleb, M.G. and Egeli, I. (1981). Some Geotechnical Problems in the Eastern Province of Saudi Arabia. *Proceedings, Symposium on Geotechnical Problems in Saudi Arabia,* v. 2, May, pp. 799-812.

ACI 201.2R-92. (1992). *Guide to Durable Concrete*. American Concrete Institute, Detroit, USA.

Ahmad, I. (1997). *Improvement of Eastern Saudi Sabkha Soils for Road Construction.* MS Thesis, Department of Civil Engineering, King Fahd University of Petroleum and Minerals, Dhahran, Saudi Arabia.

Aiban, S.A. (1994). A Study of Sand Stabilization in Eastern Saudi Arabia. *Engineering Geology*, v. 38, pp. 65-79.

Akili, W. (1981). On Sabkha of Eastern Saudi Arabia. *Proceedings, Symposium on Geotechnical Problems in Saudi Arabia,* Riyadh, v. 2, May, pp. 775-798.

Akili, W. and Ahmad, N. (1983). The Sabkhas of Eastern Saudi Arabia: Geotechnical Considerations. *Proccedings, First Saudi Engineering Conference*, King Abdulaziz University, Jeddah, May, pp. 300-322.

Akili, W. and Fletcher, E.H. (1978). Ground Conditions for Housing Foundations in Dhahran Region, Eastern Province, Saudi Arabia. *Proceedings, First International Conference on Housing Problems in Developing Countries,* Dhahran, v. 2, pp. 533-546.

Akili, W. and Torrance, J.K. (1981). The Development and Geotechnical Problems of Sabkha, with Preliminary Experiments on the Static Penetration Resistance of Cemented Sands. *Quarterly Journal of Engineering Geology*, v. 14, Part 1, pp. 59-73.

Al-Amoudi, O.S.B. (1992). *Studies on Soil-Foundation interaction in the Sabkha Environment of Eastern Province of Saudi Arabia*. PhD Dissertation, Department of Civil Engineering, King Fahd University of Petroleum and Minerals, Dhahran, Saudi Arabia.

Al-Amoudi, O.S.B. (1995). Soil Stabilization and Durability of Reinforced Concrete in Sabkha Environments. *Proceedings, Fourth Saudi Engineering Conference*, King Abdulaziz University, Jeddah, pp. 53-72.

Al-Amoudi, O.S.B. (1998). Mechanisms of Sulfate Attack in Plain and Blended Cements: A Review. *Proceedings, Symposium on Performance of Concrete Structures in the Arabian Gulf Environment*, KFUPM, Dhahran, November, pp. 172-188.

Al-Amoudi, O.S.B. (2002). Durability of Plain and Blended Cements in Marine Environments. *Advances in Cement Research*, v. 14, n. 3, July, pp. 89-100.

Al-Amoudi, O.S.B. and Abduljauwad, S.N. (1994). Modified Odometer for Arid, Saline Soils. Technical Note, *ASCE Journal of Geotechnical Engineering*, v. 120, n. 10, October, pp. 1892-1897.

Al-Amoudi, O.S.B., and Abduljauwad, S.N. (1994). Laboratory and Field Leaching Tests on Coastal Salt-Bearing Soils. *ASCE Journal of Geotechnical Engineering*, v. 120, n. 10, October, pp. 1900-1902.

Al-Amoudi, O.S.B. and Abduljauwad, S.N. (1995). Compressibility and Collapse Characteristics of Arid Saline Sabkha Soils. *Engineering Geology*, v. 39, pp. 185-202.

Al-Amoudi, O.S.B. and Maslehuddin, M. (1993). The Effect of Chloride and Sulfate Ions on Reinforcement Corrosion. *Cement and Concrete Research,* v. 23, n. 1, pp. 39-146.

Al-Amoudi, O.S.B, Asi, M.I. and El-Naggar, Z.R. (1995). Stabilization of an Arid, Saline Sabkha Soil using Additives. *Quarterly Journal of Engineering Geology*, v. 28, pp. 369-379.

Al-Amoudi, O.S.B., Maslehuddin, M. and Bader, M.A. (2001). Characteristics of Silica Fume and Its Impact on Concrete in the Arabian Gulf. *Concrete*, v. 35, n. 2, pp. 45-50.

Al-Amoudi, OS.B, Abduljauwad, S.N., El-Naggar, Z.R., Safar, M.M. (1991). Geotechnical Considerations on Field and Laboratory Testing of Sabkhas. *Proceedings, Symposium on Recent Advances in Geotechnical Engineering III,* Singapore, pp. 1-6.

Al-Amoudi, O.S.B., Abduljauwad, S.N., Rasheeduzzafar, M., and Maslehuddin, M. (1992). Effect of Chloride and Sulfate Contamination in Soils on Corrosion of Steel and Concrete. *Transportation Research Record,* n. 1345, pp. 67–73.

Al-Amoudi, O.S.B., Rasheeduzzafar, M., Maslehuddin, M., and Abduljauwad, S.N. (1994). Influence of Sulfate Ions on Chloride-induced Reinforcement Corrosion in Portland and Blended Cement Concrete. *Cement, Concrete and Aggregates,* v. 16, n. 1, pp. 3-11.

Al-Ayedi, E.S. (1996). *Chemical Stabilization of Al-Qurayyah Eastern Saudi Sabkha Soil*. MS Thesis, Department of Civil Engineering, King Fahd University of Petroleum and Minerals, Dhahran, Saudi Arabia.

Algahtani, A.S., Rasheeduzzafar, M. and Alsaadoun, S.S. (1994). Rebar Corrosion and Sulphate Resistance of Blast-furnace Slag Cement. *ASCE Journal of Materials in Civil Engineering,* v. 6, n. 2, pp. 223-231.

Al-Guwaizani, A.S. (1994). *Sedimentology and Geochemistry of Qurayyah Sabkha, Eastern Saudi Arabia*. MS Thesis, Department of Civil Engineering, King Fahd University of Petroleum and Minerals, Dhahran, Saudi Arabia.

Ali, S. M. (1999). *Interface Frictional Characteristics of Non-woven Geotextile-Sabkha and –Sand using Pull-out Tests*. MS Thesis, Department of Civil Engineering, King Fahd University of Petroleum and Minerals, Dhahran, Saudi Arabia.

Alsaadoun, S.S., Rasheeduzzafar, M., and Algahtani, A.S. (1993). Corrosion of Reinforcing Steel in Fly Ash Blended Cement Concrete. *ASCE Journal of Materials in Civil Engineering,* v. 5, n. 3, pp. 356-371.

Al-Shamrani, M.A and Dhowian, A.W. (1997). Preloading for Reduction of the Compressibility Characteristics of Sabkha Soil Profiles. *Engineering Geology,* v. 48, pp. 19-41.

Andrade, C., Castelo, V., Alonso, C., and Gonzalez, J.A. (1986). The Determination of the Corrosion Rate of Steel Embedded in Concrete by the Polarization Resistance and AC Impedance Methods. *ASTM STP 906*, American Society for Materials and Testing, Philadelphia, pp. 43-63.

Azad, A.K. (1998). Chloride Diffusion in Concrete and Its Impact on Corrosion of Reinforcement. *Proceedings, Symposium on Performance of Concrete Structures in the Arabian Gulf Environment*, KFUPM, Dhahran, pp. 262-273.

Barrow, N.J., Bowden, J.W., Posner, A.M. and Quirk, J.P. (1981). Describing The Adsorption of Copper, Zinc and Lead on a Variable Charge Mineral Surface. *Australian Journal of Soil Research*, v. 19, n. 4, pp. 309-321.

Boggs, Sam Jr. (1995). *Principles of Sedimentology and Stratigraphy*. 2nd edition, Prentice Hall, Upper Saddle River, New Jersey.

Broomfield, J.P. (1997). *Corrosion of Steel in Concrete: Understanding, Investigation and Repair.* E & FN Spon, London.

Butler, G.P. (1969). Modern Evaporite Deposition and Geochemistry of Coexisting Brines, the Sabkha, Trucial Coast, Arabian Gulf., reprinted from:

Jour. Sed. Petrol., v. 39, pp. 70-81, published in: *Marine Evaporites: Origin, Diagenesis, and Geochemistry*, Edited by: Douglas W. Kirkland and Robert Evans, Dowden, Hutchinson & Ross, Inc., pp. 91-103.

Bungey, J.H. (1982). *The Testing of Concrete in Structures.* Surrey University Press, New York.

Bush, P. (1973). Some Aspects of the Diagenetic History of the Sabkha in Abu Dhabi, Persian Gulf. in: *The Persian Gulf: Holocene Carbonate Sedimentation and Diagenesis in a Shallow Epicontinental Sea.* Editor B. H. Purser, Spriger-Verlag, Berlin, pp. 395-408.

Bye, G.C. (1999). *Portland Cement: Composition, Production and Properties.* 2nd edition, Thomas Telford, London.

Dehwah, H.A.F., Maslehuddin, M., and Austin, S.A. (2002). Long-term Effect of Sulfate Ions and Associated Cation Type on Chloride-induced Reinforcement Corrosion in Portland Cement Concretes. *Cement & Concrete Composites,* v. 24, n. 1, pp. 7–25.

Dewar, J. D. (1988). Composite Cements, Ground Granulated Blastfurnace Slag and Pulverized Fuel Ash Ready-mixed Concrete. *Municipal Engineer*, v. 5, pp. 207-216.

Eglinton, M.S. (1987). *Concrete and Its Chemical Behavior.* Thomas Telford, London.

El-Naggar, Z.R. (1988). Foundation Problems in Sabkhah Deposits. *Short Course: Foundation Engineering for Practicing Engineer*, KFUPM, Dhahran, April, SD1-SD54.

Fookes, P.G., French, W.J. and Rice, S.M.M. (1985). The Influence of Ground and Groundwater Geochemistry on Construction in the Middle East. *Quarterly Journal of Engineering Geology*, v. 18, pp. 101-128.

Haque, M.N. and Kawamura, M. (1990). Carbonation and Chloride Induced Corrosion of Reinforcement in Fly Ash Concretes. *ACI Materials Journal,* v. 89, n. 1, pp. 41-48.

Harrison, T.A., and Spooner, D.C. (1996). The Properties and Use of Concretes Made with Composite Cements. *Cement and Concrete Association*, Interim Technical Note No. 10.

Haynes, H. (2000). Sulphate Attack on Concrete – Laboratory versus Field Experience. *Fifth CANMET/ACI International Conference on Durability of Concrete*, Supplementary Papers, Barcelona, Spain, pp. 57-72.

Hobbs, D.W. and Matthews, J.D. (1998). Minimum Requirements for Concrete to Resist Deterioration due to Chloride-induced Corrosion; Minimum Requirements for Durable Concrete. *British Cement Association*, pp. 43-47.

Hsu, K.J. and Schneider, J. (1973). Progress Report on Dolomitization – Hydrology of Abu Dhabi Sabkhas, Arabian Gulf. in: *The Persian Gulf: Holocene Carbonate Sedimentation and Diagenesis in a Shallow Epicontinental Sea*. Editor B.H.Purser, Spriger-Verlag, Berlin, pp. 409-422.

Hussain, S.E. and Rasheeduzzafar, M. (1993). Influence of Micro-silica on Protection from Chloride-induced Corrosion of Reinforcing Steel. *ASCE Journal of Materials in Civil Engineering,* v. 5, n. 2, pp. 155-161.

Hussain, S.E. and Rasheeduzzafar (1994). Corrosion Resistance Performance of Fly Ash Blended Cement Concrete. *ACI Materials Journal,* v. 91, n. 3, pp. 264-272.

Irassar, E.F., Diamaio, A., and Batic, O.R. (1996). Sulfate Attack on Concrete with Mineral Admixtures. *Cement and Concrete Research*, v. 26, n. 1, January, pp. 113-123.

James, A.N. and Little, A.L. (1994). Geotechnical Aspects of Sabkha at Jubail, Saudi Arabia. *Quarterly Journal of Engineering Geology*, v. 27, n. 2, May, pp. 83-122.

Kassler, P. (1973). The Structural and Geomorphic Evolution of The Persian Gulf. in: *The Persian Gulf: Holocene Carbonate Sedimentation and Diagenesis in a Shallow Epicontinental Sea*. Editor B.H.Purser, Spriger-Verlag, Berlin, pp. 11-32.

Kendall, A. C. and Harwood G. M. (1996). Marine Evaporites: Arid Shorelines and Basins. published in: *Sedimentary Environments: Processes, Facies and Stratigraphy*. Edited by: Readings, H. G., 3rd Edition, Blackwell Science.

Kinsman, D.J.J. (1969). Modes of Formation, Sedimentary Associations, and Diagnostic Features of Shallow-Water and Supratidal Evaporates. reprinted from: *Amer. Assoc. Petroleum Geologists Bull.*, v. 53, pp. 830-840, published

in: *Marine Evaporites: Origin, Diagenesis, and Geochemistry*. Edited by: Douglas W. Kirkland and Robert Evans, Dowden, Hutchinson & Ross, Inc., pp. 80-90.

Kosmatka, S.H., Kerhoff, B. and Panarese, W.C. (2002). *Design and Control of Concrete Mixtures,* 14th edition, Engineering Bulletin 001, Portland Cement Association, Skokie, Illinois, United States of America.

Kropp, J. (1995). Chlorides in Concrete. published in: *Rilem Report 12, Performance Criteria for Concrete Durability*. edited by Kropp J and Hilsdorf H K, E & FN Spon, an imprint of Chapman & Hall, London.

Kumar, V. (1998). Protection of steel reinforcement for concrete – A review. *Corrosion Reviews*, v. 16, n. 4, pp. 317-358.

Lea, F.M. (1983). *The Chemistry of Cement and Concrete.* 3rd edition, Edward Arnold, London.

LeDred and Wey (1965). Formation Et Application De Complexes Mica-vermiculite-chlorue De Sodium. *Clays and Clay Minerals.* v. 13, n. 2, pp. 177-186.

Malhotra, V.M. and Mehta, P.K. (1997). *Pozzolanic and cementitious materials,* London.

Maslehuddin, M., Rasheeduzzafar, M., Page, C.L., and Al-Mana, A.I. (1995). Influence of Some Parameters Relevant to the Arabian Gulf Environment on Corrosion of Reinforcing Steel in Concrete. *Arabian Journal for Science and Engineering*, v. 20, n. 2, pp. 239-257.

Maslehuddin, M., Saricimen, H., Al-Mana, A.I., and Shamim, M. (1990). Performance of Concrete in a High Chloride-Sulfate Environment. *ACI–SP 122*, American Concrete Institute, Detroit, pp. 419-494.

Mehta, P.K. (1987). Natural Pozzolans. *Supplementary Cementing Materials for Concrete.* editor: Malhotra, V.M., CANMET, Ottawa, Canada.

Mehta, P.K. (2000). Sulphate Attack on Concrete – Separating Myths from Reality. *Fifth CANMET/ACI International Conference on Durability of Concrete.* Supplementary Papers, Barcelona, Spain, pp. 1-12.

Mitchell, J.K. (1993). *Fundamentals of Soil Behavior.* 2nd edition, John Wiley & Sons, Inc., New York, United States of America.

Montemor, M.F., Simoes, A.M.P., and Ferreira, M.G.S. (2003). Chloride-induced Corrosion on Reinforcing Steel: from the Fundamentals to the Monitoring Techniques. *Cement and Concrete Composites*, v. 25, n. 4-5, May-July, pp. 491-502.

Mosley, W.A., Hulse, R., and Bungey, J.H. (1996). *Properties of Reinforced Concrete Reinforced Concrete Design to Euro Code 2 (EC2).* Macmillan Press Ltd.

Neville, A.M. (1995). *Properties of Concrete.* 4th Edition, Marshfield, Mass.: Pitman Pub., London.

Neville, A.M. (1998). Concrete Cover to Reinforcement or Cover up?. *Concrete International,* v. 20, pp. 25-29.

Novokshchenov, V. (1995). Deterioration of Reinforced Concrete in the Marine Industrial Environment of the Arabian Gulf - A Case Study. *Materials and Structures*, v. 28, pp. 392-400.

Özturan, T. and Güneyisi, E. (2000). Effect of Binder Type on Strength and Chloride Ion Permeability of High Strength Concrete. *Fifth CANMET/ACI International Conference on Durability of Concrete.* Supplementary Papers, Barcelona, Spain, pp. 241-271.

Page, C.L., Short, N.R., and El-Tarras, A. (1981). Diffusion of Chloride Ions in Hardened Cement Pastes. *Cement and Concrete Research,* v. 11, n. 3, pp. 395-406.

Parrott, L.J. (1991). Factors Influencing Relative Humidity in Concrete. *Magazine of Concrete Research,* v. 43, n. 154, pp. 45-52.

Patterson, R.J. and Kinsman, D.J.J. (1981). Hydrologic Framework of a Sabkha along Arabian Gulf. *A.A.P.G. Bulletin,* v. 65, n. 8, pp. 1457-1475.

Purser, B.H. (1973). The Persian Gulf. in: *The Persian Gulf: Holocene Carbonate Sedimentation and Diagenesis in a Shallow Epicontinental Sea.* Editor B. H. Purser, Spriger-Verlag, Berlin, pp. 471.

Purser, B.H. and Seibold, E. (1973). The Principal Environment Factors Influencing Holocene Sedimentation and Diagenesis in the Persian Gulf. in: *The Persian Gulf: Holocene Carbonate Sedimentation and Diagenesis in a Shallow Epicontinental Sea*. Editor B. H. Purser, Spriger-Verlag, Berlin, pp. 1-10.

Rasheeduzzafar, M. (1992). Influence of Cement Composition on Concrete Durability. *ACI Materials Journal,* v. 89, n. 6, pp. 574-586.

Rasheeduzzafar and Hussain, S.E. (1993). Durability Mechanisms of Blended Cement Concretes. *Proceedings, 4th International Conference: Deterioration and Repair of Reinforced Concrete in the Arabian Gulf*, Bahrain, v. 2, October, pp. 909-926.

Rasheeduzzafar, M., AlSaadoun, S.S. and AlGahtani, A.S. (1992). Reinforcement Corrosion-resisting Characteristics of Silica Fume Blended Cement Concrete. *ACI Materials Journal*, v. 89, n. 4, pp. 337-366.

Rasheedduzzafar, Al-Amoudi, O.S.B., Abduljauwad, S.N., and Maslehuddin, M. (1994). Magnesium-Sodium Sulfate Attack in Plain and Blended Cements. *ASCE Journal of Materials in Civil Engineering*, v. 6, n. 2, May, pp. 201-222.

Roberts, M.H. (1962). Effect of Calcium Chloride on the Durability of Pretensioned Wire in Prestressed Concrete. *Magazine of Concrete Research,* v. 14, n. 42, pp. 143-154.

Sabtan, A., Al-Saify, M. and Kazi, A. (1995). Moisture Retention Characteristics of Coastal Sabkhas. *Quarterly Journal of Engineering Geology*, v. 28, part 1, February, pp. 37-46.

Santhanam, M., Cohen, M.D., and Olek, J. (2003). Effects of Gypsum Formation on the Performance of Cement Mortars during External Sulfate Attack. *Cement and Concrete Research*, v. 33, n. 3, March, pp. 325-332.

Scherer, G.W. (1999). Crystallization in Pores. *Cement and Concrete Research*, v. 29, n. 8, pp. 1347-1358.

Shearman, D.J. (1966). Origin of Marine Evaporates by Diagenesis. reprinted from: *Inst. Mining Met., Trans.*, v. 75, pp. 208-215, published in: *Marine Evaporites: Origin, Diagenesis, and Geochemistry*. Edited by: Douglas W. Kirkland and Robert Evans, Dowden, Hutchinson & Ross, Inc., pp. 61-68.

Siddiqi, Z.U. (2000). *Effects of Geotextiles on the Load-Carrying Capacity of Pavements on Sabkha*. MS Thesis, Department of Civil Engineering, King Fahd University of Petroleum and Minerals, Dhahran, Saudi Arabia.

Smith, B.G. (1998). Microsilica Concrete, Towards 2000 in the Arabian Gulf Environment. *Proceedings, Symposium on Performance of Concrete Structures in the Arabian Gulf Environment*, KFUPM, Dhahran, November, pp. 120-134.

Sonnenfeld, P. (1984). *Brines and Evaporites.* Academic Press, Inc., London.

Taylor, H.F.W. (1992). *Cement Chemistry.* Academic Press Limited, London.

Technical Report No. 40 (1991). The Use of GGBS and PFA in Concrete. Report of a Concrete Society Working Party.

Treadaway, K.W.J., Page, C.L., and Macmillan, G.L. (1987). The Prediction of Reinforcement Corrosion: From Laboratory Study to Exposure Trials. *Durability of Construction Materials*, v. 3, London: Chapman and Hall, pp. 1323–1329.

Turner-Fairbank (2002). *Blast Furnace Slag User Guideline HNR20.* U.S. Department of Transportation,.

CURRICULUM VITAE

Family name: Ali Nimary

First names: Walid Mohammed El-Mahdi Siddig

Date of birth: 3rd August 1976

Nationality: Sudanese

Education:

Institution Sudan University of Science and Technology
(Jan 1993 – July 1998)

Degree obtained Bachelor of Technology in Civil Engineering – Structures
(Second degree – First division)

Institution King Fahd University for Petroleum and Minerals
(Sept 1999 – Jan 2004)

Degree obtained Master of Science in Civil Engineering – Geotechnical
(GPA. 3.54)

Years of experience

July 1998 – Aug 1999 worked as structural engineer in Galandar Consultants (Khartoum/Sudan)

Membership of professional bodies:

ACI Saudi Arabia chapter – Eastern Province (Student membership)

Sudanese engineering society (junior engineer)

Other skills:

First aid certificate from the Sudanese Red Crescent (1989)